ES NOT CIRCULATE

UNIVERSITY OF MICHIGAN
MAY 28 1954
MEDICAL LIBRARY

ACTA RADIOLOGICA

CONDITA A GÖSTA FORSSELL

EDITA IUSSU SOCIETATUM RADIOLOGICARUM DANIAE, FENNIAE, NORVEGIAE ET SUECIAE

Editor ERIK LINDGREN, Stockholm / *Editor adiuvans* OLLE OLSSON, Lund

Redactores

Dania: P. Flemming Möller, Köbenhavn; C. Krebs, Århus
Fennia: G. Jansson, Helsingfors; S. Mustakallio, Helsingfors
Norvegia: T. Dale, Oslo; J. Frimann-Dahl, Oslo
Suecia: S. Hultberg, Stockholm; F. Knutsson, Upsala

INDEX

The roentgen diagnosis of polycystic kidneys. By *Lars Billing* 305

An electrokymographic study of auricular arrhythmia in total heart block. By *Arne Carlsten* and *Ulf Rudhe* 316

Pantomography in theory and use. By *Yrjö V. Paatero* 321

Experiences with Telepaque, a new cholecystographic medium. By *Lars Renck* 336

Clinical investigations on the use of radioactive gallium (Ga^{66} and Ga^{67}) in bone diseases. By *J. Th. van der Werff* 343

Dose measurements on secondary roentgen radiation. By *Rune Walstam* . 348

Secondary roentgen radiation. By *Bo Lindell* 353

La méthode tomographique dans la mesure du volume d'un viscère plein. Application au cœur. Par *Joseph Duhamel, Pierre-Louis Martin, Michel Guillon* et *Jean Broussin* 377

VOL. 41 APRIL 1954 Fasc. 4

ACTA RADIOLOGICA

EDITORIAL NOTICE

ACTA RADIOLOGICA publishes original papers relating to medical radiology and nuclear medicine. The articles are printed in English, French or German according to the wishes of the author. Contributions from all countries are accepted but priority is given to those from Scandinavian sources. Papers are published on the clear understanding that they are contributed exclusively to Acta Radiologica. They are subject to editorial revision and the right is reserved to introduce such changes as may be necessary to make the contributions conform to the editorial standards but Acta Radiologica does not hold itself responsible for any statements made or opinions expressed by authors. Contributions should be as concise as possible. Papers of more than 24 pages, including space for figures and tables, cannot be accepted for publication without special permission from the Editor. More extensive articles may be published as supplements at the author's own expense. These are not subject to editorial revision. Manuscripts from Denmark, Finland and Norway should be forwarded to the Sub-Editors of the respective countries, and other manuscripts direct to the Editorial Secretary, Acta Radiologica, Stockholm 2, Sweden.

Manuscripts must be typewritten with double spacing (at least 1 cm between each line) and adequate margins and a short summary should be included with each. All manuscripts should bear the name and full address of the contributor. A copy of the manuscript should always be retained by the author so that it may be available in the event of the original being lost in transit. Alterations to print are costly and, with the exception of small corrections, will be charged to the author. Footnotes should be avoided as far as possible, since they break the reading of the text and are expensive.

Illustrations and tabular material should be unmounted, and attached to the manuscripts in an individual cover. Numbering should be indicated in pencil lightly on the back and never appear on the front. The illustrations must be provided with suitable short legends and so worded that they are comprehensible without reference to the text. These legends should be typewritten on a separate sheet and not under the respective figures. Care should be taken that the illustrations only show the necessary details and essential features. Drawings and charts for reproduction should be in *black* (never in blue). The Editor reserves the right to reduce the size of illustrations as considered appropriate.

A bibliography must be added and the references should be arranged in alphabetical order of the author's name followed by his initials, full title of the paper and name of the journal — abbreviated according to *Fishbein: Medical Writing* or the *Quarterly Cumulative Index Medicus*. The volume number, year and number of first page of article should follow. Reference to books and monographs should indicate the author, the title, the edition, the name and city of the publisher, and the year of publication.

Example:

TILLINGER, K. G.: Papillary cystadenolymphoma. Acta radiol. 28 (1947), 241.

CAFFEY, J.: Pediatric X-Ray Diagnosis, Second Edition. The Year Book Publishers, Chicago 1950.

Fifty reprints will be presented to the author or divided among joint-authors. Additional reprints may be purchased at cost price but the necessary order must be given when the proof is returned.

Annual subscription rate 70 Swed. Kr. (plus 6 Sw. Kr. postage outside Scandinavia) payable in advance. (Two volumes, each of 6 numbers, appear annually.) Single copies 7 Sw. Kr. (plus postage Sw. Kr. 0:50) The subscription will be considered automatically renewed if not cancelled at the latest 10 days before the publication of a new volume.

All communications in regard to advertising, subscriptions, change of address, etc., should be sent to Acta Radiologica, Stockholm 2, Sweden.

ACTA RADIOLOGICA
EDITA IUSSU SOCIETATUM RADIOLOGICARUM
DANIAE, FENNIAE, NORVEGIAE, ET SUECIAE

VOL. 41 APRIL 1954 FASC. 4

THE ROENTGEN DIAGNOSIS OF POLYCYSTIC KIDNEYS

by

Lars Billing

The roentgen diagnosis of a polycystic kidney in an advanced stage is relatively easy, but difficulties arise when the task is to differentiate between an early stage of the condition and normal or pathologic variations in the shape and size of the kidney and pelvis. In such cases the descriptions given in the text books do not appear to be always altogether adequate. In support of this the following two cases are quoted.

Case 1. Male, aged 23: On two occasions during the last months, pain in the region of the left kidney and gross haematuria. Urography (Fig. 1): Right kidney normal. Left kidney large and the pelvis elongated; the major calyces appear to be a little elongated. No deformity of the pelvis or the renal outline to indicate larger cysts. Preliminary diagnosis: Probable multiple cysts in one kidney or unilateral polycystic kidney (according to BELL. Cf p. 307).

Case 2. Female, aged 36: Uncharacteristic pain in the upper part of the abdomen but no obvious symptoms referable to the kidneys. Urography (Fig. 2): The kidneys are large and the pelves long. The outlines are not embossed. Possibly the calyces are somewhat elongated but there are no obvious deformities of the pelves. Preliminary diagnosis: Probable early stage of bilateral polycystic kidney.

The reports on these cases prompted me to sum up the roentgen findings in fourteen patients examined during the last four years at Sahlgrenska Sjukhuset, and in whom the diagnosis of polycystic kidney appeared to be confirmed by operation, aortography or typical urographic findings. Intravenous urography with compression of the ureters was performed in all the cases, and retrograde pyelography in only one case (on a kidney with much decreased function). Aortography was performed in five cases, but one of these was not technically successful. For the purposes of comparison, the urograms of fifty patients with kidneys

Submitted for publication, July 3, 1954.

From Roentgen Department III (Director: Docent Ingmar Wickbom), Sahlgrenska Sjukhuset, Gothenburg, Sweden.

Fig. 1. Case 1. Urography. Left kidney: large pelvis and calyces elongated.

Fig. 2. Case 2. Urography. Large kidneys, elongated calyces.

Table 1

Group of signs	No.		27 Polycystic Kidneys					100 Normal Kidneys
			+	—	?	0	%+	% +
a	1	Length of the kidney > 14 cm	27	0	0	0	100	1
	2	Embossed, polycyclic outline	3		24		11	1
b	3	Thickness of the parenchyma > 3 cm	25	1	0	1	93	0
	4	Length of the pelvis > 9 cm	21	5	1	0	78	1
	5	Elongation of a calyx	17	8	1	1	63	4
	6	Multiple cyst impressions in the pelvis	24	1	1	1	89	0
	7	Lateral position of the pelvis	3	23	0	1	11	2
	8	Long axis of the pelvis parallel to the spine	17	9	0	1	63	3
	9	Horn-shaped pelvic ampulla (a & b)	20	5	0	2	74	20
		a. Horizontal horn	9				33	1
		b. Oblique horn	11				41	19
c	10	Worm-eaten cortex in the aortographic nephrogram	8	—	—	—	—	—

\+ = Sign positive.
— = Sign negative.
? = Impossible to judge if positive or negative.
0 = Not determined: insufficient distinguishable outlines or incomplete contrast filling of the pelvis.

considered clinically and roentgenologically normal, were studied. The results of this investigation are shown in Table 1. A brief review of some features of the pathology and clinical features of polycystic kidneys will be given in connection with the discussion of the roentgenologic signs and their value in the diagnosis.

Frequency. According to BELL, the incidence of polycystic disease in post-mortem examinations varies between 1 : 350 and 1 : 620. About 8 per cent of the cases are unilateral. In a series of kidneys examined roentgenologically the frequency should not be less than this, as we are here dealing with a selection of patients with kidney symptoms.

The clinical diagnosis of polycystic kidney was suspected only in one of the fourteen patients in my material, when referred for urography. The signs and symptoms that occasioned the roentgen examination were: haematuria, pyelitis, albuminuria, ureterolithiasis or uncharacteristic pain. BELL writes: "Gross haematuria is found in about one-third of the cases from time to time."

The roentgen appearances reflect the pathology of polycystic disease. The kidney is enlarged by innumerable cysts of diameters varying from

Fig. 3. Polycystic kidney (later operated), retrograde pyelography. Pelvis without major calyces. Thickness of parenchyma: 4.5 cm. Length of kidney > 16 cm. Length of pelvis 8 cm. No cyst impressions.

Fig. 4. Polycystic kidney. Urography. (Somewhat rotated position). Small ampulla; long and elongated major calyces; pelvis parallel to the spine.

< 1 mm to several cm and situated in both the cortex and the medulla, particularly in the former. Over a long period, the cysts become larger and cause a pressure athrophy of the parenchyma. The roentgen findings are dependent on: I. The type of pelvis with the two extremes of (a) a large ampulla with only minor calyces and no major calyces (Fig. 3) and (b) a small ampulla and several long major calyces (Fig. 4); II. The presence, as well as the situation of larger cysts.

The ten roentgen signs described below, may be divided into three groups (a—c).

(a) Changes seen in the outline of the kidney. When the kidney is very large the outline is often difficult to distinguish, probably due to reduction of the perirenal fat.

Fig. 5. Polycystic kidney. Urography: Thickness of the parenchyma 3.5 cm; no embossed outlines; some cyst impressions. Length of kidney > 16 cm and of pelvis 10 cm.

Fig. 6. Polycystic kidney. Urography: Multiple cyst impressions (↓). The pelvic ampulla forms an oblique horn.

1. The size of the kidney. The length was measured in the films (100 cm focus-film distance) and was 11—13 cm in 99 of the 100 normal kidneys, the remaining kidney measuring 14 cm. All the 27 polycystic kidneys were more than 14 cm, often 16—20 cm. A polycystic kidney in the early stages may be < 14 cm while a kidney without cysts but enlarged by reason of congenital abnormalities, hydronephrosis, lone function, growth etc., may be > 14 cm. The breadth has not been measured because the medical contour is so often difficult to distinguish. Thus a length of > 14 cm may only raise suspicions as to the condition.

2. An embossed polycyclic outline may be caused by several larger cysts near the surface. In non-cystic kidneys the outline may be dented by scars or persisting congenital lobulation. This sign may only be defined if a major part of the outline is distinguishable which seldom occurs in the larger polycystic kidneys; when marked, it is most suggestive.

(b) Changes seen in the contrast-filled pelvis (urography or retrograde pyelography).

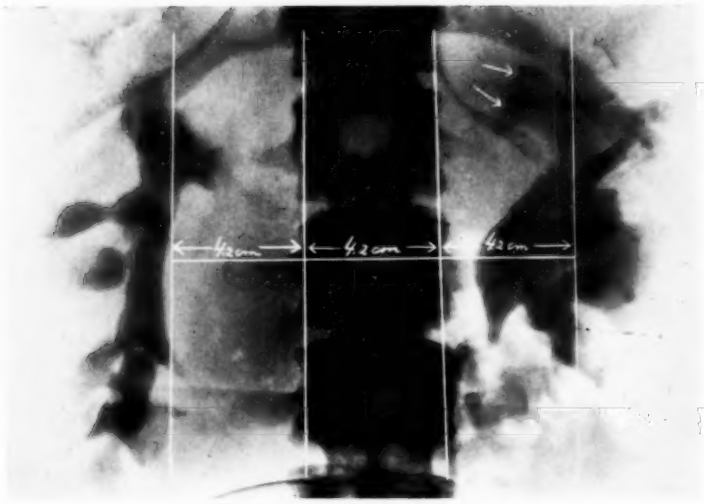

Fig. 7. Polycystic kidneys. Urography: Right pelvis (but not the left) lies more laterally than the breadth of a vertebral body from the spine. Right pelvis (14 cm) is almost parallel to the spine, but the left (10 cm) is in an intermediate position.

3. Increased thickness of the parenchyma measured as the distance between the lateral outline and the nearest laterally directed minor calyx. In the normal kidneys this distance was 2—2.7 cm and in only one instance reached 3 cm. In all the polycystic kidneys but two, it was > 3 cm (max. 4.5 cm). In one polycystic kidney, the thickness of the parenchyma was 2.8 cm, but in the contralateral kidney was 4 cm. In one kidney it was not possible to measure the thickness. Thus a thickness of the parenchyma > 3 cm, if not caused by a local expanding process, seems to be an almost pathognomonic sign. More experience of normal, malformed and diseased kidneys is, however, necessary in order that the value of this sign may be assessed.

4. Elongation of the pelvis. The distance between the most superior and most inferior major calyces is measured. This measurement was 6—8.5 cm in 99 and 9 cm in 1 of the 100 normal kidneys. In the polycystic kidneys, the distance generally exceeded 9 cm, in one instance reaching 14 cm. The significance of this sign is the same as that of sign 1.

5. Elongation of a calyx is a sign difficult to judge as the normal variations are great. If pronounced, this sign may be characteristic (Fig. 4).

6. Deformity of a calyx by a larger cyst situated close to it (Figs. 5, 6, 7, 8). Such impressions if multiple form an almost pathognomonic sign.

Fig. 8. Contra-lateral kidney to Fig. 3. Urography: Pelvis 12 cm long. Multiple cyst impressions (↓). The pelvic ampulla forms a horizontal horn.

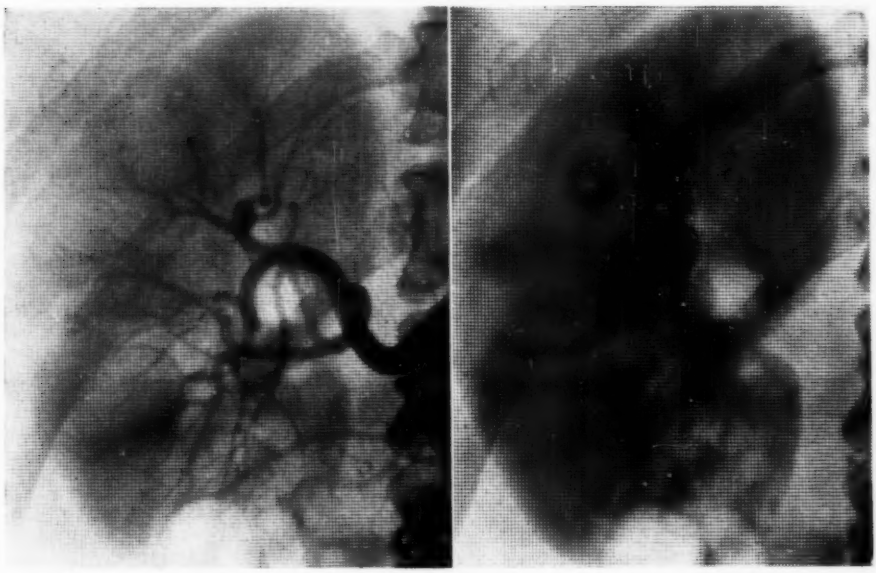

a. b.

Fig. 9. Normal kidney. Arteriographic (a) and nephrographic (b) phase of aortography. In (b) the cortical substance is opacificated, best seen in the renal columns around the interlobar arteries.

Fig. 10. Polycystic kidney. Nephrographic phase of aortography. 'Worm-eaten' appearance of cortical substance due to innumerable small cysts.

7. A lateral displacement of the pelvis may indicate enlargement of the parenchyma medial to the pelvis. I consider this sign as being positive when the distance to the spine is more than the breadth of a vertebral body, measured as in Fig. 7. This sign is of less significance as it is often absent in polycystic kidneys and may also occur in normal cases.

8. The long axis of the pelvis parallel to the spine (Fig. 4) and not to the psoas. This is a sign of enlargement or forward displacement of the kidney which, accordingly, will lie closer to the spine than to the psoas. This sign is often difficult to define as intermediate positions are also seen in normal cases; it is thus by no means pathognomonic and of only little value.

9. The pelvic ampulla has a horn shape. This may indicate a deformity of the pelvis due to enlargement of the parenchyma close to the ampulla, but may also be caused by an unusually low position of the kidney. The 'horn' may lie horizontally (Fig. 8) or obliquely (Fig. 6). However, doubtful cases are frequent, especially as regards the oblique 'horn', which is sometimes seen in normal cases. The sign is therefore not of importance.

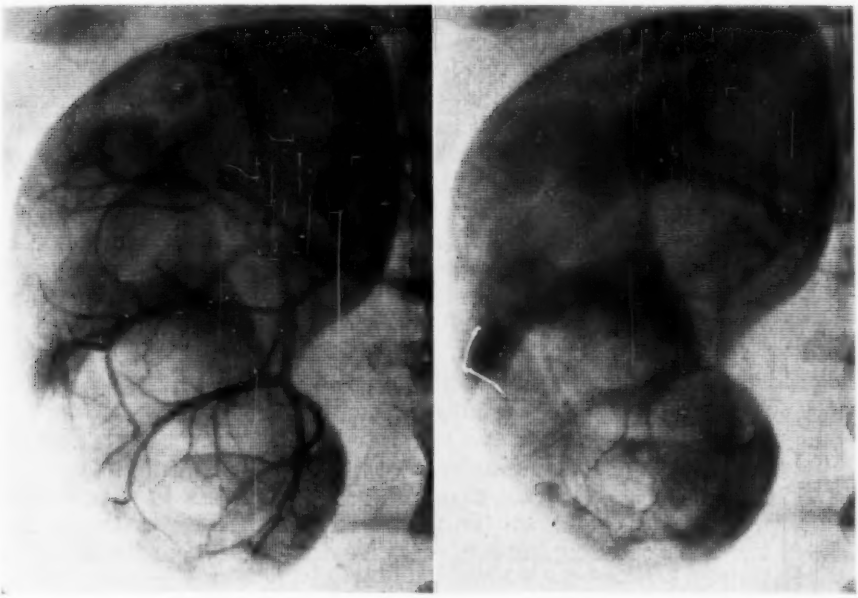

a. b.

Fig. 11. Case 2, right kidney. (a) Late arteriographic and (b) nephrographic phase of aortography. No cysts visible in the cortex.

(c) Changes seen in aortography. In a large polycystic kidney the branches of the renal artery are stretched, but this is difficult to assess in the early stages and may occur in all enlarged kidneys, *e. g.* in hydronephrosis.

10. The nephrographic appearances on the other hand, are, in my opinion, pathognomonic. The opacification of the parenchyma seen in films exposed a few seconds after injection into the aorta, is not of the same nature as that seen in urography in cases with acute obstruction of the ureter. The former is due to the capillaries being filled with contrast medium, whereas the second is caused by accumulation of medium in the various segments of the nephron. Thus in the former case, mainly the cortex, but in the second, the whole of the parenchyma is rendered opaque. Figs. 9 a and b are the arteriographic and nephrographic phases in an aortography of a normal kidney. The opaque cortical substance both in the periphery of the kidney and in the renal columns around the interlobar arteries is seen. Fig. 10 is the nephrographic phase of a poly-

cystic kidney. The opaque cortex does not constitute a homogeneous layer, but has a worm-eaten appearance due to the presence of innumerable cysts of varying size.

Signs 1, 2, 4, 5 and 6 are described in the text books but no information as to the measurements appears to have been given. Signs 7, 8 and 9 are discussed, among others, by HENNINGER and WEISS, but the value of signs 3 and 10 have not been stressed previously.

As seen from the table and from what has been said above, only signs 3, 6 and 10 are of decisive importance. However, the other signs should not be undervalued. In cases with indistinct outlines and incomplete contrast-filling of the pelvis (due to decreased function), every sign may prove valuable in pointing to the nature of the lesion and indicate retrograde pyelography or aortography. With more experience of signs 1—9, I consider that aortography is seldom necessary for the diagnosis, but a successful aortography is a deciding factor in a doubtful case.

As to the two suspected cases quoted above, neither can be diagnosed as polycystic kidney of the ordinary type with multiple cysts in the cortex. In Case 1, the length of the kidneys was 11 and 15 cm and the length of the pelvis 6 and 10 cm on the right and left sides, respectively. In Case 2, the corresponding measurements were 16 and 15 cm for the kidneys and 12 and 11 cm for the pelves. The thickness of the parenchyma was < 2.5 cm in all four kidneys and there were no defects to suggest the presence of larger cysts. In both cases, there are no cysts visible in the opaque cortical substance. (Case 2: Figs. 11 a and b.) The cause of the gross haematuria from the left kidney in Case 1 was not clarified.

Addendum

On account of pain the kidneys of Case 2 were surgically explored in January 1954. The kidneys were found to be large but there was no evidence of cysts or other pathology.

SUMMARY

The roentgen findings in polycystic kidneys are briefly described and the signs enumerated and discussed in detail. The importance of a successful aortography producing a characteristic nephrogram as a deciding factor in the differential diagnosis, is stressed.

ZUSAMMENFASSUNG

Die Röntgenbefunde bei polyzystischen Nieren werden kurz beschrieben; die Symptome werden aufgezählt und eingehend besprochen. Die Bedeutung einer erfolgreichen Aortographie, die ein für die Differentialdiagnose entscheidenes charakteristisches Nephrogramm gibt, wird hervorgehoben.

RÉSUMÉ

La symptomatologie radiologique du rein polykystique est brièvement décrite et les signes sont énumérés et étudiés en détail. L'auteur insiste sur l'importance d'une aortographie réussie, donnant une néphrographie caractéristique, comme élément décisif du diagnostic différentiel.

REFERENCES

1. Bell, E. T.: Renal diseases. Lea & Febiger, Philadelphia 1947.
2. Henninger, H. & Weiss, K.: Zur Klinik der kongenitalen Cystenniere. Ztschr. urol. Chir. 44 (1938/39), 221.

FROM THE ROENTGENOLOGIC RESEARCH LABORATORY AND THE LABORATORY OF CLINICAL PHYSIOLOGY, KAROLINSKA SJUKHUSET, STOCKHOLM, SWEDEN

AN ELECTROKYMOGRAPHIC STUDY OF AURICULAR ARRHYTHMIA IN TOTAL HEART BLOCK

by

Arne Carlsten and *Ulf Rudhe*

Auricular arrhythmia is often observed in total A—V block (ERLANGER and BLACKMAN 1909—10, HECHT 1913, PARSONNET and MILLER 1944 and others). The auricular intervals which include a ventricular contraction, are as a rule shorter than the intervals appearing in ventricular diastole. This auricular arrhythmia seems to be dependent on the vegetative tone (ROTH and KISCH 1948, CARLSTEN 1953), but the mechanism underlying it, is unknown at present.

We have tried to obtain information on the origin of this arrhythmia in total A—V block by the aid of electrokymographic examination of the right auricle. Our intention has been to study the degree of filling and emptying of the right auricle in different heart cycles and to relate this to the auricular rhythm.

Methods

The electrocardiogram (ECG), phonocardiogram (PCG) and electrokymogram (EKyG) were recorded simultaneously. The ordinary amplifier electrocardiograph (Triplex, Elema) was used. The phonocardiogram was recorded in the 15—100/sec. frequency range with a piezo-electric microphone. The electrokymograph and the roentgen ray unit were the same as described in earlier papers (ENGSTRÖM, KJELLBERG, PERSSON and RUDHE 1949, KJELLBERG, RUDHE and SJÖSTRAND 1951). The roentgen rays were emitted from a condensor apparatus. Its effect, as well as the current from the photocell connected with a direct current amplifier, have in earlier experiments been found to be practically constant even

Submitted for publication Aug. 21, 1953.

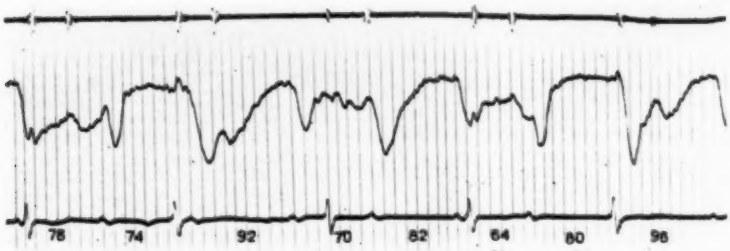

Fig. 1, Case 1. PCG, EKyG and ECG. P—P intervals are measured in 1/100 sec.

on continuous operation for 20 minutes (KJELLBERG, RUDHE and SJÖSTRAND 1951). The investigation was always performed with the patients in voluntary apnoea. They were instructed to avoid straining. In all the examinations the diaphragmatic dome was arrested at a level — adjusted for each individual — marked on the fluorescent screen.

The intention was to record border electrokymograms from the right auricle. As interest was focussed on auricular volume changes, all curves which showed any appreciable influence from ventricular activity of the type due to positional changes were rejected.

Material

Five subjects with total A—V block were examined. Because of the difficulty of obtaining 'pure' right auricular electrokymograms satisfying the criterion mentioned above, only two of the five subjects were accepted for analysis.

Case 1. Male, aged 17 years. D. Ventricular septal defect. No symptoms or signs of cardiac decompensation. ECG showed a ventricular rate of 40—45 and an auricular rate of 63—102 beats a minute. QRS slurred. RS—T depressed in leads I, II, CR7 and IV R. T negative in leads I—III, CR7 and IV R, positive in CR2.

Case 2. Male, aged 78 years. D. Carcinoma of the gingiva + arteriosclerosis. No symptoms or signs of cardiac failure. ECG showed a ventricular rate of 40—45 and an auricular rate of 65—80 beats a minute. Slight depression of the RS—T segment in leads II, CR7 and IV R. QRS slightly slurred. Otherwise normal findings.

Results

Figs. 1 and 2 represent a short part of the recordings from Case 1 and Case 2 respectively. The record in Fig. 1 and the upper record in Fig. 2 demonstrate heart periods with wide variations in the depth of deflection in the EKyG. A pronounced auricular arrhythmia is present

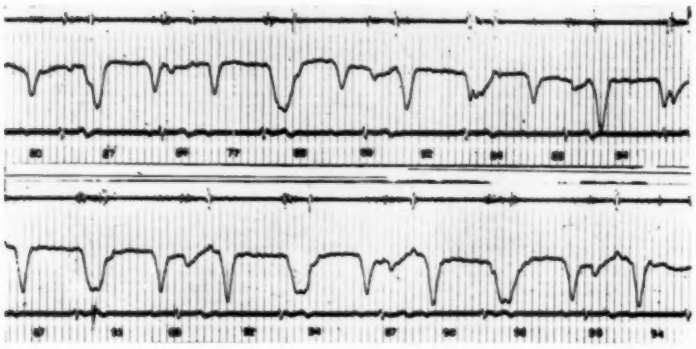

Fig. 2, Case 2. PCG, EKyG and ECG. P—P intervals are measured in 1/100 sec.

(P—P intervals vary between 0.64 sec.—0.96 sec. and 0.77 sec.—0.94 sec. respectively). In the lower record of Fig. 2 the depth of the deflection in the EKyG at the auricular systole is more constant. The auricular rhythm is here less irregular (P—P intervals between 0.87 sec.—0.96 sec.).

The results of the analysis are demonstrated graphically in diagram 1 and 2. From these figures it is evident that there is a relationship between the depth of auricular systolic deflection in the EKyG and the time interval to the next auricular systole in the ECG. In Case 1, it was observed in addition that the deepest deflections occurred when auricular and ventricular systole were simultaneous, while the smallest deflections were found in P—P intervals including a ventricular systole without simultaneous auricular and ventricular contractions. In Case 2, this tendency towards separation of different deflections in groups of P—P intervals is less marked.

Discussion

Several theories have been advanced to explain the auricular arrhythmia occurring in 25—75 % in different reported materials of total A—V block. A review of these theories will be given in a later paper (Carlsten 1954). The present investigation seems to throw some light upon the mechanism underlying the arrhythmia.

We think we are justified in assuming that the deflections in the EKyG represent a relative indication of the auricular volume changes because the influence on the records of the ventricular contraction is reduced to a minimum in the selected cases. The deeper the deflection of the EKyG over the right auricle as a result of an auricular contrac-

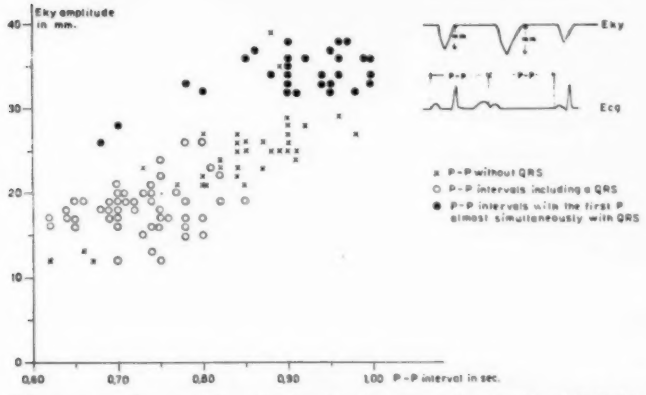

Diagram 1, Case 1. The relationship between the depth of EKyG deflection and the P—P intervals.

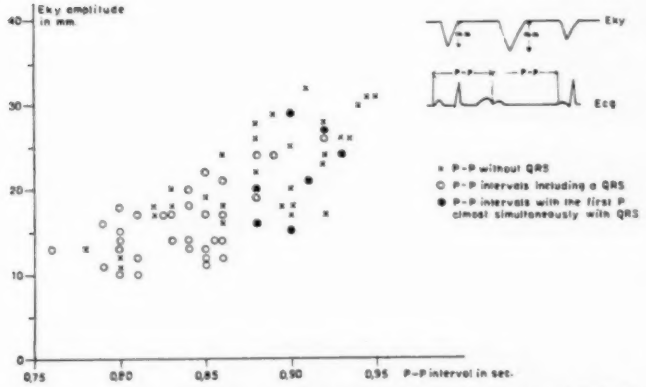

Diagram 2, Case 2. The relationship between the depth of EKyG deflection and the P—P intervals.

tion, the longer is the interval to the next auricular contraction. Consequently haemodynamic factors (the degree of filling and emptying of the right auricle) might play some rôle in the mechanism of the arrhythmia. However, any definite conclusions cannot be drawn from the present analysis. Further investigations of the problem of auricular activity in total A—V block should include a closer study of these haemodynamic conditions.

SUMMARY

Two cases with total heart block, showing auricular arrhythmia, have been studied with simultaneous registration of the electrocardiogram, phonocardiogram and right auricular electrokymogram. In both cases there was a tendency for longer auricular intervals following deep deflections in the electrokymogram and vice versa. The results suggest that the auricular arrhythmia in total heart block is influenced by the filling and emptying of the auricles.

ZUSAMMENFASSUNG

Zwei Fälle mit totalem Herzblock, die aurikuläre Arhythmie aufwiesen, sind mit Hilfe von gleichzeitiger Registrierung des Elektrokardiogrammes, des Phonokardiogrammes und des rechten aurikulären Elektrokymogrammes untersucht worden. In beiden Fällen lag eine Neigung zu längeren Vorhofsintervallen nach tiefen Inflexionen im Elektrokymogramm und umgekehrt vor. Die Ergebnisse deuten an, dass die aurikuläre Arhythmie beim totalen Herzblock durch die Füllung und Entleerung der Vorhöfe beeinflusst wird.

RÉSUMÉ

Deux cas de bloc total du coeur, avec arythmie auriculaire, ont été étudiés par enregistrement simultané de l'électrocardiogramme, du phonocardiogramme et de l'électrokymogramme auriculaire droit. Dans les deux cas il y avait tendance à l'allongement des intervalles auriculaires suivant de profondes inflexions de l'électrokymogramme et vice versa. Ces résultats font penser que l'arythmie auriculaire dans bloc total du coeur est influencée par la réplétion et l'évacuation des oreillettes.

REFERENCES

Carlsten, A.: On the vegetative control of auricular and ventricular rates and rhythms in total heart blocks. To be published in Acta med. Scandinav.

Engström, B., Kjellberg, S. R., Persson, L. & Rudhe, U.: Some aspects of the use of electrokymography in cardiac investigations. Acta radiol. 31 (1949), 435.

Erlanger, J. & Blackman, J. R.: Further studies in the physiology of heart-block in mammals. Heart 1 (1909—1910), 177.

Hecht, A. F.: Der Mechanism der Herzaktion im Kindesalter. Erg. inn. Med. 11 (1951), 49.

Kjellberg, S. R., Rudhe, U. & Sjöstrand, T.: The relationship between the pulmonary blood content, the heart volume and the filling rate of the left ventricle. Acta physiol. Scandinav. 24 (1951), 49.

Parsonnet, A. E. & Miller, R.: Heart Block. Am. Heart J. 27 (1944), 676.

Roth, J. R. & Kisch, B.: The mechanism of irregular sinus rhythm in auriculoventricular heart block. Am. Heart J. 36 (1948), 257.

FROM THE INSTITUTE OF DENTISTRY (DIRECTOR: PROFESSOR EERO TAMMISALO),
UNIVERSITY OF HELSINKI, HELSINKI, FINLAND

PANTOMOGRAPHY IN THEORY AND USE

by

Yrjö V. Paatero

Since publishing an advance report in 1949 (5) of a new method of tomographic roentgenography (which I subsequently named pantomography), I have had an opportunity of developing the method. In 1950—1951 I worked for a year and a half at the Dental School of the University of Washington in Seattle, Wash., carrying out research and experiments and submitted a report on the results for publication in the United States. Later, in Finland, I have attempted to improve pantomography and develop it into a reliable and useful method of roentgenography (6, 7, 8, 9). As pantomography has now been in constant use at this Institute for more than a year and, by and large, has met my expectations, I avail myself of the opportunity of describing the method in its entirety.

Pantomography enables the recording on ordinary flat film of roentgenograms of any curved layers of an object, *e. g.* the human skull. Pantomographic roentgenograms, *i. e.* pantomograms, are, in a way, panoramas of the layers.

Thus, pantomographic roentgenography must be distinguished from all previous tomographic methods which produce roentgenographic representations of level surfaces, either longitudinal (3), transverse (1, 3) or of parts of the object near the outer surface (4).

Before the principle of pantomography is considered, the special terminology which has been evolved must be given.

Nomenclature used in Pantomography

Pantomograph: A device used with a normal roentgen apparatus, which produces pantomographic roentgenograms = pantomograms.

Submitted for publication, August 11, 1953.

Pantomogram: A panoramic roentgenogram of a curved layer, either internal or external, of the object.

Image layer: The layer of the object visible in the pantomogram.

Thickness of image layer: The dimension in depth of the layer visible.

Image surface: The mathematical surface of the image layer which travels at the same linear speed as the roentgen film. (The image surface has no thickness.)

Rotational speed: The angular velocity of the rotating parts of the pantomograph.

Location: The distance of the image layer or the roentgen film from the rotational axis (in cm or mm).

Divergence: The angle in the horizontal plane of the outermost rays of the roentgen beam. Unless specifically mentioned, the vertical divergence is ignored.

Width of roentgen beam: The width of a bunch of roentgen rays in a horizontal plane.

Object holder: A ring attached to a rotating chair, the front being detachable for admitting the patient's neck. The centre of the ring must lie on an imaginary extension of the rotation axis of the chair.

Cephalostat: A device attached to the object holder and designed to hold the patient's head in the correct position during the exposure.

Film holder: A circular plate on which the film cassette is placed and which is rotated by means of friction of the object holder.

Principle of Pantomography

The principle of pantomography is depicted in the schematic drawing in Fig. 1. It shows the object holder (Oh) and film holder (Fh), each of equal diameter. Their rotational axes are O_1 and O_2, respectively. The arrows indicate the directions of rotation. A roentgen beam (R) is aimed through the rotational axes, from right to left in the drawing. For the time being, the roentgen beam is assumed to be a mathematical surface with no width. It is further assumed that the object holder, when rotated, energizes the film holder through friction as the edges of the holders engage. As the diameters of the object holder and film holder are equal, they rotate with identical angular velocity. Consequently, all points at an equal distance from the rotational axis have the same linear speed. Further, if the points in question travel in the same linear direction through the roentgen beam (R), they remain stationary in respect of one another. This applies, for instance, to the part of the roentgen beam between the axes (O_1 and O_2). It therefore follows that circles 1, 2, 3 and 4

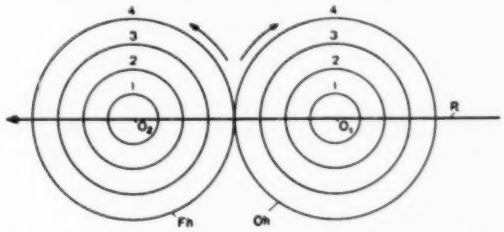

Fig. 1. A roentgen beam (R) is aimed through the rotational axis (O_1) of the object holder (Oh) and the rotation axis (O_2) of the film holder (Fh). As both the object holder and film holder rotate at the same angular speed, a layer of the object which is equally far from its rotational axis as the film is from its axis, is projected on a film bent on the film holder (the film and the layer have an identical linear speed on the part of the roentgen beam between the axes).

of the object holder and the corresponding circles of equal size of the film holder travel at the same linear speed through the roentgen beam and thus are stationary in relation to one another. On the other hand, circles of different size, though travelling at the same angular speed, have a different linear velocity. The linear speed of circle 3 is larger than that of circle 2 but smaller than that of circle 4. Hence, the greater the distance of a point from the rotational axis, the greater its linear speed. The linear speed of the points on the axis are equal to zero, a fact to be remembered.

Now if a roentgen film (in its cassette) is placed on the film holder alongside circle 3 and an object is put in the object holder, a continuous representation of the cylindrical layer of the object on circle 3 of the object holder is projected on the film when the machine is rotated and the object exposed to the roentgen beam. If for instance a pantomogram of an elliptical layer on a horizontal plane is desired, it suffices to bend the film cassette into an elliptical shape. The parts of the film which are more distant from the axis record a representation of the outermost layers of the object, while those closer to the axis record the inner layers according to their distance from the rotational axis.

The parts of the object whose distance from the rotational axis differ from that of the film, travel at a linear speed different from that of the film, and are therefore not sharply projected in the view. They only leave linear 'fog traces' or nothing at all, dependent on the density, location and other characteristics of the object.

From the foregoing it is clear that the shape and location of the roentgen film determine the situation and shape of the object's layer of which the pantomogram is formed, *e. g.* if spherical roentgen films were available, it would be possible to record spherical surfaces or layers.

Existing films are capable of reproducing cylindrical and conical surfaces as well as intermediate shapes since they may be suitably bent.

If a representation of several layers is desired with one exposure, it is only necessary to place the corresponding number of films on the film holder and bend them to the shape desired. Each film records only its 'own' surface, the linear speed of which corresponds to that of the film concerned. By using a voltage of 80 kV it is easy to obtain a picture of many as three layers at one exposure, provided the cassettes are fitted with thin intensifying screens.

Thickness of Image Layer

While theoretically it is possible to discuss an image surface, in practice it is not possible to produce a pantomogram of a mathematically thin layer, and the layer projected onto the film will always possess a dimension of thickness. The thickness of the image layer is determined by two factors: the location of the object in relation to the rotational axis and the range of the divergence of the bunch of roentgen rays in the horizontal plane. The farther the part to be reproduced from the rotational axis, the thicker the image layer; the greater the horizontal divergence, the thinner the image layer will be.

Effect of Divergence on Location of Film

For the sake of clarity I have, in explaining the principle of pantomography, assumed the roentgen beam to be a vertical, mathematical plane without width. In reality this is never the case. The theory would be valid if roentgen tubes with linear foci (6) were available.

In existing roentgen apparatus, the rays emerge as a diverging bundle from a point-like focal spot. This fact must be borne in mind in studying the theory of pantomography.

Because of divergence, a roentgenogram, as well as a pantomogram, is always larger than the object. A pantomogram is horizontally wider than the layer reproduced, or, to be specific, wider than the image layer flattened out into a plane. It therefore follows that the film must travel at a greater linear speed than that of the respective image surface in order to accommodate the projection of the image on the film as the object and film holder rotate an equal number of degrees on their axes. In practice, this requires that the film be placed further from its axis than the corresponding surface (layer) to be recorded is from its rotational axis. The correct position of the film may be accurately calculated in each case, but for practical purposes its determination may be made

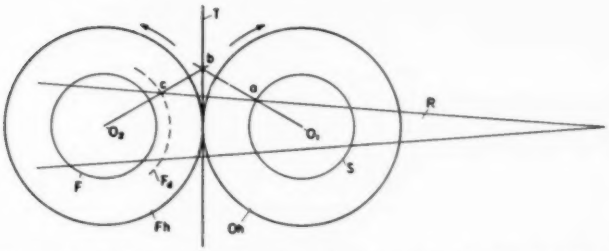

Fig. 2. The effect of the divergence of a roentgen beam on the positioning of the film. The correct distance may be determined by drawing a straight line from point O_1 through point a to the tangent T; another straight line is drawn from point b to point O_2. Point c shows the position of the film.

graphically as depicted in Fig. 2; for the sake of clarity, I have given the roentgen beam a considerably larger divergence than used so far in pantomography. If one wishes to determine the correct position of the film in relation to the image surface (layer) (S) of the object, this can be done by drawing a straight line from the axis (O_1) through the intersection (a) of the outermost ray and the circle (S). This line meets the tangent (T) at point b. From this point another straight line is drawn to the axis (O_2) of the film holder. The intersection (c) of this line and the outermost ray of the roentgen beam indicates the exact distance (depicted by the dotted circle F_d) of the film. If parallel rays could be used (6) the film would be on circle F, which is equal to circle S.

By thus locating the positional circles of the film for respective image surfaces of varying size, it is possible to draw a diagram which quickly shows the correct position of the film in each case. This I have done in Fig. 3. The diagram is valid in regard for all divergence angles which I

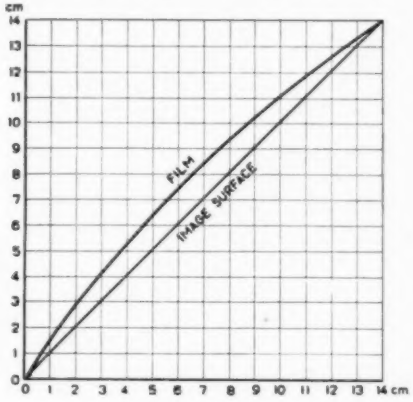

Fig. 3. A diagram showing the interrelation between the layer to be shown and the film. The X-axis shows the distance of the image layer from its rotational axis, while the Y-axis indicates the corresponding distance of the film.

generally have used in pantomography so far. The horizontal X-axis shows the distance of the surface from its axis (O_1) in centimeters, while the vertical Y-axis indicates the corresponding position of the film from the axis O_2. In this research, the distance of the focal spot from the axis of the object holder was 51 cm, while the diameter of both the object holder and film holder was 28 cm. The width of the lead slit in front of the roentgen tube was about 4 mm, its distance from the focal spot being 31 cm. With these factors the width of the roentgen beam at a distance of the axis of the film holder is about 11.5 mm. An anode voltage of 80 kV has generally proved suitable for roentgenographing adults, as compared with 75 kV in the case of children. The pantomograph used rotates around its axis once every 20 seconds. As the current output of the roentgen unit is 38 mA, the mAs in a jaw exposure amounts to about 450. A scrutiny of the diagram shows that the graph is relatively straight for the entire distance (5—9 cm) of cranial pantomography. The adjustment required for divergence is thus about 1.5 cm.

To obviate unnecessary calculations in taking films, 'corrected' circles, corresponding to the mathematical circles one centimeter apart of the object holder, are inscribed on the surface of the film holder.

Projection of Film from Stray Radiation

In pantomography, as in roentgenography generally, it is desirable to shield the roentgen film as carefully as possible from stray radiation. For this purpose a lead shield with a vertical slit, is placed between the object holder and film holder. This shield is, of course, stationary while the other parts rotate. The roentgen beam is projected onto the film through the slit, the remainder of the film lying behind the lead safe from stray (secondary) radiation.

Since the roentgen beam in pantomography is relatively narrow, it is obvious that secondary radiation emanates from only a narrow portion of the object. Horizontal secondary radiation thus is negligible and capable of being largely eliminated through the lead shield. On the other hand, vertical secondary radiation is considerably more pronounced, as the roentgen beam in cranial reproductions is about 30 cm high. The lead shield cannot therefore protect the film from vertical secondary radiation. This I have observed experimentally. If a Lysholm grid is placed in front of the slit so that its lead strips are in a vertical position, the grid does not appreciably improve the contrast. But if the grid is in a horizontal position a marked improvement of the contrast can be noticed, as in that case the film is not subjected to vertical secondary radiation.

In experiments using a broad roentgen beam for the achievement of a very thin image layer, it has proved necessary to use the Lysholm

grid, as the wide slit of the lead shield, in this case, would be of no consequence. The Lysholm grid might be placed so that the strips are slightly oblique to the horizontal plane, thereby avoiding horizontal lines in the film.

My experiments on secondary and stray radiation were carried out with live subjects and such phantoms as emit a great deal of secondary radiation.

Positioning of Object in Object Holder

The object (the patient's head) may be placed in various positions in the object holder depending upon the specific purpose in view. I find it practical to use the mandible as a directional base. Fig. 4 schematically depicts three principal positionings. When a good representation of the entire skull or jaws is required it is advisable to place the object symmetrically to the sagittal diameter of the object holder, *i. e.* concentrically to the rotational axis (positions 1 and 2). If a clear view of the temporomandibular joints is desired, position 1 is recommended, whereas position 2 is better if the teeth are to be shown. If both the temporomandibular joints and teeth are to be depicted, an intermediate position

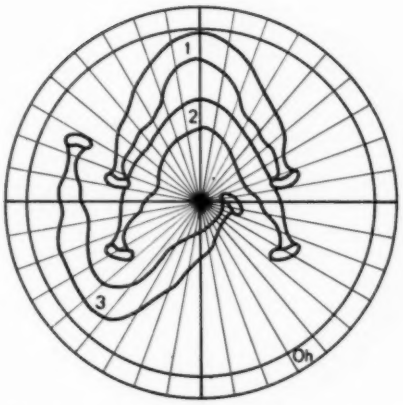

Fig. 4. Different positions of the object (the mandible) in relation to the object holder.

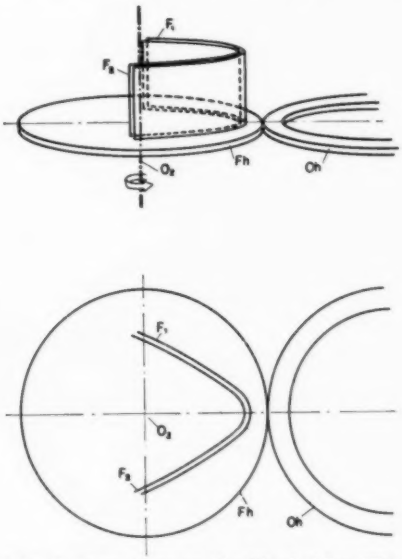

Fig. 5. Two films on the film holder (Fh). The outer film (F_1) and the inner film (F_2) are bent into the shape of a jaw.

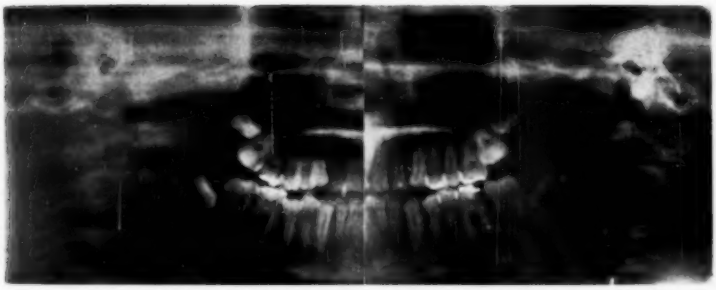

Fig. 6. A pantomogram taken eccentrically of the teeth.

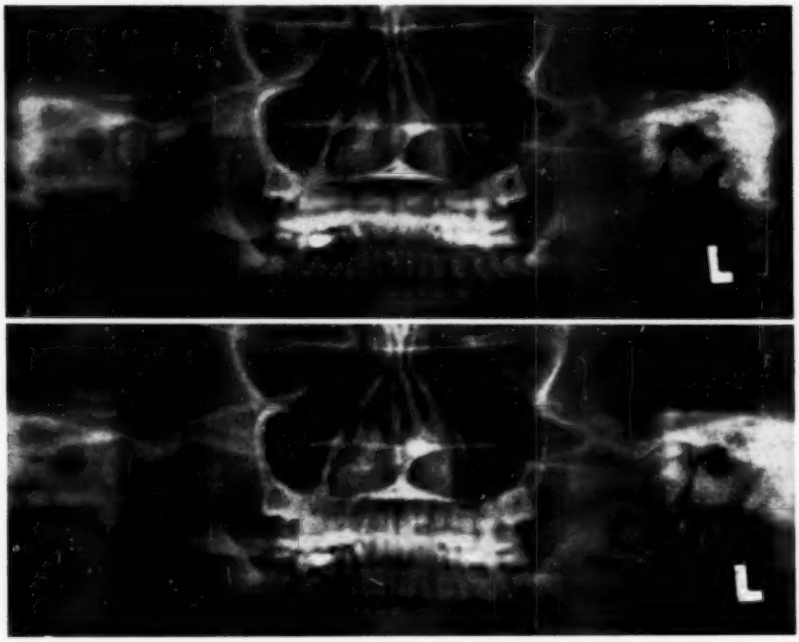

Fig. 7. Double pantomograms of the jaws made with films 5 mm apart. Stereoscopically, a 'plastic' panorama is obtained.

is selected. Radii drawn on the drawing (Fig. 4) enable the observer to judge the direction in which the roentgen beam penetrates the different parts of the object. The pantomograms in Figs. 7 and 8 are taken with the concentric method.

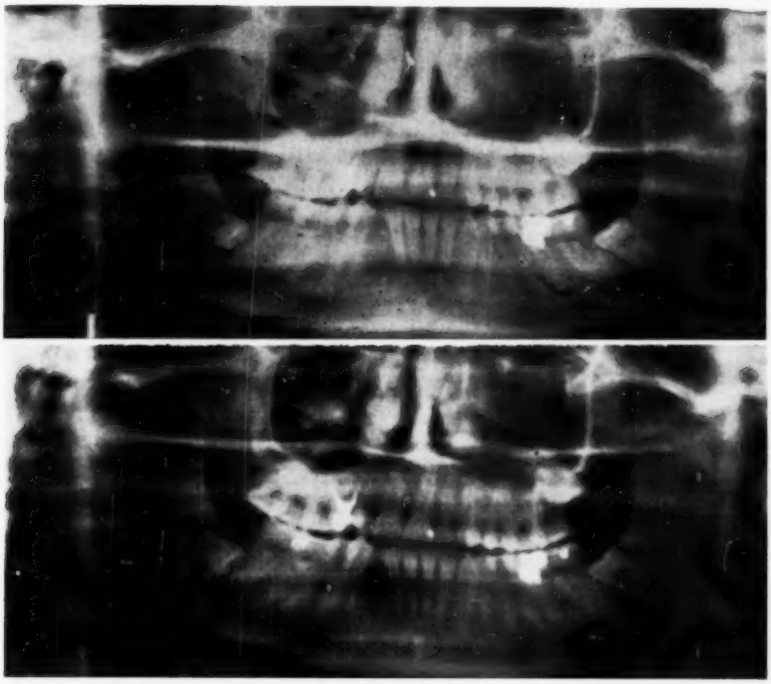

Fig. 8. Stereopantomograms taken of the jaw with a vertical tube shift.

In order to examine the jaws and teeth as orthoradially as possible one must resort to the eccentric technique: the object must be placed assymmetrically to the object holder. This method is represented by 'mandibular position 3'. It can be seen that in this case the roentgen beam penetrates the jaws at almost a perpendicular angle, whereby the teeth generally appear clearly without overlapping. A drawback of this technique is that exposures must be made for each side of the jaws or skull, with consequent re-positioning of the patient.

Placing the patient in position and carrying out the procedure do not require much time in the present stage of pantomography. The entire process can easily be done by an experienced person in three minutes.

Joint pantomograms, taken eccentrically of a 14-year-old boy are shown in Fig. 6. The films were obtained especially for the teeth.

Apart from the patient's position in respect to the rotational axis it is important that he be suitably placed in relation to the horizontal plane. Good results have been obtained by positioning the head in such a manner

that the Frankfurt plane is horizontal. Camper's plane has also been used as an orientation plane.

As for the elevation ratio between the roentgen tube and the object, keeping the focal spot of the roentgen tube level with the external auditory meatuses, has proved advantageous for general purposes. In taking films of the teeth alone, I consider it desirable to lower the focal spot to the height of the occlusal plane which is placed horizontally. The roentgen beam will then be directed through the upper and lower teeth at the best possible vertical angle.

Thickening the Image Layer with Double Films

The two factors which decide the thickness of the image layer and which make possible, within limits, the advance selection of the thickness, have been mentioned. This does not mean that the thickness of the image layer is adjustable within millimeters, but rather that it is possible to portray a relatively thick or thin layer of one or two centimeters or of a few millimeters.

In this connection I wish to present another method whereby the image layer may be thickened and made more clearly visible in the pantomogram. If two films in close proximity are used instead of one so that the sharp picture of the first film seems to extend to the sharp picture of the second film, a very clear vision of the image layer is produced when the pictures are viewed stereoscopically.

With the same exposure the outer film produces a picture of a layer slightly further away than the inner film. The distance between the films may suitably be 4—6 mm. If examined stereoscopically either with the naked eye or with a stereoscope, one eye sees a deeper layer than the other. The pictures blend together, resulting in a 'plastic' panorama of the layer under observation. The reader is invited to look at Fig. 7 in the manner described. As the oral and nasal cavities are in the image layer, they are clearly visible. The incisors in this case are slightly outside the image layer.

The use of double films is schematically explained in Fig. 5. F_1 is the outer film, F_2 the inner one, in either the same or separate cassette, with an interposed sheet of felt keeping them apart. The bending of the films corresponds to the shape of the jaws. The edge of the film holder (Fh) engages with that of the object holder (Oh) (only part of it is visible). When the object holder is rotated, it turns the film holder by means of friction.

Pictures taken in the manner described above may be viewed in their normal position or 'sidewise' as in Fig. 7. Occasionally and in certain situations a definite stereoscopic effect may be observed.

Stereoscopic Pantomography

Stereoscopy may profitably be adapted to pantomography by abiding to the general principles of stereoscopy. The roentgen tube may be moved either vertically or horizontally between exposures. As the focus—film distance in my pantomographic technique has been about 70 cm, a suitable tube shift has been 67 mm (2). Instead of moving the roentgen tube, the object may be correspondingly turned.

For several reasons I consider a vertical tube shift superior to a horizontal. Pictures thus produced must naturally be held 'sidewise' for observation. Stereo views taken vertically are, moreover, individually symmetrical and may as such be used for comparison of opposite sides. On the other hand, those obtained horizontally are, by reason of their assymmetricallity, not useful for this purpose.

Figure 8 shows a pantomogram pair taken with a vertical tube shift. In parallel viewing of the films, the observer sees the jaws from within, as if he were in the nape of the patient's neck. By viewing with 'crossed eyes', the jaws appear as from without.

Construction and Use of the Technical Devices Needed in Pantomography

The largest and most expensive piece of equipment is the pantomograph itself, to be used in conjunction with any suitable roentgen unit. The principal parts of a pantomograph are the base, the seat rotated by an electric motor, and the object holder with its cephalostat. The seat may be raised and lowered at will, the object holder remaining stationary. Figure 9 represents the upper part of a pantomograph with a patient in position. On the left is a part of the roentgen tube and a cube-shaped case provided with slit diaphragms. At the middle of the upper rail of the cephalostat is a small wheel by means of which the vertical ear rods may be adjusted symmetrically further from, or nearer to, each other. The upper part of the cephalostat can be moved forward and backward so that the small horizontal ear plugs at the lower ends of the ear rods may be placed directly above, in front of, or behind the diameter of the object holder. The various adjustments of the ear plugs may be read from the scale on the cephalostat. At the upper part of the left ear rod is a scale which directly measures the distance of the tip of the ear plugs from the axis, this being necessary for correct positioning of the film. This scale is more clearly visible in the photograph of the upper part of the cephalostat shown in Fig. 10. The left ear rod moves horizontally in front of the scale, while the extreme edge of the rod functions as an indicator. The lower zero-line is used when the ear plugs are on the diameter. If,

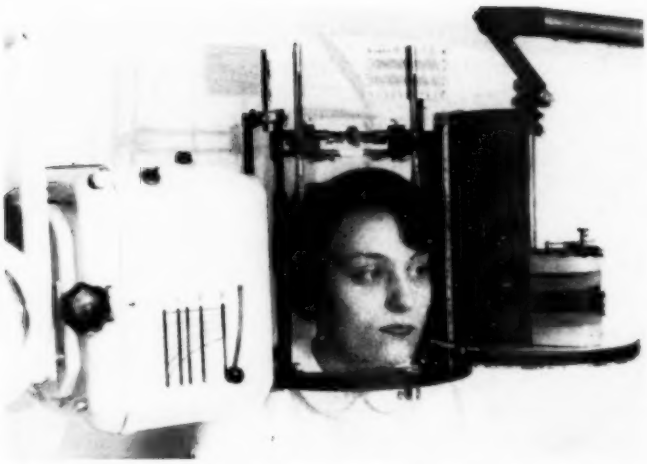

Fig. 9. Ear plugs at the lower ends of vertical rods are placed in the patient's external auditory meatuses for immobilization.

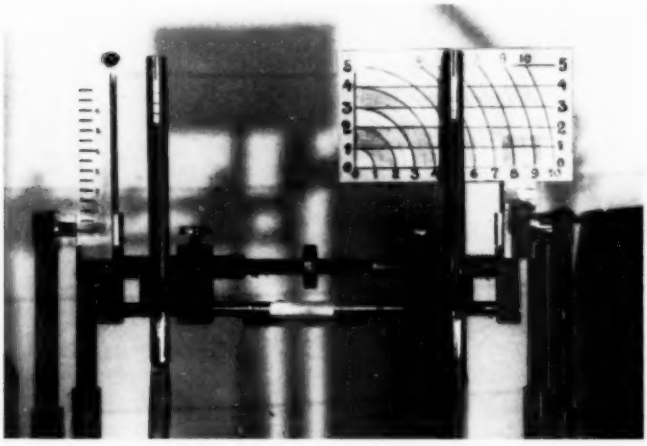

Fig. 10. The adjustment device with scales of the cephalostat.

again, the ear plugs are, say, 3 cm in front of or behind the diameter, the distance in question is discernible on the horizontal line marked with the number 3. In the present instance line 1 is being used and the position of the ear plugs is about 5.5 cm. The corresponding point of the film

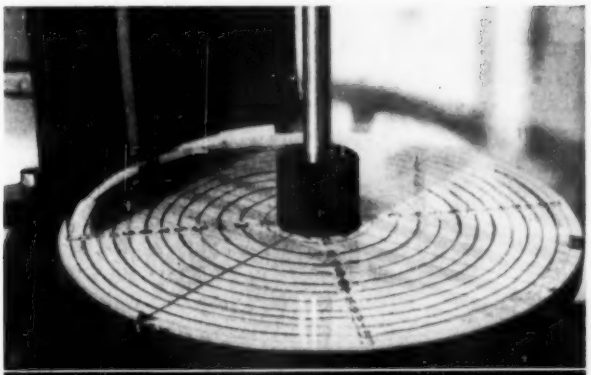

Fig. 11. The film holder with circular scale.

Fig. 12. A jaw film cassette bent on its support.

must be 5.5 cm + 1.5 cm = 7.0 cm distant from the axis of the film holder in accordance with diagram 3.

In Figures 9, 10 and 11, the stationary curved lead shield, mentioned earlier, is visible; it is provided with a vertical slit designed to prevent the access of secondary radiation to the film rotating on the film-holder.

Figure 11 is a near-view of the film-holder with its circles permitting the correct positioning of the film. The radii of the circles are shown in centimeters and they make provision for the divergence adjustment in question, thus obviating recurring additions. Besides the circles, the upper surface of the film holder is marked with lines which correspond to the sagittal position of the ear plugs of the object holder.

Figure 12 represents the film cassette and its bending and attachment with rubber bands to the cassette support. It has been previously mentioned that the cassettes are made of non-transparent stiff paper or black plastic cloth. Inside are two intensifying screens, and the general construction is such as to allow easy bending. One of the cassette's long

sides is open and may be rendered light-proof with a cover of the same shape, extending to half the height of the cassette.

The cassette support is made of two pieces of wood, one a replica in reverse of the other, shaped to resemble the halves of the jaw. They are joined in front by means of a hinge. The surface of the support is coated with lead and at its upper part there is a locking arrangement which keeps the whole in the shape into which it is bent. There are larger cassettes and supports for pantomography of the skull. A suitable lead sheet thick enough to maintain its shape may be employed in place of the cassette support. If a pantomogram is desired of a small area only, small film sizes may be used. For one half of the skull a 24 × 30 cm film suffices, while a view of a jaw may be recorded on a 12 × 30 cm.

I have tentatively experimented with pantomography of the thorax and the results are encouraging.

I avail myself of this opportunity of thanking the Cultural Fund of Finland (Suomen Kulttuurirahasto), Helsinki, and the Sigrid Jusélius Foundation (Sigrid Jusélius Stiftelse), Helsinki, for the considerable grants which have made this investigation, as well as the purchase of the equipment, possible.

Professor Eero Tammisalo, Director of the Institute of Dentistry, among others, is also thanked for his assistance and many kindnesses.

Addendum

With this article in press I find that K. Heckmann, in Die Röntgenperspektive und ihre Umwandlung durch eine neue Aufnahmetechnik [Fschr. Röntgenstr. 60 (1939), 144], presented, *inter alia*, an idea similar to one which formed one of my starting-points.

SUMMARY

A new roentgenographic method, pantomography, enabling the recording on flat film of the curved outer and inner thin layers of an object, is described.

The pantomograph consists of a motor-driven chair and rotating film-holder. With the object and film revolving at identical angular velocities a pantomogram of a curved thin layer of the object is obtained. It is necessary only to bend the film into the shape of the layer to be radiographed, for a representation of the layer in question to be registered.

The theory and practical application of the apparatus which has been developed by the author are discussed in detail.

ZUSAMMENFASSUNG

Eine neue röntgenographische Methode, die Pantomographie, wird beschrieben. Sie ermöglicht die Wiedergabe gekrümmter äusserer und innerer dünner Schichten eines Objektes in einer Filmebene.

Der Pantomograph besteht aus einem elektromotorisch bewegten Stuhl und einem rotierenden Filmträger. Rotieren Objekt und Film mit identischen Winkelgeschvindigkeiten, so erhält man ein Pantomogramm einer gekrümmten dünnen Schicht des Objek-

tes. Der Film muss nur der zu untersuchenden Schicht angeformt werden, damit eine Darstellung der in Frage stehenden Schicht registriert werden kann.

Die Theorie und die praktische Anwendung des vom Verf. entwickelten Apparates werden eingehend besprochen.

RÉSUMÉ

L'auteur décrit une nouvelle méthode radiographique, la pantomographie, qui permet de radiographier sur un film plat de minces couches courbes externes et internes d'un objet.

Le pantomographe consiste en une chaise mue par un moteur et un porte-film tournant. Quand l'objet et le film tournent avec la même vitesse angulaire, on obtient une pantomographie d'une mince couche courbe de l'objet. Il suffit de donner au film la courbure de la couche à radiographier pour obtenir une représentation de cette couche.

La théorie et l'application pratique de l'appareil qui a été réalisé par l'auteur sont étudiées en détail.

REFERENCES

1. Gebauer, A. and Wachsmann, F.: Geometrische Betrachtungen und technische Fragen zur Herstellung transversaler (horizontaler) Körperschichtaufnahmen. Röntgenblätter 2 (1949), 215.
2. Jerman, C.: Modern X-Ray Technic. Bruce Publishing Company, Saint Paul, Minneapolis 1928.
3. Kieffer, J.: The laminagraph and its variations. Am. J. Roentgenol. 39 (1938), 497.
4. Olsson, O.: Eine neue Methode zur isolierten Oberflächenradiographie. Acta radiol. 23 (1942), 420.
5. Paatero, Y. V.: A new tomographical method for radiographing curved outer surfaces. Acta radiol. 32 (1949), 177.
6. — Viivafokuksen käyttö pantomografiassa. Suom. hammaslääk. toim. 48 (1952), 11.
7. — Pantomographische Röntgenphotographie. Fschr. Kieferorthopädie 13 (1952), 115.
8. — La radiopantomographie. Rev. stomat. (Fr.) 53 (1952), 691.
9. — Radiography of the temporo-mandibular joint. A new method. Ann. Chir. et gynaec. fenn. (Fld). 42 (1953), 259.

Pantomography has also been treated in Finnish in Suom. hammaslääk. toim., Vol. 48 (1952) and 49 (1953).

FROM THE ROENTGEN DIAGNOSTIC DEPARTMENT (DIRECTOR: PROFESSOR K. LINDBLOM), KAROLINSKA SJUKHUSET, STOCKHOLM, SWEDEN

EXPERIENCES WITH TELEPAQUE, A NEW CHOLECYSTOGRAPHIC MEDIUM

by

Lars Renck

Many attempts have been made during recent years by investigators to obtain a new cholecystographic medium with better properties than the original tetraiodo-phenolphtalein (4). The introduction of contrast media of the di-iodine-phenylic-propionic acid type (Bilitrast, Priodax) in 1941 constituted a definite improvement, mostly by decreasing side-effects; further, the instructions given to the patient were simplified. The new media, however, could not be used entirely without side-reactions, and it was often necessary to repeat the dose to obtain adequate filling even in patients with functioning gall-bladders.

In 1944 a preparation of another type, called Monophen, was introduced. This, a di-iodated derivative of cyclohexanecarboxylic acid with approximately the same iodine content as the earlier media, was prescribed in doses of 3—4 g contained in rather large capsules and gave about the same frequency of filling and similar side-effects as Priodax.

In 1949, LEWIS and ARCHER synthetized the medium Telepaque with an iodine content of 66.7 per cent by weight as compared with 52 per cent in the former media. The preparation is chemically composed of 3-(3-amino-2,4,6-tri-iodophenyl)-2-ethyle-propanic acid and thus contains three iodine atoms instead of two. The toxicity has been determined in animal experiments to be one third that of Priodax, and the L. D. 50 for mice is reported to be as high as 12 000 mg. The excretion of the medium does not take place by the renal route but through the intestines.

Telepaque is prescribed in a dose of 3 g and is distributed in the form of tablets containing 0.5 g. The preparation is slightly photo-sensitive

Submitted for publication, Sept. 5, 1953.

and is packed in light-proof plastic containers. It is quickly absorbed from the intestine and within four to six hours the filling of the gall-bladder is said to be satisfactory for diagnostic purposes.

Fig. 1. Telepaque filling; calculi present.

Own investigation: The purpose of the investigation was to compare the usefulness of Telepaque with Bilitrast and a series of 130 unselected patients, sixty-six of whom were given Bilitrast and 64 Telepaque, were examined. Both preparations were given on the evening before the examination together with a fat-free meal, after which the patients were not allowed to take anything more by mouth before the examination. Telepaque was administered in a dose of 3 g and Bilitrast in a dose of 6 g. The next morning a survey film was obtained, and if the filling of the gall-bladder was unsatisfactory the dose was repeated and the patient re-examined twenty-four hours later. If the filling was saticfactory, the examination was completed.

Table 1

Roentgen diagnoses of the two series (per cent)

	Normal findings	Cholelithiasis	No definite diagnosis
Telepaque	49	42	9
Bilitrast	53	38	9

The two series turned out to be composed of cases comparable from the roentgen diagnostic point of view (Table 1). As far as sex and age was concerned, however, the group given Telepaque showed a slight preponderance of females and younger age-groups (Table 2). The number of in-patients and out-patients was about equal in both series.

The frequency of side-reactions was also studied in both series. The patients were asked about the two most common and easily recognized symptoms: vomiting and diarrhoea (Table 3). The patients in the Telepaque series were also questioned about the occurrence of nausea, which occurred in eleven per cent of the cases.

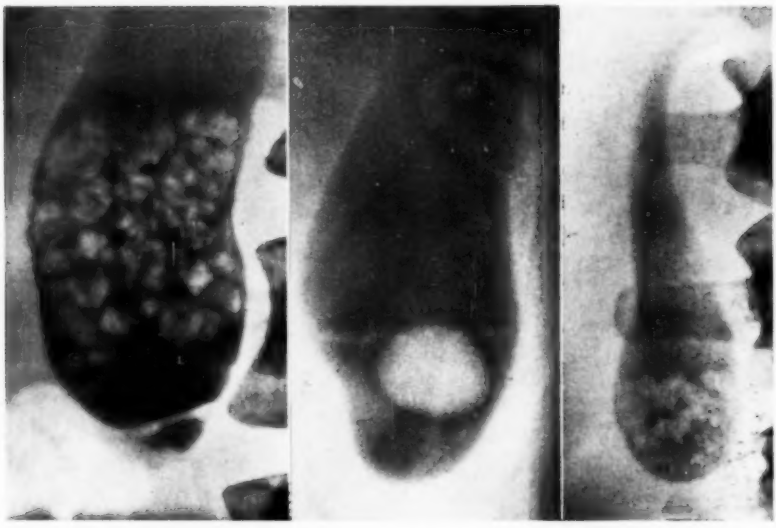

a. b. c.

Fig. 2. a. Filling of gall-bladder containing a great number of small stones, the larger of which lie at the fundus. b. One large stone and a group of smaller stones lying at a level in the contrast medium. c. Gall-bladder filled, before fatty meal. (All films erect.)

Table 2

Age and sex distribution of the series (number of cases)

	♂	♀	21—30	31—40	41—50	51—60	61—70	71—80
Telepaque .	15	49	15	19	13	9	6	2
Bilitrast ..	23	43	13	15	14	16	6	2

Table 3

Frequency of side-reactions (per cent)

	Vomiting	Diarrhoea
Telepaque	3	23
Bilitrast	6	30

Side-reactions have been reported to occur less often with Telepaque than with Bilitrast (1, 2, 3, 5). Telepaque has, on the other hand, been given with a fat-free meal, as is usual with Bilitrast, and it has been

reported that its side-effects may be further decreased by administering it with an ordinary meal or even with a meal with a high fat content (4).

The evaluation of the contrast filling of the gall-bladders was made by one examiner not informed in advance as to which contrast medium had been used in any particular case. The filling was classified into four different groups: excellent filling with high contrast; ordinary filling; unsatisfactory filling, in which some filling had definitely occurred but the low concentration rendered diagnostic assessment difficult; and finally, no distinguishable filling. The results are shown in Table 4.

Fig. 3. Emptying appearances most commonly encountered.

The difference between the frequency of filled and non-filled gall-bladders in both series was not statistically significant. The contrast filling of the functioning gall-bladders, however, was much more intense with Telepaque. The relative number of excellent fillings with Telepaque was more than twice as common as with Bilitrast but the frequency of

Table 4

Filling of the gall-bladder in the two series (per cent)

	Excellent	Ordinary	Unsatisfactory	No filling
Telepaque	74	11	8	7
Bilitrast	35	42	9	14

unsaticfactory filling was almost the same. It has been pointed out in reports from other countries that the increased density may involve risk of radio-opaque concretions being hidden by the contrast medium. This danger may partly be avoided by using a higher kilovoltage or by repeating the examination with a smaller dose. One of the advantages of the high degree of contrast concentration is that even in the erect position almost the whole of the gall-bladder is filled and the settling of the contrast medium to the fundus is less pronounced.

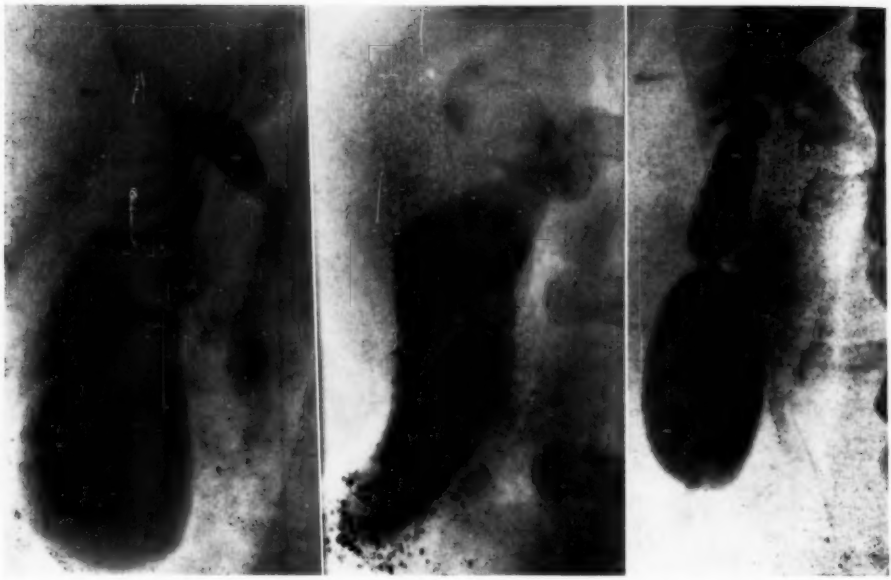

a. b. c.

Fig. 4. a—b. Filling of all the biliary ducts including some of the hepatic branches. c. Stone partly occluding cystic duct: no stones in the gall-bladder. (All films supine.)

In all the cases belonging to the Telepaque series, films following a fatty meal were also obtained in order to study the contraction of the gall-bladder and the filling of the biliary ducts. These films were taken fifteen to thirty minutes after the meal as a routine measure and no other attempt to obtain improved filling was made. Filling of the ducts was established in the greater number of cases. In a shorter series consisting of fourteen cases of the Bilitrast material the same procedure was carried out. The results are shown in Table 5 in which the number of positive

Table 5

Frequencies of filling of the biliary ducts (per cent unless otherwise stated)

	Cystic duct		Bile duct		Hepatic duct (all parts)	
	Good	Poor	Good	Poor	Good	Poor
Telepaque	56	13	25	14	2	6
Bilitrast	9	10	1 case	2 cases	None	None

fillings of the cystic duct in the Bilitrast material is representative of all the material and not only of those cases which were given a fatty meal; good filling of 'this duct' is often obtained even without any emptying procedure.

The relatively high frequency of filling of the ducts with Telepaque is quite obvious. No case of duct concretion has, however, been demonstrated, but a few cases of stones in the first part of the cystic duct have been encountered.

It has recently been discovered that the filling of the ducts may be further improved if films are obtained with the patient in the supine position, having been kept in this position for a few minutes preceding the exposure to allow the heavier and denser fraction of the contrast medium to enter the ducts.

A repetition of the dose in accordance with the above-mentioned requirements was considered necessary in forty-four per cent of the Bilitrast cases but only in twenty per cent of the Telepaque series. Contrary to what has been stated earlier, the filling was often considerably increased after a second dose of Telepaque.

Unabsorbed residues of the contrast medium, mostly lying in the colon, were evident in fifty-three per cent of the Telepaque cases, but the Bilitrast series also showed as high a percentage as thirty-nine. It has been pointed out that this fact may be a sign that the dose of the contrast medium has been too large (2). In the Bilitrast series a routine dose of 6 g was given. This is twice the dosage most commonly used and explains the exceptionally high incidence of unabsorbed medium. As regards Telepaque, many authors (1, 2) have also reported a high frequency of residues in the alimentary tract. These remnants are easily dealt with in most cases and seldom disturb the evaluation. The filling frequencies of Telepaque have also proved to be the same both in cases with and without unabsorbed residues. Smaller doses of 2 g have been given in a few cases not belonging to the material to patients of light weight, and excellent filling has been achieved.

The introduction of Telepaque has thus proved to constitute valuable progress in cholecystography. One clear advantage is the improved filling of the gall-bladder. Moreover, the possibility of studying the biliary ducts in a relatively high number of cases is of importance both from clinical and anatomic points of view especially when an operative procedure is indicated.

SUMMARY

A comparison between the gall-bladder contrast media, Bilitrast and Telepaque, carried out in a series of 130 unselected cases, is presented. Telepaque proved to give better filling of the gall-bladder but the side-effects were about the same for both media

in the material. The emptying of the gall-bladder after a fatty meal was also studied and Telepaque produced filling of the ducts in a considerably higher frequency of cases than the earlier medium.

ZUSAMMENFASSUNG

Die beiden Gallenblasenkontrastmittel Bilitrast und Telepaque wurden in einer Serie von 130 nicht besonders ausgewählten Fällen miteinander verglichen. Es zeigte sich, dass Telepaque eine bessere Füllung der Gallenblase ergab. Die Nebenwirkungen waren jedoch im Material für beide Kontrastmittel ungefähr gleich. Die Entleerung der Gallenblase nach einer Fettmahlzeit wurde ebenfalls studiert; nach Telepaque füllten sich die Gallenwege bedeutend häufiger als nach dem erstgenannten Kontrastmittel.

RÉSUMÉ

L'auteur présente une étude comparative entre les produits de contraste cholécystographiques Bilitrast et Telepaque établie sur une série de 130 cas pris au hasard. Le Telepaque a donné un meilleur remplissage de la vésicule biliaire mais les effets secondaires ont été à peu près les mêmes pour les deux produits dans les cas étudiés.

L'évacuation de la vésicule après un repas gras a aussi été étudiée; le Telepaque a rempli beaucoup plus souvent les voies biliaires que le Bilitrast.

REFERENCES

1. Christenssen, W. & Sosman, M.: A Preliminary Report on Telepaque, a New Cholecystographic Medium. Am. J. Roentgenol. 66 (1951), 764.
2. Dunne, E., Jenssen, E. & Hughes, R.: Telepaque. A New Medium for Cholecystography. Radiology 60 (1953), 210.
3. Morgan, R. & Stewart, H.: Clinical Experience with Telepaque, a New Gallbladder Compound. Radiology 58 (1952), 231.
4. Scott, W. & Simril, W.: Newer Radioopaque Media for Oral Cholecystography. Am. J. Roentgenol 69 (1953), 78.
5. Shehadi, W. H.: Telepaque. Am. J. Roentgenol. 68 (1952), 360.
6. — Personal communication, July 1953.
7. Whitehouse, W. & Martin, O.: A Comparative Clinical Study of Priodax and Telepaque, Including 1000 Examinations. Radiology 60 (1953), 215.

FROM THE ST. CANISIUS-ZIEKENHUIS, NIJMEGEN, THE NETHERLANDS

CLINICAL INVESTIGATIONS ON THE USE OF RADIOACTIVE GALLIUM (Ga^{66} AND Ga^{67}) IN BONE DISEASES

by

J. Th. van der Werff

Since 1949 intensive studies have been made on the use of radioactive gallium in cases of pathologic conditions in bone, mainly by H. C. DUDLEY and his co-workers at the laboratories of the U. S. Naval Medical Research Institute and the National Naval Medical Center, Bethesda, Maryland. Attention was drawn to these new isotopes during the study of the properties of the rare element itself. Having made a great number of investigations on the distribution and excretion of gallium when injected in the form of gallium lactate or gallium citrate and on the toxic levels with different animals, DUDLEY and co-workers found that intravenously injected tracer-dosages of Ga^{72} were selectively concentrated in primary and secondary malignant bone tumours in such quantities that even early metastases could be detected with the Geiger-Müller counter before these could be identified by roentgen films. One of Dudley's co-operators, F. R. LANG summarized the main properties in 1951, as follows:

1. In the form of its lactate salt it is very quickly absorbed following intramuscular injection.

2. It is rapidly transported to and deposited in the bony structures of the body.

3. It is excreted extremely slowly.

4. While retained in the body of the animal for a long period of time, it is relatively inert and non-toxic at the dosage levels required for radioisotope tracer studies and also at the dosage estimated to provide sufficient radioactivity for attempting eradication or control of bone malignancies.

Paper read at the Seventh International Congress of Radiology, Copenhagen, 1953.
Submitted for publication, September 24, 1953.

5. It produced no demonstrable pathologic effects on the brain, liver, kidneys or, in fact, any other organ or system of the bodies of laboratory animals.

In the same article, LANG published his experiences in twelve cases, six with carcinoma of the prostate, two with carcinoma of the breast, one with bronchogenic carcinoma, one with gastric carcinoma, one with osteogenic sarcoma and one with osteochondrosarcoma, all these patients having bone mestastases.

In all cases tracer-studies were carried out by injecting 350 to 400 microcuries of the isotope Ga^{72} intravenously. By using Geiger-Müller counters, it was found that eighty per cent of the gallium^{72} became localized within two hours after its intravenous injection in human subjects. In normal bone the localization reached a maximum in one hour. In malignant conditions of bone the maximum localization in the pathologic bone areas was attained within ten hours. Moreover, the remarkable fact was noted that the concentration of the isotope in the malignant bone lesions was twenty-fold higher than in normal bone. This made it possible to detect metastases in areas before these produced clinical symptoms or were revealed roentgenographically. It also appeared that it might be possible to destroy bone tumours by administrating high therapeutic doses. In two cases this was attempted by giving 1,300 mC of Ga^{72}. It is clear that if these findings were confirmed, radioactive gallium must be an essential new and important therapeutic measure against the malignant bone diseases.

It was for this purpose that I made tracer studies in a group of fifteen patients all suffering from bone diseases. However, instead of using the isotope Ga^{72}, which was generally employed by the American authors, I made use of the isotopes Ga^{66} and Ga^{67}. These have several advantages. The isotope Ga^{72} is obtained in the uranium reactor from gallium in the form of Ga_2O_3. The maximum activity is 125 mC per gram. Thus, if one wants to apply a therapeutic dosage of 1,300 mC, this means that one has to start from a quantity of 10 grams of Ga_2O_3. As gallium is a very precious substance, the cost of the application would be so high that its clinical use would be prohibitive.

Moreover, gallium is a very toxic material which again limits its dosage by reason of the great amount of non-active carrier required. Another disadvantage of Ga^{72} is its relatively short half-life of 14.3 hours, which causes considerable loss during transport and during the time which elapses from it leaving the reactor and its injection into the patient. On the other hand Ga^{72} emits very hard gamma-radiation of 2.53 MeV and beta-radiation of 2.50 MeV which makes its detection by G. M. counters very easy. Now, it is well known that a number of other isotopes

of gallium exist and it was proved by HALBERSTADT, working with the Philips synchro-cyclotron at Amsterdam that it was possible to obtain great amounts of the isotopes Ga^{66} and Ga^{67} by a transmutation reaction in the cyclotron.

If zinc, which is relatively cheap, is bombarded by deutons, about six isotopes of gallium arise, most of which possess very short half-lives of less than one hour. Two of them, however, have reasonable half-lives viz. Ga^{66} of 9.5 hours and Ga^{67} of 78 hours. Ga^{66} emits very hard beta rays of up to 4.15 MeV (64 per cent), k radiation of 8.7 MeV (36 per cent) and gamma radiation of up to 4.8 MeV Ga^{67} emits k radiation (100 per cent) followed by relatively soft gamma-rays of up to 388 keV.

The production of these isotopes is very high. By means of the Philips cyclotron, 40—50 mC of Ga^{66} per hour and 6—7 mC of Ga^{67} could be obtained per hour. The chemical isolation of the mixture of both isotopes is simple and may be carried out in a few hours.

As these preparations can be obtained carrier-free, it is clear that they are non-toxic and may be employed in any amount, apart, of course, from the toxic effect of the radiation emitted. By reason of these useful properties we used the mixture of the two isotopes in an attempt to confirm the findings of the American authors as to the concentration of gallium in malignant bone. We injected gallium citrate intravenously in fifteen patients and compared the concentration in the primary foci or in the metastases with symmetrical sites in the normal bone.

Let it be said at once that we could not agree that the differences in concentration were so high as reported by the American authors. In some cases there was no difference at all, in others up to 100 per cent difference and only in one case was there a three-fold increase in the affected area. Biopsy, performed later, revealed a chronic osteomyelitis. The following forms a review of all fifteen cases:

	R.	L.
1. recurrence of osteogenic sarcoma in left humerus	1,500 k/m.	1,750 k/m.
2. recurrence of osteogenic sarcoma in right femur	800 k/m.	500 k/m.
3. osteogenic sarcoma in right femur	1,750 k/m.	1,100 k/m.
4. metastasis in left os pubis	1,000 k/m.	950 k/m.
5. chronic osteomyelitis in left femur	3,400 k/m.	1,200 k/m.
6. metastasis in right femur	1,250 k/m.	1,200 k/m.
7. metastasis of hypernephroma in right femur	900 k/m.	900 k/m.
8. chondrosarcoma in left 4th rib	1,600 k/m.	1,600 k/m.
9. metastasis of carcinoma of the prostata in left ileum ..	1,110 k/m.	1,250 k/m.
10. osteomyelitis of right acetabulum	615 k/m.	420 k/m.
11. healing fracture of left ulna	880 k/m.	990 k/m.

			R.		L.
12. healing fracture of right tibia			740 k/m.		720 k/m.
13. treated Ewing-sarcoma of right femur			800 k/m.		600 k/m.
14. metastasis of carcinoma mammae in cervical spine	C 1	C 3	C 5	C 7	
	345	330	440	440 k/m.	
	Th 1	Th 6	Th 10	L 1	L 5
15. metastasis of carcinoma mammae in Th 6	540	900	750	750	720 k/m.

The measurements at the pathologic sites are underlined.

As may be seen, there are differences in the concentration of gallium in the bone lesions, but never to such an extent as to justify treatment by the giving of a very heavy dosage.

Attempts were naturally made to find out whether the discrepancy was due to some difference in the technics used. The measurements were made by means of a count-rate meter with an accuracy of one per cent. The head of the heavily shielded G.M. tube had a diameter of 3 cm. If the pathologic area was very small, we not only measured the radiation from that area, but also from the neighbouring normal bone, which, of course, might partly hide the excess of the radiation from the pathologic bone. (But some of the lesions examined were quite large and no significant difference was noted.)

The influence of the carrier was then considered. One presumes that the excess of gallium in the tumour only occurs if sufficient carrier is added to the radioactive gallium. A measurement with a tracer dosage of 0.75 mC carrier-free gallium was therefore made, and after a few days a new tracer dosage with a surplus of 5 mg non-active gallium citrate added. Again this made no difference.

The conclusions of the investigations are perhaps a little disappointing. It is only to be hoped that some error has been made and that gallium isotopes may be accepted as being of value in the therapy of bone lesions.

SUMMARY

The author attempted to confirm the findings of American authors (DUDLEY and co-workers) that radioactive gallium selectively concentrates in bone tumours to such a degree that its therapeutic exhibition would be warranted. Employing Ga^{66} and Ga^{67} instead of the Ga^{72} used by these authors, some differences between the concentrations in pathologic and normal bone were noted, but not to the extent as reported. The value of the general use of radioactive gallium as a therapeutic agent for bone tumours must be considered doubtful.

ZUSAMMENFASSUNG

Der Verf. versuchte die Befunde amerikanischer Autoren (DUDLEY u. Mitarb.) zu bestätigen, nämlich dass radioaktives Gallium selektiv in solchem Ausmasse in Knochentumoren konzentriert wird, dass seine therapeutische Anwendung gesichert sein würde. Bei der Anwendung von Ga^{66} und Ga^{67} an Stelle von Ga^{72}, welches obengenannte Verfassern benutzten, wurden einige Konzentrationsunterschiede in pathologischen und gesunden Knochen beobachtet, jedoch nicht so grosse wie in den mitgeteilten Befunden. Der Wert einer allgemeinen Anwendung radioaktiven Galliums als Heilmittel für Knochentumoren muss als zweifelhaft angesehen werden.

RÉSUMÉ

L'auteur s'est efforcé de confirmer les résultats d'auteurs américains (DUDLEY et coll.) d'après lesquels le gallium radioactif se concentre électivement dans les tumeurs osseuses à un degré qui justifierait son emploi thérapeutique. Employant le Ga^{66} et le Ga^{67} au lieu du Ga^{72} utilisé par ces auteurs, il a observé certaines différences entre les concentrations dans l'os pathologique et dans l'os normal, mais pas dans la même mesure que ces auteurs. L'intérêt de l'emploi général du gallium radioactif comme agent thérapeutique des tumeurs osseuses doit être considéré comme douteux.

REFERENCES

BRUCER, M.: Distribution of Gallium in man; autopsy evidence. Nucl. Sc. Abstr. 5 (1951), 2105.

DUDLEY, H. C.: The biological significance of Ga^{72}. Nucl. Sc. Abstr. 3 (1949), 1177.

DUDLEY, H. C. and MADDOX, G. E.: Deposition of Ga^{72} in skeletal tissue. J. Pharmacol. & Exper. Therap. 96 (1949), 224.

DUDLEY, H. C., IMERIE, G. W. and ISLOCK, J. T.: Deposition of Ga^{72} in proliferating tissue. Radiology 55 (1950), 571.

LANG, F. R.: A study of the use of Radioactive Gallium in Medicine. Ann. Int. Med. 35 (1951), 1237.

MULRY, W. C. and DUDLEY, H. C.: Studies of radio gallium as a diagnostic agent in bone tumors. J. Lab. & Clin. Med. 37 (1951), 239.

FROM THE INSTITUTE OF RADIOPHYSICS OF THE KING GUSTAF V JUBILEE CLINIC
(DIRECTOR: PROF. ROLF M. SIEVERT), STOCKHOLM, SWEDEN

DOSE MEASUREMENTS ON SECONDARY ROENTGEN RADIATION

by

Rune Walstam

Measurements on the secondary roentgen radiation dose have been published to a very small extent. In 1947 LORENTZON (3) investigated the dose-rate from certain materials of practical importance and estimated the quality of the secondary radiation from the point of view of radiation protection. This investigation clearly showed the importance of the fluorescence rays, as earlier pointed out by CHRISTEN (1).

In order to complete the survey of secondary radiation data given by LINDELL (2), I have used about the same arrangement as LORENTZON and measured the secondary dose-rate from some elements with particularly regard to the softest radiation components. The arrangement is shown in Diagr. 1.

A cardboard ionization chamber with graphite-covered walls about 0.15 mm thick was used. (The air between the radiator and the chamber brought in an additional absorption, equivalent to about 0.4 mm of card-

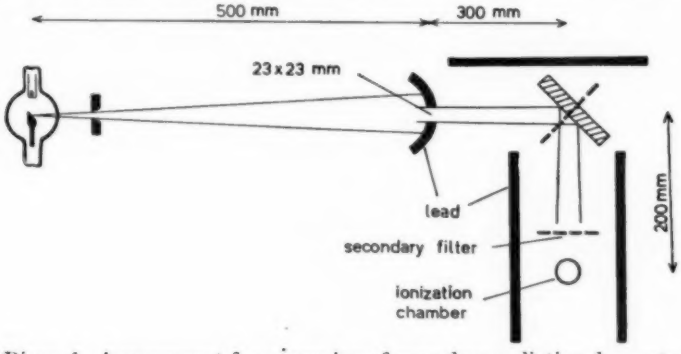

Diagr. 1. Arrangement for measuring of secondary radiation dose-rate.

Submitted for publication, June 12, 1953.

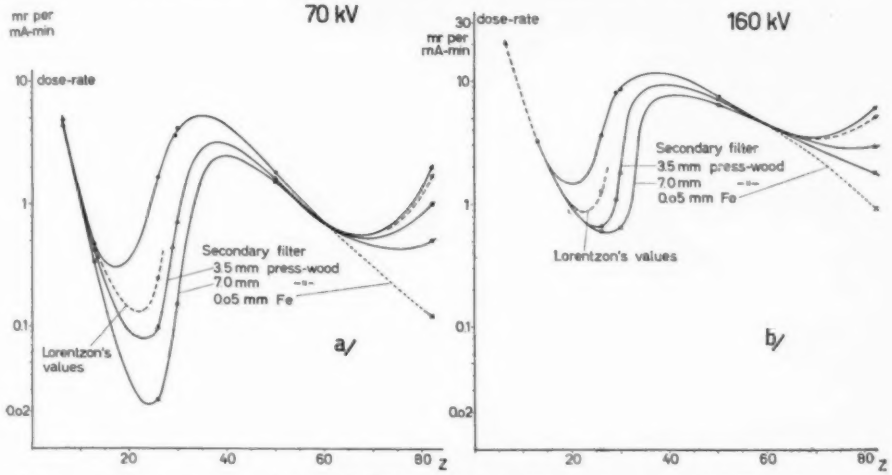

Diagr. 2. Dose-rate per mA at a) 70 kV and b) 160 kV constant potential. The dose-rate is related to the field area and distances used in this investigation and should only be used for comparison of different absorbers as to their secondary radiation efficiency.

board.) Measurements of the wave-length dependence had shown that there was no disturbing influence of heavy elements. The wave-length dependence of an ionization chamber is due partly to the effect of deficient air-equivalence of the walls and partly to wall absorption, and a correction factor is usually required for radiation quality. However the chamber constant for radium γ-rays was used for all qualities. This constant gave the best measure of the ionization inside the chamber and it would have been meaningless to make a correction for wall absorption for example, especially as the radiation to be measured was composed of very different qualities and the absorption of the softest radiations was one of the phenomena to be studied.

The results of the dose-measurements are shown in Diagr. 2. The dose-rate for light elements caused by Compton scattered radiation, decreases with increasing atomic number, until the fluorescence radiation from heavier elements brings about an increase.

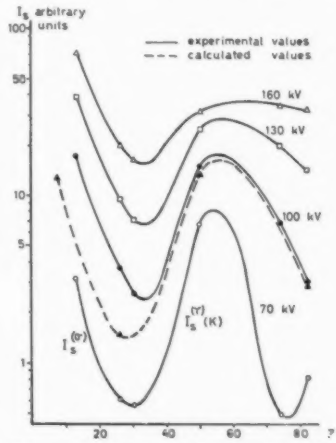

Diagr. 3. The total secondary intensity as a function of atomic number (LINDELL).

The high dose efficiency of the softest K rays has made the dose-rate minimum move towards low atomic numbers in comparison with the intensity minimum from Lindell's intensity curves.

A secondary filter of 3.5 mm of press-wood, however, reduces the K radiation dose-rate from Fe to an absolute minimum. It is apparent how the soft K radiation from Fe, Cu and Zn will affect the measurements, but in practice it will give a low integral dose in large objects. The relatively hard K radiation from Sn is only slightly dependent on light secondary filtering. The L radiation from Pb gives the same effect as soft K radiation.

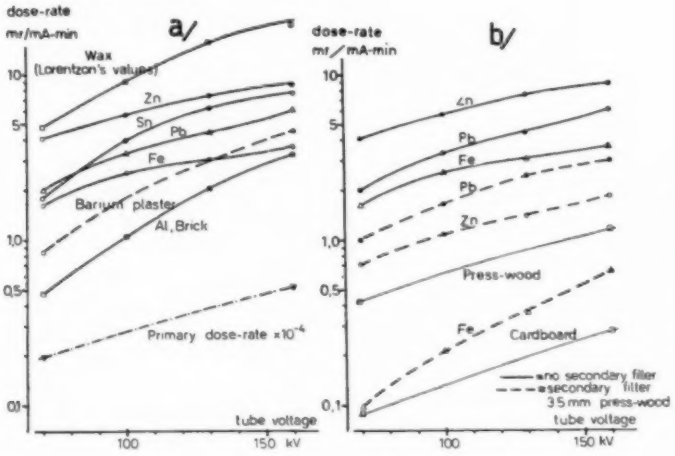

Diagr. 4. The secondary dose-rate at constant tube-current as a function of voltage for some elements and wall-materials. a) Without secondary filter. b) Dependence of secondary filtering.

As an example of practical measurements, LORENTZON's values are also shown. The results to be expected, if a chamber with an arbitrary wall-thickness is used, may easily be estimated from the curves. The air between the chamber and the secondary radiation source will often be equivalent to a few mm of cardboard.

The curves also show the depth dose distribution obtainable in the secondary radiation from any element.

In Diagr. 4 certain wall and protective materials are collected together with some other elements of interest. The secondary dose-rate is given as a function of tube voltage. As may be seen from Diagr. 5 the slope of the curves is steeper the greater the proportion between the mean dose-contributing quantum energy and the highest primary quantum energy. This fact is illustrated by the curve for Fe before and after secondary filtration, and the curve for Sn, the K energy of which decreases with increasing tube voltage in comparison with the peak energy corresponding to the tube voltage. As a rule the secondary radiation dose-rate from light

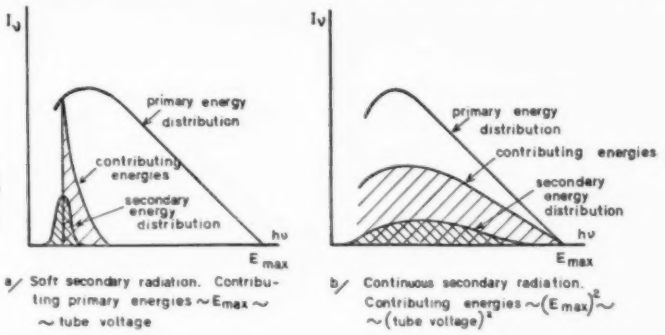
primary energy distribution
contributing energies
secondary energy distribution
hν
E max
a/ Soft secondary radiation. Contributing primary energies ~ E max ~ ~ tube voltage
primary energy distribution
contributing energies
secondary energy distribution
hν
E max
b/ Continuous secondary radiation. Contributing energies ~ (E max)² ~ ~ (tube voltage)²

Diagr. 5. The reason of varying slope of the dose-rate curves in Diagr. 4.

elements (with the scattered photons having almost the same energy as the primary) shows the greatest voltage dependence.

Most of this voltage dependence is caused by the increased primary radiation efficiency at higher voltages, as may be seen from the curve showing how the primary dose-rate increases with the tube voltage. However, even at the same primary dose-rate there is an increase with the voltage up to a maximum of secondary radiation intensity at some hundred kV, *e.g.* voltages used in ordinary deep therapy. At still higher voltages, the secondary intensities will decrease again. Another factor of importance is the varying angular distribution at different energies.

Diagr. 4 also shows the dose-rate from non-saturation layers of cardboard (1 mm = 0.058 g/cm²) andpress-wood (3.5 mm = 0.34 g/cm²) indicating the increase to be expected if some other material is covered with such layers.

Dose-rate measurements also were made on the transmitted secondary radiation. The dependence of absorber thickness is shown in Diagr. 6 for Sn.

As the secondary radiation here consists of monochromatic fluorescence rays, a single optimum thickness was obtained for both intensity and dose-rate.

From Fe higher dose-rates were obtained the thinner the absorber even down to around 0.1 mm, as the photons with the highest dose-efficiency were carried by the very soft K radiation.

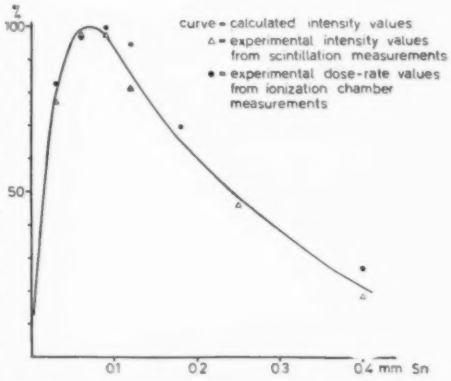

Diagr. 6. Transmitted secondary radiation from thin layers of Sn as a function of absorber thickness 100 kV, 1 Al. (Scintillation measurements according to LINDELL).

The dose measurements described here confirm the conclusions on the dose-rate from different elements made by LINDELL in a just published paper.

It can be seen that Fe is the element that should be used if the secondary radiation dose has to bekept low.

Light elements (water, tissue, wood) give high dose-rates and penetrating radiation and are from the protection point of view the most dangerous ones.

The K radiation from elements as Cu and Zn can easily be reduced by thin absorbers and will therefore give low integral doses.

Heavy elements give very penetrating K radiation and their L radiation may affect the dose-rate in the same way as soft K radiation from lighter elements.

SUMMARY

Dose measurements have been made at 70 and 160 kV constant potential on the secondary radiation from some materials of practical interest. The dose-rates have been measured with a thinwalled ionization chamber. It is shown that light elements give high dose-rates and penetrating radiation, heavy elements penetrating K radiation and soft L radiation. Iron has been found to give a practical minimum of dose-rate.

ZUSAMMENFASSUNG

Dosismessungen der von Materialien von praktischem Interesse ausgehenden Sekundärstrahlung sind bei 70 und 160 kV konstanter Spannung ausgeführt worden. Die Dosisleistungen sind mit einer dünnwandigen Jonisationskammer gemessen worden. Es wird gezeigt, dass leichte Elemente hohe Dosisleistungen und penetrierende Strahlung, schwere Elemente penetrierende K-Strahlung und weiche L-Strahlung geben. Man fand, dass Eisen ein praktisches Minimum der Dosisleistung gibt.

RÉSUMÉ

L'auteur a mesuré les doses de rayonnement secondaire émises sous des potentiels constants de 70 et 160 kV par des substances d'intérêt pratique. Les doses ont été mesurées avec une chambre d'ionisation à paroi mince. L'auteur montre que les éléments légers donnent des doses élevées et un rayonnement pénétrant, les éléments lourds un rayonnement K pénétrant et un rayonnement L mou. Le fer donne pratiquement une dose minimum.

REFERENCES

1. CHRISTEN, TH.: Sekundärstrahlen und Härtegrad. Fortschr. Röntgenstr. 25 (1917), 55.
2. LINDELL, B.: Secondary Roentgen Radiation. Acta radiol. 41 (1953), 353.
3. LORENTZON, L.: Secondary Roentgen Radiation from Wax, Al, Fe and Pb at Tube Voltages Between 40 and 170 kV. Acta radiol. 41 (1953), 201.

FROM THE INSTITUTE OF RADIOPHYSICS (DIRECTOR: PROFESSOR ROLF M. SIEVERT), KING GUSTAF V JUBILEE CLINIC, STOCKHOLM, SWEDEN

SECONDARY ROENTGEN RADIATION

by

Bo Lindell

Although secondary radiation in connection with roentgen rays was recognized by RÖNTGEN (37) himself and investigated by PUPIN (30) as early as 1896, there is still some confusion about this phenomenon among those actively concerned with this type of radiation. This paper does not contain anything previously not known but has been written to give a general survey of the subject, illustrated by the results of measurements recently carried out at the Institute of Radiophysics.

The two phenomena giving rise to secondary radiation are 'scattering' and 'fluorescence'. Scattered rays formerly seemed to be primary radiation with merely altered direction (BARKLA (2), THOMSON (41)) in contrast to fluorescence rays which had obviously a much greater wave-length than the primary rays (BARKLA (3)).

In consequence of this, scattering could not be connected with any true absorption of energy, as any change of the energy conveyed by the rays would cause a change in wave-length. The true absorbed energy, *i. e.* energy taken from the radiation and transferred into kinetic energy of electrons, was then identical with the loss of energy that was to be expected from the difference in wave-length between the primary and the fluorescence rays.

Thus the total 'absorption' coefficient (extinction coefficient) could be written:

$$\mu = \sigma + \tau \quad \ldots\ldots\ldots\ldots\ldots\ldots\ldots\ldots \quad (1)$$

where σ was the 'scattering coefficient' and τ the 'true absorption coefficient'.

Detailed study showed however that the scattered radiation had not exactly the same wavelength as the primary rays, the difference being explained by the energy given off to the scattering electrons (COMPTON 9, 10), DEBYE (12)). The scattering coefficient had to be divided into two

Submitted for publication. June 12, 1953.

parts, as it is now usually written. The old conception of the two phenomena 'scattering' and 'absorption' is nowadays replaced by knowledge of two others: the Compton effect and the photoelectric effect, each of which contributes to the secondary radiation as well as to the true absorption.

The Compton effect, seen as an elastic collision between a roentgen ray quantum and a single electron, has been treated theoretically fairly completely by KLEIN and NISHINA (23). σ now means the part of the radiation energy extinction which is caused by this effect and τ the remaining extinction caused by the photoelectric effect. The total absorption coefficient may still be written as above, but with a different meaning as it is no longer divided into terms accounting for absorbed and non-absorbed energy. However, this division is still easily performed. If σ_a and τ_a account for the energy transformed into kinetic energy of Compton and photo electrons respectively while σ_s and τ_s account for the energy radiated from the point of absorption, the total absorption coefficient is

$$\mu = (\sigma_s + \tau_s) + (\sigma_a + \tau_a) = \mu_s + \mu_a \ldots\ldots\ldots\ldots \quad (2)$$

The generation of secondary rays will then depend upon the values of σ_s and τ_s. Although these coefficients are theoretically well known, the interaction between the different extinction phenomena will be rather complicated in the actual absorber. There will be multiple scattering (RAJEWSKY (34)) and extinction of scattered and fluorescence radiation, and this complexity has deterred many from trying to estimate theoretically the quality and quantity of secondary radiation for any given material.

Let us assume that with a certain voltage and filtering condition of a roentgen tube, *i. e.* at a known energy distribution of the primary rays, we want to know how the secondary radiation depends on the absorber. Is there any simple law or thumb-rule to be found? In the following section we will see how to derive this dependence under very simplified assumptions.

Basic Theoretical Estimation of Quantity and Quality of Secondary Roentgen Radiation

The following assumptions will be made:

1. The distance between the absorber and radiation source (and between the absorber and measuring device) is great enough to make the angles φ and ψ independent of x.

2. The primary radiation intensity (energy per unit area and time) I_0 at the surface of the absorber is known, together with its energy distribution $I_{\nu}(\nu) = dI_0/d(h\nu)$.

3. At the depth x, I_ν will be reduced to $I_\nu \cdot e^{-\mu(h\nu)\frac{x}{\cos\varphi}}$. The secondary radiation intensity that should be added to this value will be neglected, which means that all multiple secondary radiation is neglected. Thus $\mu(h\nu)$ in the expression above will be identical with the total extinction coefficient at the photon energy $h\nu$.

Assume a volume element at the depth x of $A \cdot dx$, A being the field area. The secondary radiation (scattered and fluorescence rays) from this element is

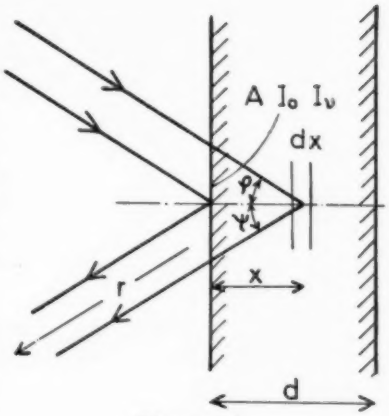

Diagram 1.

$$d^2P_s(x, \nu) = AI_\nu\mu_s(\nu)e^{-\mu(\nu)\cdot\frac{x}{\cos\varphi}}dx\,d\nu \quad \ldots\ldots\ldots\ldots \quad (3)$$

where $\mu_s(\nu)$ is the part of the total extinction coefficient that accounts for re-radiated energy.

With no especially preferred direction of radiation, the intensity of the secondary radiation at the distance r from the secondary source (the absorption of the secondary rays not yet considered) would be

$$d^2I_s(x, \nu) = \frac{1}{4\pi r^2} \cdot d^2P_s(x, \nu) \quad \ldots\ldots\ldots\ldots \quad (4)$$

This is valid for the fluorescence radiation but not for the Compton rays, the angular distribution of which has to be calculated according to the formula of Klein and Nishina.

If we begin with the approximation that the Compton rays are scattered as the classical formula predicts, we have to add a correction factor $F(\nu, \varphi, \psi)$ to make the formula agree with the Klein-Nishina theory. The intensity of the radiation scattered from one single electron is then

$$I_e = I_{prim} \cdot \frac{e^4}{(m_0c^2)^2} \cdot \frac{1}{r^2} \cdot \frac{1 + \cos^2(\varphi + \psi)}{2} \cdot F(\nu, \varphi, \psi) \ldots\ldots \quad (5)$$

where (cf. Fig. 2 a)

$$F(\nu, \varphi, \psi) = \{1 + a[1 + \cos(\varphi + \psi)]\}^{-3} \cdot \left\{1 + \frac{a^2(1 + \cos(\varphi + \psi))^2}{[1 + \cos^2(\varphi + \psi)][1 + a(1 + \cos(\varphi + \psi))]}\right\} \ldots\ldots \quad (6)$$

a means $h\nu/m\,c^2 = h\nu/510$ if $h\nu$ is measured in keV $e^4/(m_e c^2)^2$ has the numerical value $\frac{1}{4\pi} \cdot 10^{-24}$.

If we want to sum up the intensities in order to obtain the total scattered intensity from one atom we must take into consideration the fact that the different electrons may interact to build up a greater intensity than would be expected if they were all independent. This happens when the wave-length is much greater than the distances between the electrons; all scattered rays from the atom will then have almost the same phase, thus giving rise to an increased intensity.

For short waves, however, we may consider an atom as carrying electrons each giving the same contribution to the total scattered radiation from the atom

$$I_a = Z \cdot I_e \quad \ldots\ldots\ldots\ldots\ldots\ldots\ldots\ldots \quad (7)$$

Z being the atomic number.

For long waves we have to use a correction factor to make the calculated, total, scattered intensity from the atom agree with the interference theory given above

$$I_a = S \cdot Z \cdot I_e \quad \ldots\ldots\ldots\ldots\ldots\ldots\ldots \quad (8)$$

S is called the 'scattering factor'. According to WENTZEL (46), the scattered radiation from an atom consists of two components: coherent rays (in definite phase relation to each other) and incoherent rays, the latter combined with the electron recoils predicted by the theories of Debye and Compton. The coherent rays will be important only for long waves and follow the laws of classical electrodynamics. The scattering factor may be calculated from

$$S = \frac{\left(\sum_1^z f_n\right)^2}{Z \cdot F(h\nu)} + \left(1 - \frac{\sum_1^z f_n^2}{Z}\right) \quad \ldots\ldots\ldots\ldots\ldots \quad (9)$$

Here $f_n = \int_0^\infty u_n(a) \cdot \frac{\sin ka}{ka}\, da$ is the electronic structure factor for the n:th electron, and $u_n(a)\,da$ the probability that this electron will lie between the radii a and $a + da$ from the centre of the atom. The factor k is

$$k = \frac{4\pi}{\lambda} \sin \frac{\varphi + \psi}{2} \quad \ldots\ldots\ldots\ldots\ldots\ldots \quad (10)$$

The values of $\sum f_n$ have been calculated by JAMES and BRINDLEY (20). Values of $\sum f_n$ and $\sum f_n^2$ are also given in Compton and Allison's monograph (11).

For large k-values $S = 1$ and $I_a = Z \cdot I_e$. For small k-values $\sum f_n = \sum f_n^2 = Z$, which makes $I_a = Z^2 I_e$. Thus the influence of S will be most important for heavy atoms.

As there are $\varrho N/W$ atoms per cubic centimeter of any material (ϱ being the density, W the atomic weight and $N = 6.02 \cdot 10^{23}$, the number

of atoms per gram atom) the intensity scattered from a volume unit will be[1]

$$I_s^{(e)} = \frac{\varrho N}{W} \cdot \frac{I_p}{r^2} \cdot \frac{e^4}{(m_0 c^2)^2} \cdot SZF \cdot \frac{1+\cos^2(\varphi+\psi)}{2} = \Bigg| \\ = \frac{I_p}{4\pi r^2} \cdot 0.3\, SF \cdot \frac{\varrho S}{w}(1+\cos^2(\varphi+\psi)) \Bigg| \quad \ldots\ldots (11)$$

As mentioned previously, fluorescence radiation is independent of direction and Eq. (4) holds true.

$$d^2 I_s^{(f)} = \frac{d^2 P_s}{4\pi r^2} \quad \ldots\ldots (12)$$

For the combined secondary radiation from the volume element a factor $\mathrm{Exp}\left(-x\frac{\mu'}{\cos\psi}\right)$ must account for the extinction of the secondary rays, the extinction coefficient of which has to be referred to the frequency of the secondary radiation.

$$\mu'(\nu) = \mu(\nu') \quad \nu' < \nu \quad \ldots\ldots (13)$$

As the function $\mu'(\nu)$ is ambiguous (different values for fluorescence and scattered radiation) we have to divide the extinction factor into two parts. Thus the total intensity of the secondary radiation is composed of contributions from scattered and fluorescence rays according to the following expression

$$I_s = I_s^{(e)} + I_s^{(f)} = \frac{A}{4\pi r^2} \cdot 0.3 \cdot \frac{\varrho Z}{W} \cdot (1+\cos^2(\varphi+\psi)) \int_0^\infty I_\nu SF \cdot \frac{1-e^{-d\left(\frac{\mu}{\cos\varphi}+\frac{\mu'_{sc}}{\cos\psi}\right)}}{\frac{\mu}{\cos\varphi}+\frac{\mu'_{sc}}{\cos\psi}} d\nu + \\ + \frac{A}{4\pi r^2} \int_0^\infty I_\nu \tau_s \frac{1-e^{-d\left(\frac{\mu}{\cos\varphi}+\frac{\mu'_{FL}}{\cos\psi}\right)}}{\frac{\mu}{\cos\varphi}+\frac{\mu'_{FL}}{\cos\psi}} d\nu \quad \ldots\ldots (14)$$

Practical Example

If we now assume that all measurements are made on an absorber with saturation thickness, the exponential term may be neglected.

[1] As the distance between the atoms is not small compared with the wave-length, interference between different *atoms* will only occur if they form a uniform space-lattice. This influence is neglected here as it requires a more well defined primary beam than is usual in practice.

For most practical materials we shall also see from the absorption coefficients that $I_s^{(a)}$ may be neglected when $I_s^{(f)}$ is important and vice versa. If we consider the special case in which $\varphi = \psi = 45°$ we have

$$I_s^{(a)} = \frac{A}{4\pi r^2} \cdot \frac{0.3}{\sqrt{2}} \cdot \frac{\varrho Z}{W} \cdot \int_0^\infty \frac{I_\nu SF}{\mu + \mu'_{sc}} d\nu \quad \ldots\ldots\ldots\ldots \quad (15)$$

$$I_s^{(f)} = \frac{A}{4\pi r^2} \cdot \frac{1}{\sqrt{2}} \cdot \int_0^\infty \frac{I_\nu \tau_s}{\mu + \mu'_{FL}} d\nu \quad \ldots\ldots\ldots\ldots\ldots \quad (16)$$

The fact that the fluorescence radiation may often be neglected when scattering is important will not necessarily mean that it is not generated, but rather that it may be so soft as to be completely absorbed in the secondary radiation source itself. For the *absorption* of both primary and secondary rays, however, the photoelectric effect may be important, making μ and μ'_{sc} much greater than the pure Compton coefficient. As $\mu + \mu'_{sc}$ increases with increasing atomic number more rapidly than $\varrho ZS/W$, the result is that *the intensity of scattered radiation from an absorber with saturation thickness will decrease with increasing atomic number of the absorber.*

Numerical Calculations

We have assumed that the energy distribution $I_\nu(\nu)$ of the primary radiation is known. If not, it is easily determined from the transmission factor, Exp $(-\mu d)$, of the roentgen ray tube and the assumption that the intensity of the Bremsstrahlung has a linear distribution when plotted as a function of energy (KRAMERS (26)).

With the constants A, ϱ, Z and W known, functions $S(\nu)$, $F(\nu)$, $\mu(\nu)$, $\mu'(\nu)$ and $\tau_s(\nu)$ remain to be obtained. The scattering factor S may be calculated from the values of the electronic structure factor given in Compton and Allison's monograph. The Klein-Nishina formula is simplified to (cf. Diagram 2 b).

$$F(\nu) = \frac{1 + \frac{a^2}{1+a}}{(1+a)^2} \quad \ldots\ldots\ldots\ldots\ldots \quad (17)$$

$\mu(\nu)$ may be taken from any modern table of absorption coefficients and $\mu'(\nu)$ from the same source, being equal to $\mu(\nu')$, as the relation $\nu'(\nu)$

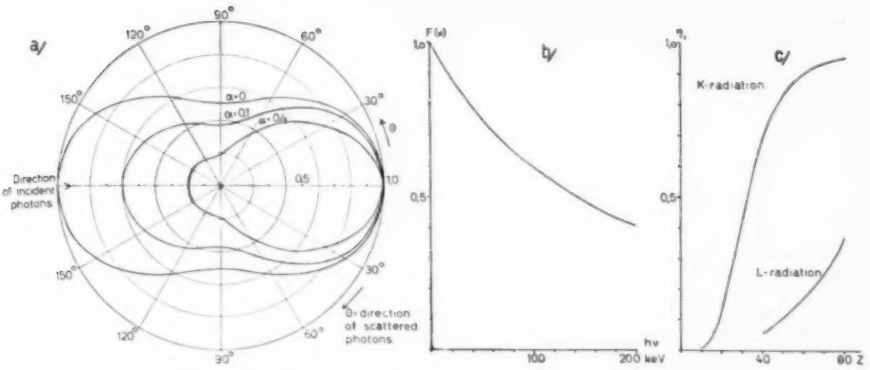

Diagram 2. a) Angular distribution of scattered photon energies. b) The function F (ν) in the case $\varphi = \psi = 45°$. c) Fluorescence radiation efficiency according to Burhop.

is known from the theories of Compton and Debye or from the tabulated wave-lengths of the fluorescence rays.

τ_s may need some introduction. It has to account for the re-radiated part of the energy given off to an atom through the photoelectric effect.

If the energy of an electron in the i:th level is E_i we have

$$\tau_s \approx \frac{E_i}{h\nu} \cdot \eta_i \cdot \tau \quad \ldots\ldots\ldots\ldots\ldots\ldots \quad (18)$$

Here τ is the total photoelectric extinction coefficient. In most cases K radiation will occur, E_i then being the energy of the K photons. The corresponding L radiation can be neglected, as it is either too soft to come out of the absorber, or of small intensity compared with the L radiation produced by primary photons with energies below the K absorption edge. $\tau(\nu)$ may be calculated from (Victoreen's (47) formula or taken as $\mu(\nu) - \sigma(\nu)$ from any table of absorption coefficients.

η_i is the fluorescence efficiency accounting for the fact that the energy E_i is not always transferred to fluorescence radiation but may sometimes be given up to Auger electrons. $1 - \eta_i$ is called the internal conversion probability (Burhop (7)) and is defined as the ratio between the number of Augerelectrons and the total number of photoelectric processes. For light elements, the fluorescence efficiency is far below 100 %, resulting in smaller intensities of the fluorescence rays than are often assumed (see Diagram 2 c).

The high self-absorption of the soft fluorescence rays from light elements, together with the influence of η_i, will cause *the fluorescence*

intensity to increase with increasing atomic number of the absorber, until the decreasing amount of primary radiation above the K edge may make it drop.

The two parts of the secondary radiation may both be written as

$$I_s = \int_0^\infty \Phi(\nu, Z)\, d\nu \quad \ldots\ldots\ldots\ldots\ldots\ldots (19)$$

Here $\Phi(\nu\ Z)$ may be regarded as the distribution of the energy contributions to the secondary radiation as a function of the primary energy. As the real photon energies corresponding to each value of Φ is smaller than the primary energies, the energy distribution of the secondary intensity is

$$\frac{dI_s}{d\nu} = \Phi[\nu_1(\nu),\ Z] \quad \ldots\ldots\ldots\ldots\ldots\ldots (20)$$

where $\nu_1(\nu)$ is the inverse function to $\nu'(\nu)$.

Diagram 3 shows examples of $\Phi(\nu)$ for H_2O, Fe, Sn and Pb. Very heavy elements such as Pb will, apart from the K radiation, also show L radiation of importance, thus compensating the intensity drop mentioned above.

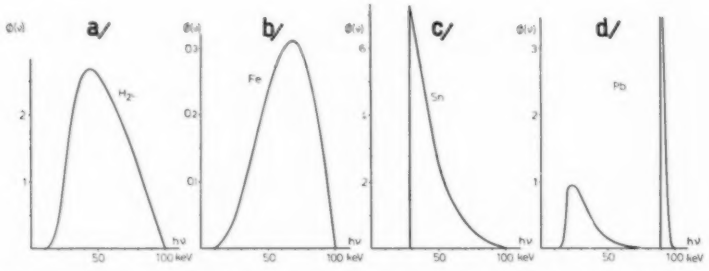

Diagram 3. Energy distribution for the primary photons contributing to the secondary radiation at 100 kV. (Total filter supposed to be 1 mm Al.) The intensities are given in arbitrary units but are comparable with each other.

The Transmitted Secondary Radiation

The secondary radiation transmitted through the absorber may be estimated from about the same assumptions we have already made.

Assume that the distance between absorber and primary radiation source and between absorber and measuring device is great and that all multiple secondary radiation can be neglected. The total secondary radiation at the distance r from the absorber will be

$$I_s = I_s^{(a)} + I_s^{(t)} = \frac{A}{4\pi r^2} \cdot 0.3 \cdot \frac{\varrho Z}{W} (1 + \cos^2(\varphi - \psi)) \int_0^\infty I_\nu \, SF \, \frac{e^{-\frac{d\mu}{\cos\varphi}} - e^{-\frac{d\mu'_{sc}}{\cos\psi}}}{\frac{\mu'_{sc}}{\cos\psi} - \frac{\mu}{\cos\varphi}} \, d\nu +$$

$$+ \frac{A}{4\pi r^2} \int_0^\infty I_\nu \tau_s \cdot \frac{e^{-\frac{d\mu}{\cos\varphi}} - e^{-\frac{d\mu'_{FL}}{\cos\psi}}}{\frac{\mu'_{FL}}{\cos\psi} - \frac{\mu}{\cos\varphi}} \, d\nu \quad \ldots\ldots\ldots\ldots\ldots\ldots \quad (21)$$

This formula corresponds to Eq. (14) and, if we give $\Phi(\nu)$ the same meaning as in Eq. (19), we can write the transmitted secondary radiation in a given direction as

$$I_s = \int_0^\infty \Phi(\nu) \cdot B(\nu, d) \, d\nu \quad \ldots\ldots\ldots\ldots\ldots\ldots \quad (22)$$

Here

$$B(\nu, d) = \frac{\mu' \cos\varphi + \mu \cos\psi}{\mu' \cos\varphi - \mu \cos\psi} \left\{ e^{-\frac{d\mu}{\cos\varphi}} - e^{-\frac{d\mu'}{\cos\psi}} \right\} \quad \ldots\ldots \quad (23)$$

and it may be shown that when $\frac{\mu}{\cos\varphi} = \frac{\mu'}{\cos\psi}$ we have

$$B(\nu, d) = 2d \cdot \frac{\mu}{\cos\varphi} \cdot e^{-d \cdot \frac{\mu}{\cos\varphi}} \quad \ldots\ldots\ldots\ldots\ldots\ldots \quad (24)$$

The function B (d) has a different maximum value for each photon energy $h\nu$. This means that thin absorbers will not give as much secondary radiation as thick ones, since the former do not extinguish as much primary radiation. Nor will very thick absorbers give as much secondary radiation as thinner ones, since the primary intensity will decrease too much before it has reached the region from which the secondary radiation can emanate.

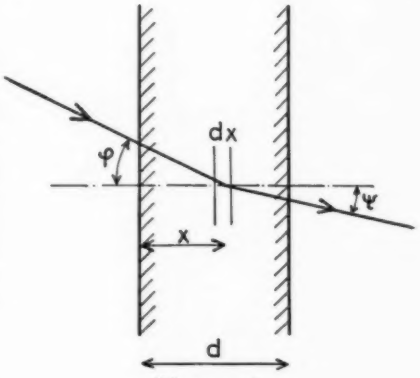

Diagram 4.

The optimum thickness for a given quantum energy is obtained from differentiating B (d)

$$d_{opt}(\nu) = \frac{\ln \frac{\mu' \cos\varphi}{\mu \cos\psi}}{\frac{\mu'}{\cos\psi} - \frac{\mu}{\cos\varphi}} \quad \ldots\ldots\ldots\ldots\ldots\ldots \quad (25)$$

And in the case of $\frac{\mu}{\cos\varphi} = \frac{\mu'}{\cos\psi}$ we have

$$d_{opt}(r) = \frac{\cos\varphi}{\mu} \quad \ldots\ldots\ldots\ldots\ldots\ldots \quad (26)$$

The order of magnitude of the optimum absorber thickness for a continuous distribution of energies may be obtained if the values of μ and μ' for the mean energy are used. It should be noticed that the optimum thickness for secondary *dose-rate* is quite different from the value giving maximum *intensity*, as the mean dose-contributing energy is lower than the mean intensity-contributing energy.

Measurement of Secondary Radiation Energy Distributions

In order to demonstrate the behaviour of the secondary radiation as suggested in the preceding section, a scintillation counter was used combined with a differential discriminator (ÅSTRÖM (51)) in the following arrangement.

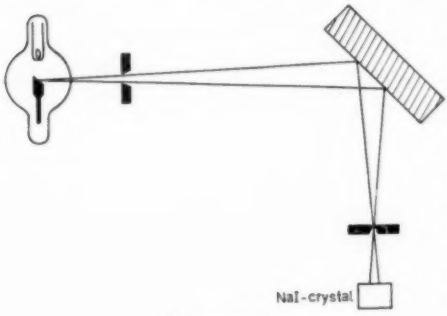

Diagram 5.

The detector was a sodium iodide crystal of sufficient thickness (10 mm) to procure a satisfactory absorption of the primary radiation, the absorbed energy of which gave scintillations detected by an EMI 5311 photo-multiplier.

A calibration of the energy scale was made with the help of the fluorescence rays (cf. Diagram 6 b). The width of the channel was proved to vary very little over the energy range studied.

The resolution was different for high and low energies, depending upon the small number of photons reaching the photomultiplier at low energies, thus giving high statistical fluctuations (cf. Diagram 6 a). It might have been possible to increase the efficiency of the collection of photons from the crystal, but not without great difficulties, as the window had to be very thin in order to let in soft radiation. The window absorption was due to a 0.015 mm Al foil and the non-determinable oil film that protected the crystal from the air.

A diaphragm cut down the primary beam to a circular field area of 2.5 sq.cm at the absorber. A second diaphragm, 3 mm in diameter, defined the secondary beam as shown in Diagram 5.

The primary results consisting of energy distributions of the number of photons have been transformed into energy distributions of the radiated energy simply by multiplying each number of photons Nr with the corresponding photon energy hr. At the same time the spread has been transformed to the same representation limiting the resolution as shown in Diagram 6 a.

The primary radiation source was a Metalix roentgen tube without any added filter and with an inherent filtration equal to about one mm of Al.

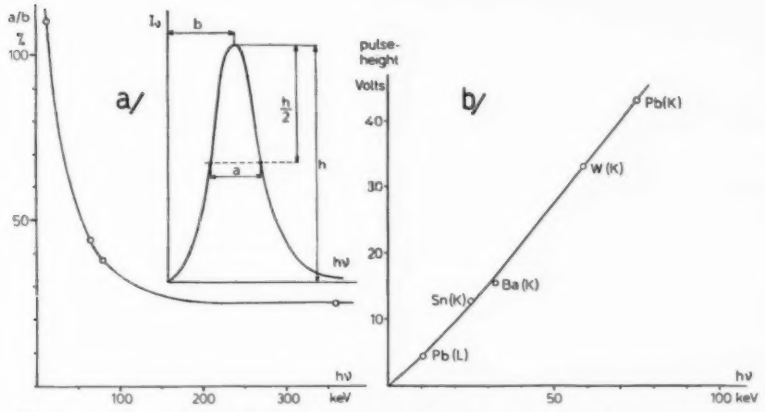

Diagram 6. a) Resolution of the scintillation spectrometer at different photon energies. b) Energy calibration of the pulse heights using fluorescence radiation.

Diagram 7 shows examples of energy distributions of the secondary radiation intensity from different elements when $\varphi = \psi = 45°$.

Before each measurement was carried out, a check was made that the absorber was thick enough to give saturation. As the aperture of the detector limited the absorber volume that could be used, the thickness

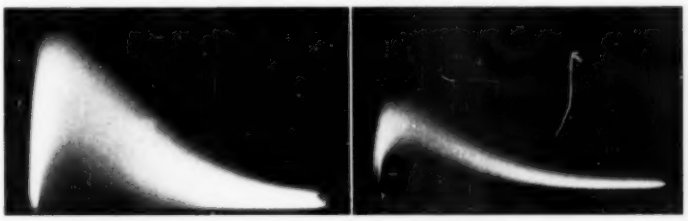

a. b.

c.

Fig. 1. Oscilloscope pictures of the pulse height distribution from a) Al, scattered radiation, b) Sn, K radiation, and c) Pb, L and K radiation.

had to be below 20 mm. That did not procure saturation for Al at voltages over 100 kV (constant potential). Saturation conditions could not be reached for paraffin or press-wood.

Pulse distributions, as they appeared on an oscilloscope screen, are shown in Fig. 1.

From Diagram 7 it can be seen that the pure scattering, shown for Fe[1], will be combined with K radiation at the higher atomic number of Zn and may be neglected in relation to the K radiation at the still higher

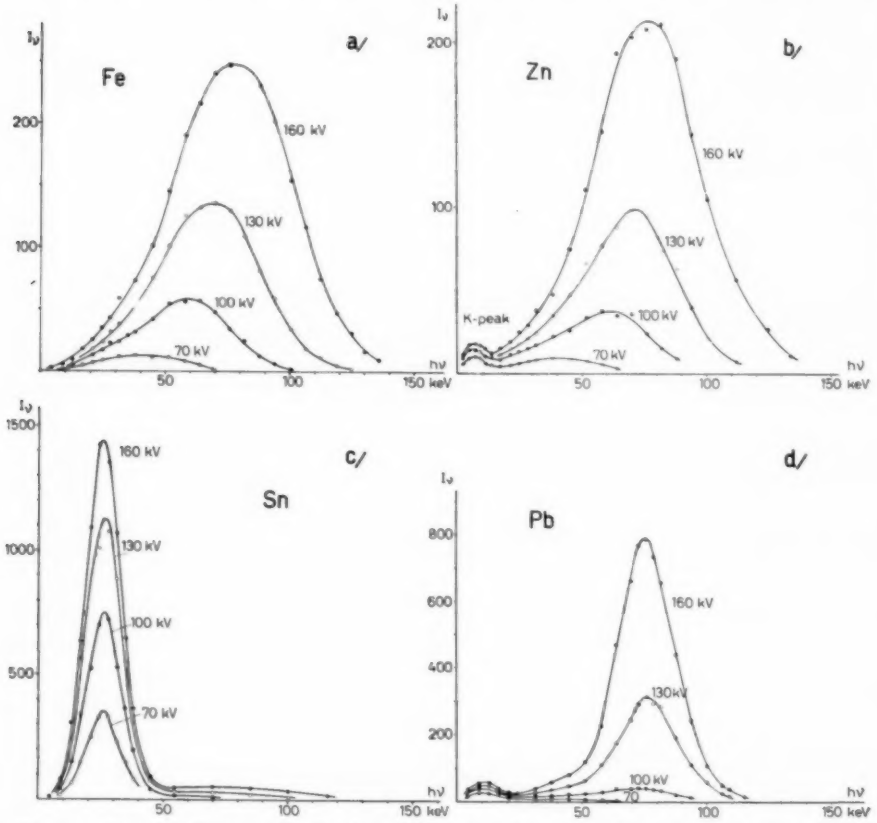

Diagram 7. a—d) Energy distribution of the secondary radiation intensity from Fe, Zn, Sn and Pb.

[1] Dose measurements revealed the presence of a very soft K radiation, the total *intensity* of which was too low to be noticeable in the measurements described above.

atomic number of Sn. Pb also shows L radiation[1]. The intensities are given in arbitrary units but are comparable with each other.

It should be noticed how the distribution of scattered radiation will move towards lower energies when the tube voltage decreases, in contrast to the fluorescence radiation which is fixed at a certain quantum energy.

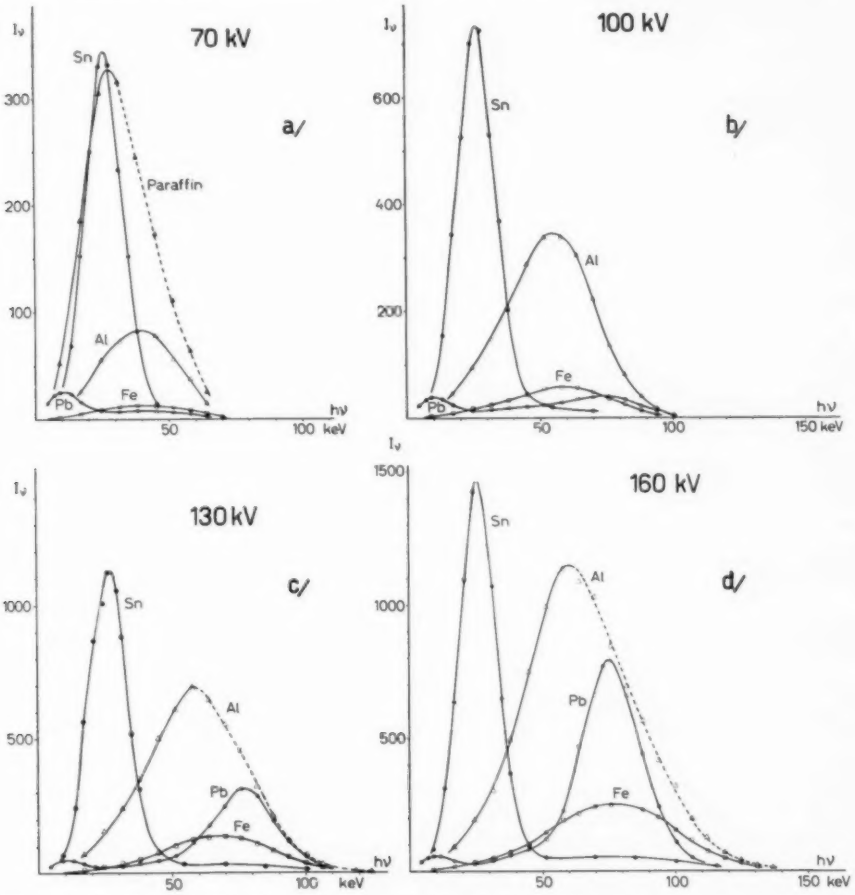

Diagram 8. Energy distributions of the secondary radiation intensity from different elements at the following tube voltages (total filter 1 mm Al): a) 70 kV b) 100 kV c) 130 kV d) 160 kV.

[1] The iodine K escape peak is slightly indicated. From measurements on tungsten it could be determined to about 3 percent in the energy distribution diagram.

Diagram 8 gives a comparison between the intensities from different elements at four tube voltages.

The primary radiation had rather soft components as no additional filter was used. Diagram 9 shows the influence of different primary filters upon the energy distribution of the secondary radiation intensity from an iron absorber.

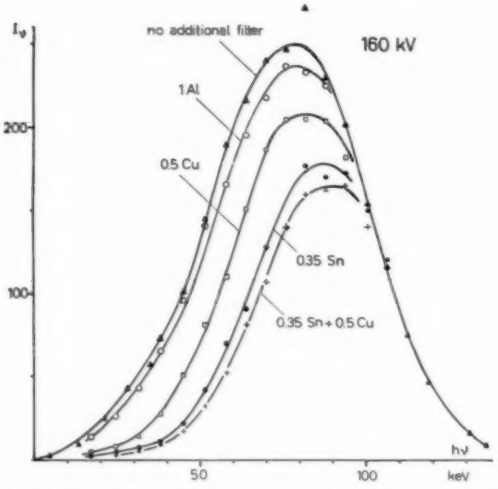

Diagram 9. The scattered radiation from Fe at 160 kV with different primary filters.

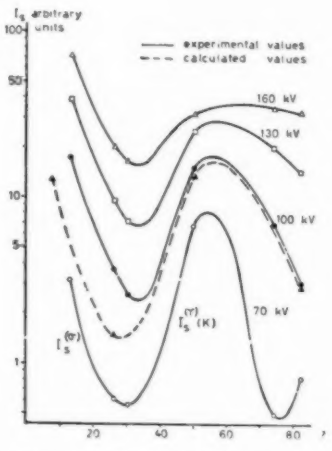

Diagram 10. The total secondary intensity as a function of atomic number.

By integrating the curves in Diagram 8, it is possible to obtain a comparison between the *total* intensities from different elements (Diagram 10).

The curves in Diagram 10 should be compared with the curve that may be expected from the theory. There seems to be a minimum of secondary radiation *intensity* from elements with atomic numbers just above 30, *i. e.* for practical use Cu and Zn.

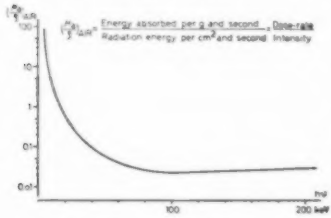

Diagram 11. The true mass-absorption coefficient for air.

Now, if we look upon these facts from a practical point of view, we may not be so interested in the intensity as in the dose-rate. We have then to consider what contribution to the total dose will be obtained from intensities carried by photons of different energies. This information is given in Diagram 11.

We see that the radiation in the low-energy range is rather significant to the

dose, though it may be of little importance considered as energy. This fact is illustrated by the results of dose measurements carried out by LORENTZON (28) and WALSTAM (45).

It depends upon the circumstances to what degree the energy of the softest K radiations should be taken into the estimation of the secondary dose-rate. If it is too soft to go deep enough to make any biologic effect, and if the dose is measured by means of an ionization chamber with walls of sufficient thickness to absorb it completely, the K radiation may of course be neglected, although it will give a rather high dose-rate where it is absorbed. It will then be neccessary to have information on the absorption of the soft components of the radiation.

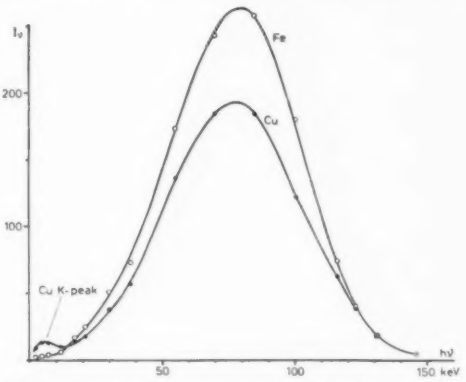

Diagram 12. The energy distribution of the secondary radiation intensity from Fe and Cu. Cu gives a lower intensity but a K radiation that may cause a higher dose-rate than the secondary radiation from Fe, the fluorescence of which cannot be seen in the diagram. 160 kV, 1 Al.

Diagram 12 shows the energy distribution of the secondary intensity from saturation layers of Fe and Cu.

The low-energy range radiation from Fe, Zn, Cu and Pb was studied in detail, the results being shown in Diagram 13.

The energy levels measured are in good agreement with the expected values. The L radiation from Pb, which gives a much higher dose-rate than the same intensity of K radiation, will often disturb measurements or cause injurious skin reactions. It is seen from Diagram 13 that this soft radiation has a half-value layer of about 3—4 mm press-wood and that it is almost completely absorbed by an iron-foil of 0.05 mm. The K radiation from Zn is still softer but still noticeable after a filter of 3.5 mm of press-wood.

The K radiation from Fe is hardly noticeable at all, the interjacent air volume and the window of the detector being too thick to let it through. Accordingly there should usually be no need to take care of it as most detectors have thicker walls, and it will probably also be too soft to cause any skin reactions (cf. WALSTAM's dose measurements). As Fe gives but a little more total secondary radiation intensity than Zn or Cu, it should be convenient to use when it is important to keep the secondary dose-rate low.

In order to obtain some idea of how much the secondary radiation

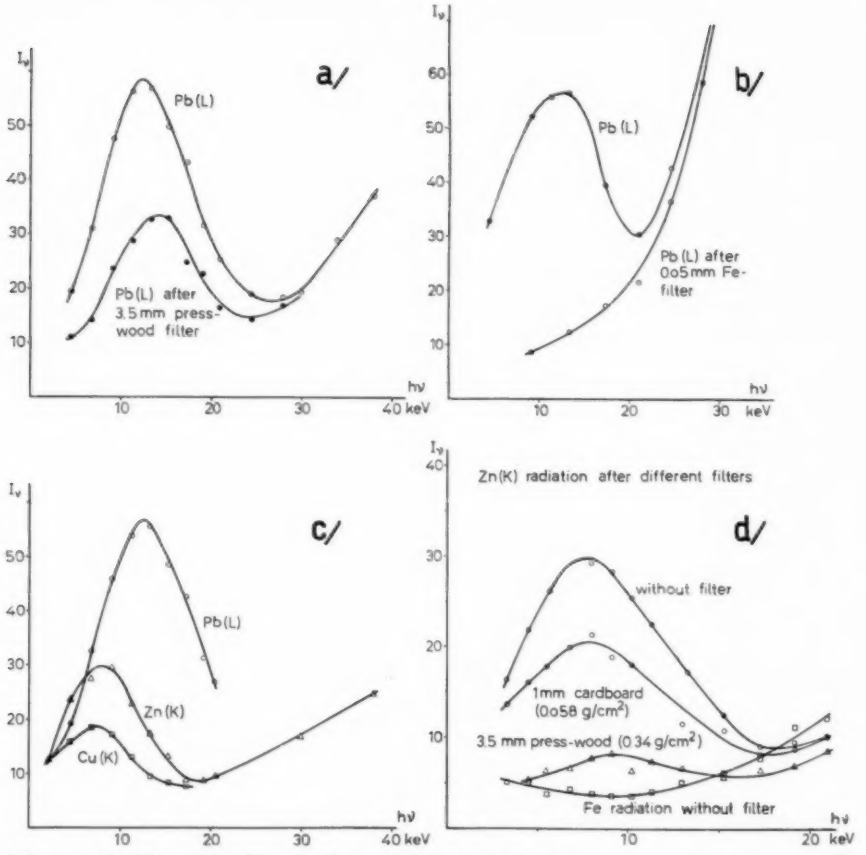

Diagram 13. The softest K radiations. a) and b) The influence of secondary filters on the L radiation from Pb. c) The soft components of the secondary radiation from Cu, Zn and Pb. d) Secondary filtering of the K radiation from Zn. All curves taken at 160 kV and with a total primary filter of 1 mm Al.

intensity would increase when a certain layer of some light element was added, measurements also were made of the intensity from Al and press-wood under non-saturation conditions. The results are shown in Diagram 14, where all intensities are given in figures comparable with those in the earlier results.

Diagram 15 shows the results of measurements on certain wall materials. The Ba K radiation with its quantum energy just above 30 keV has a higher dose efficiency than the K radiation from Pb or the

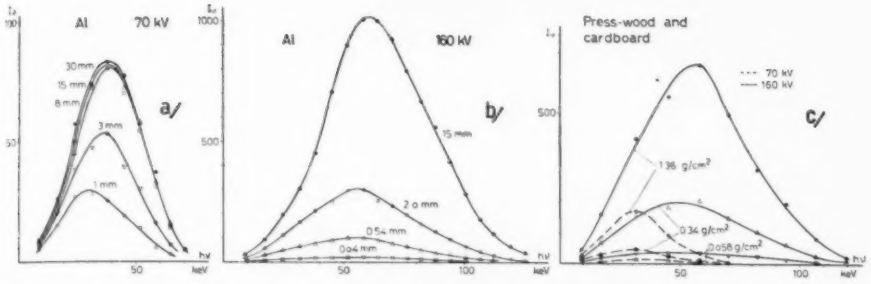

Diagram 14. a—c) The energy of the secondary radiation intensity from some light materials of different thicknesses. Primary filter about 1 mm Al.

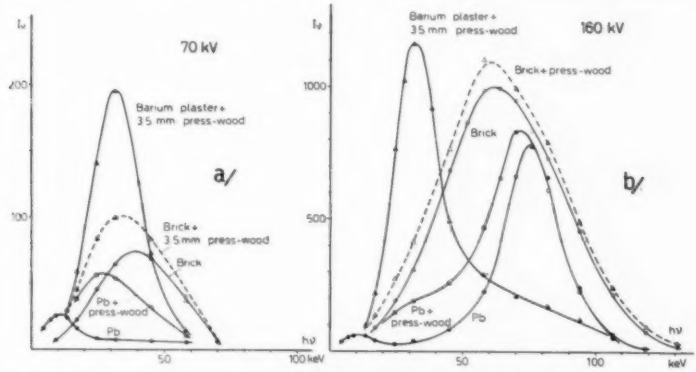

Diagram 15. The energy distribution of the secondary radiation intensity from some wall materials. a) at 70 kV, b) at 160 kV. Total filter 1 mm Al.

scattered radiation from brick. The Ba radiation, however, is softer and consequently not so penetrating. Compared with iron (the saturation thickness of which at 160 kV is for practical purposes about 3 mm) Pb, brick and barium plaster give fairly high intensities (cf. the dose measurements in the following section).

For measurements of *the transmitted secondary radiation* the same method was used as for the back-scattered radiation, only with a different angle between the absorber and the directions of radiation and collection.

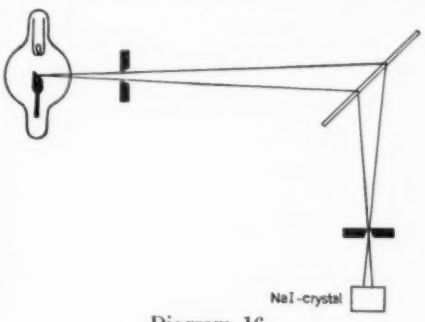

Diagram 16.

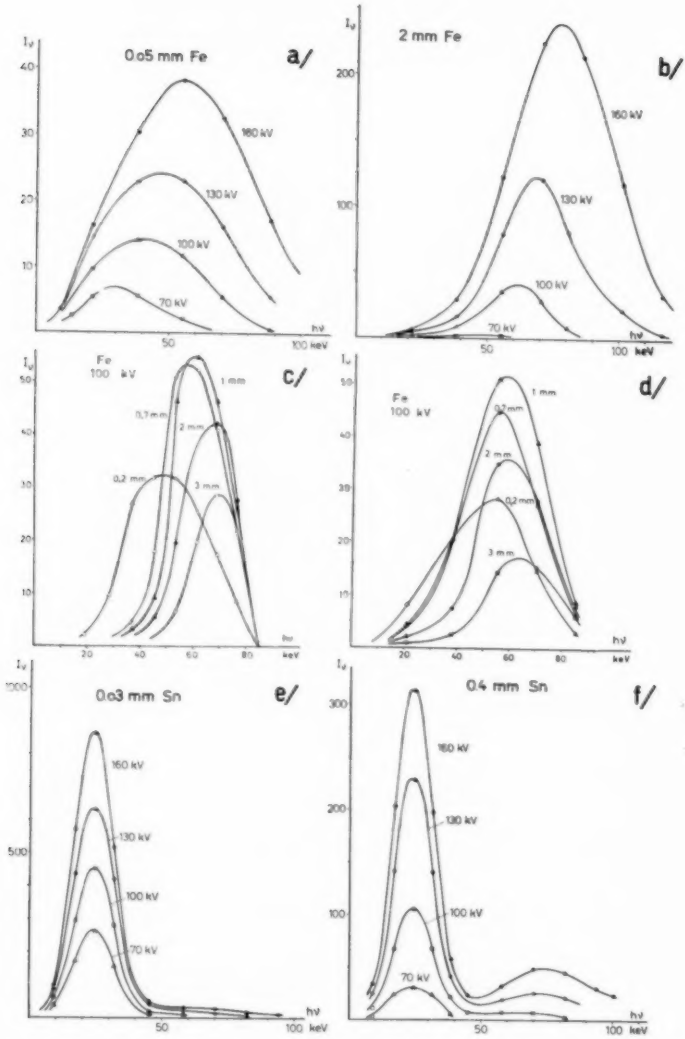

Diagram 17. The energy distribution of the transmitted secondary radiation intensity. a) From a thin Fe absorber. b) From a thick Fe absorber. Notice the self-filtering effect of the absorber. c) Calculated values of the energy distribution from Fe absorbers of different thicknesses at 100 kV, 1 Al. d) Measured energy distributions from Fe, showing the same tendency as the calculated curves. e) From a thin Sn absorber. f) From a thick Sn absorber. Self-filtering has reduced the K radiation almost to the level of the scattered radiation.

As it was not possible to obtain absorbers sufficiently thin for heavy elements such as Pb nor use the thick absorbers necessary for light elements such as Al, measurements were made only on Fe and Sn. Fe may thus represent the light elements giving no detectable fluorescence radiation and Sn the heavy elements with almost only fluorescence radiation. The results are given in Diagram 17.

The transmitted scattered radiation from Fe shows the same dependence upon tube voltage as did the back-scattered radiation. The filtering effect of the absorber itself can be seen, as well as the agreement between the calculated and measured energy distributions.

The K radiation from Sn shows a corresponding voltage dependence, with the difference that the quantum energy is fixed. The curves show how the scattering from the thicker absorber has grown more important, *i. e.* the scattered radiation has a greater value of the optimum thickness of the absorber than has the fluorescence radiation.

The total secondary intensity as a function of the absorber thickness is shown in Diagram 18. Here the values of maximum intensity have been made equal to 100 % for comparison with the calculated values. It should be noticed that these curves for Sn give only the fluorescence and not the scattered radiation which, however, from thick absorbers, may not be neglected (cf. Diagram 17 f).

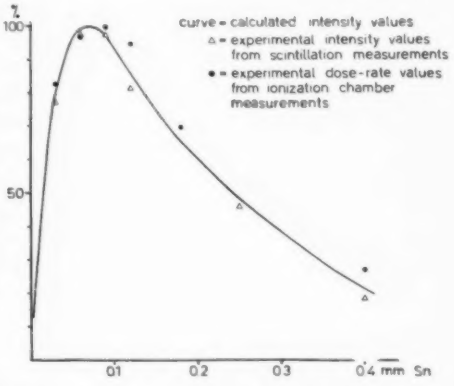

Diagram 18. The total secondary radiation intensity from the back of a Sn absorber as a function of absorber thickness. 100 kV, 1 Al.

Diagram 19 shows the transmitted secondary radiation from a compound filter. The tin filter, described by THORAEUS (42), for voltages about 170 kV usually consists of 0.44 mm Sn + 0.25 mm Cu + 1.0 mm Al. In order to obtain about the same reduction of the primary intensity with our direction of the beam we used 0.28 mm Sn.

It will be seen from Diagram 19 that the K radiation from Sn is almost completely absorbed by 0.5 mm of Cu. The Al layer only makes the scattered *intensity* increase. Earlier, it was supposed to absorb the K radiation and electrons from the Cu layer and give mechanical strength to the filter. We now know that the roentgen generated electrons may be neglected from the point of view of secondary radiation if an ordinary roentgen apparatus is used, as not even the photoelec-

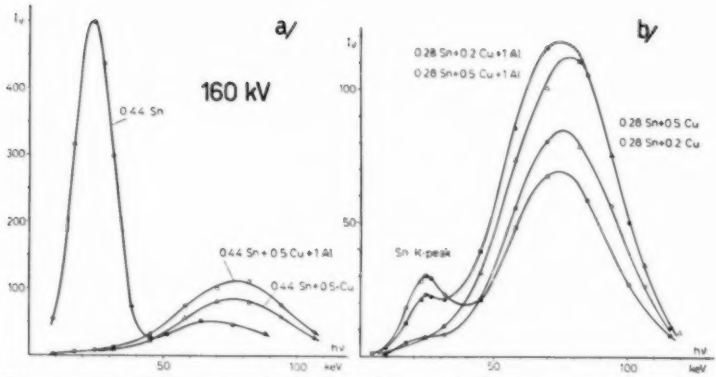

Diagram 19. The transmitted secondary radiation from a compound filter. a) With a Cu component thick enough to make the Sn K peak invisible in the energy distribution. b) With components comparable with those in a Thoraeus-filter.

trons of the highest energy can penetrate more than a few tenths of a millimetre of water.[1]

The K radiation is now left to be considered. It was clearly noticeable in the back-scattered radiation (cf. Diagram 12). In Diagram 19, however, we cannot see any sign of fluorescence radiation. The primary radiation through a compound filter, such as the one used, is so heavily filtered by the main filter that the soft components, which are the most efficient for generating K radiation from Cu, will never reach the Cu layer[2]. Thus the only reason in keeping the Al layer is that it strengthens the filter.

From Diagram 19 we see that 0.2 mm of Cu will not form a sufficient filter to absorb the K radiation from Sn 'completely' (*i. e.* completely for practical purposes). As 0.2 mm of Cu represents an actual range of 0.28 mm for the Sn K rays, the usual tin filter with 0.25 mm of Cu should not give 'sufficient' absorption (*i. e.* absorption sufficient to make

[1] The resemblance between the dependence of atomic number for the secondary roentgen radiation and the corresponding dependence for the emergent flux of secondary electrons from an absorber irradiated with γ-rays is apparent. At high γ-energies these electrons form an important part of the secondary radiation (The medical consequences of this were first considered by SIEVERT (40)). The dependence of atomic number for this radiation has been investigated by BRAGG (5), HACKET (18), EVE (13), KOVARIK (25) and WILSON (50), and good surveys on the subject have been given by QUIMBY *et al.* (33) and HINE (19), the latter showing the mechanism behind the Z dependence to be explained by the scattering of the electrons being approximately proportional to the atomic number.

[2] (When no Sn was used the K radiation was present for 0.1 mm of Cu, but had almost vanished at 0.5 mm of Cu; this gives an idea of the primary energies most efficient to generate it; the actual range in Cu for the K radiation as well as for the primary rays owing to our arrangement was thus 0.14 and 0.7 mm respectively.)

the transmitted Sn K-radiation non-detectable) of this K radiation in the direction of the primary beam. Even with a Thoraeus-filter used in the same arrangement (thus giving too high primary filtering with an actual range of 0.35 mm in Cu for the emergent K radiation) the fluorescence radiation was clearly noticeable. The most convenient backing of the Sn layer might thus be a Cu layer of about 0.5 mm and no Al. So thick a Cu layer, however, may decrease the absorption of the desired high energy primary rays too much. As a compromise with practical demands the original backing proposed by THORAEUS seems to be a good choice.

I have tried in this survey to make clear the mechanism of the secondary roentgen radiation. Most of the facts pointed out have been published earlier, but often not in a way to be easily accessible and, to my knowledge, never in one paper.

It should be once more emphasized:

Secondary radiation is composed of Compton-scattered rays and fluorescence rays. For elements heavier than Fe, the scattered rays (for the primary qualities that have been discussed) have little importance. For elements lighter than Fe, the fluorescence rays are so soft that they will often not penetrate the matter (including air) between the secondary radiation source and the point of observation.

From Fe up to the heaviest elements, the secondary radiation (from the view-point of dose-efficiency) is almost exclusively fluorescence radiation. In this connection, K radiation is the most important up to such heavy elements as W. The K radiation dose-rate increases with atomic number, and it depends upon the energy of the primary rays (*e. g.* the tube voltage) how far this increase will last.

Pb also gives L radiation of importance.

The K radiation from Fe is very soft and will be reduced to less than 10 % by a few mm of any unit density material. The remaining scattered radiation will give a lower dose-rate than any other secondary radiation. *Thus Fe is the element that should be used if the secondary radiation dose-rate is to be kept low.*

The K radiation from Cu and Zn is more penetrating than the K radiation from Fe. Thus *it will affect most dose-measurements, giving a higher dose-rate in the chamber than after some mm in, for example, tissue.*

The K radiation from Sn is rather hard. Sn also gives a very low scattered intensity and *is thus an ideal monochromatic radiation source.*

The L radiation from Pb will affect dose-measurements in the same way as the soft K radiation from lighter elements.

Elements such as Fe, Cu and Zn, which give rather high dose-rates without any secondary filter, may be covered by a thin layer of some lighter element to reduce the soft K radiation.

Light elements (water, tissue, wood) are the most dangerous from the protection point of view, since they give both high dose-rates and penetrating radiation, thus being able to cause high integral doses.

This survey is not complete without an account of dose-measurement results. The reader is referred to two papers just published. WALSTAM (45) has as a direct continuation of the intensity measurements reported here measured the secondary dose-rate as a function of atomic number. LORENTZON (28) presents an investigation from 1947 that gives practical data about the secondary dose-rate from different materials.

SUMMARY

The author gives a survey of secondary roentgen radiation illustrated by calculations of some practical examples. It is shown how the secondary radiation depends upon the quality and quantity of primary radiation and upon the atomic number of the secondary radiation source. Measurements have been made at 70, 100, 130 and 160 kV constant potential on the secondary radiation from some materials of practical interest. The energy distribution of the secondary radiation intensity has been measured with a scintillation spectrometer. It is shown how light materials give high secondary dose-rates, produced by scattered radiation. Heavy materials give fluorescence radiation, the significance of which is discussed.

ZUSAMMENFASSUNG

Der Verfasser gibt einen Überblick über die sekundäre Röntgenstrahlung und berechnen diese für einige praktische Fälle. Es wird gezeigt, wie die Sekundärstrahlung von der Qualität und Quantität der Primärstrahlung und von der Atomnummer des Sekundärstrahlers abhängig ist.

Messungen der Sekundärstrahlung einiger Materialien von praktischem Interesse sind bei 70, 100, 130 und 160 kV konstanter Gleichspannung ausgeführt worden. Die Energieverteilung der Sekundärstrahlungsintensität ist mit einem Szintillations-Spektrometer gemessen worden. Es wird gezeigt dass leichtatomige Stoffe hohe Sekundärstrahldosen durch Streustrahlung geben. Schweratomige Stoffe geben Fluoreszensstrahlung, deren Eigenschaften besprochen werden.

RÉSUMÉ

L'auteur donne une vue d'ensemble sur le rayonnement roentgen secondaire illustrée par le calcul de quelques exemples pratiques. Il montre comment le rayonnement secondaire est fonction de la qualité et de la quantité du rayonnement primaire et du nombre atomique de la source de rayonnement secondaire. Il a mesuré sous des potentiels constants de 70, 100, 130 et 160 kV le rayonnement secondaire émis par quelques substances d'intérêt pratique. Il a étudié la distribution de l'énergie du rayonnement secondaire avec un spectromètre à scintillation. Il est montré que les substances légères émettent de fortes doses de rayonnement secondaire, dues au rayonnement diffusé. Les corps lourds donnent un rayonnement de fluorescence dont l'auteur étudie l'importance.

REFERENCES

1. Barkla, Ch. G.: Der Stand der Forschung über die sekundäre Röntgenstrahlung. Jahrb. d. Radioakt. und Elektronik 5 (1908), 246.
2. Barkla, Ch. G.: Röntgen Rays and Scattered Röntgen Rays. Phil. Mag. 15 (1908), 288.
3. Barkla, Ch. G.: Die Spektren der fluoreszierenden Röntgenstrahlungen. Jahrb. d. Radioakt. und Elektronik 8 (1911), 471.
4. Bernstedt, R.: Secondary Radiation from Protective Walls in Hard Roentgen Radiation. Acta radiol. 19 (1938), 85.
5. Bragg, W. H. and Madsen, J. P. V.: An Experimental Investigation of the Nature of X-Rays. Phil. Mag. 16 (1908), 918.
6. Breitländer, K.: Wie Gross ist der Rückstreuungsbetrag? Strahlentherapie 23 (1926), 79.
7. Burhop, E. H. S.: The Auger Effect and Other Radiationless Transitions. Cambridge University Press, Cambridge 1952.
8. Christen, Th.: Sekundärstrahlen und Härtegrad. Fortschr. Röntgenstr. 25 (1917), 55.
9. Compton, A. H.: Secondary Radiation Produced by X-Rays. Bull. of the Nat. Res. Counc. 4, II (1922), 19 (Nat. Acad. of Sciences, Wash.)
10. Compton, A. H.: A quantum theory of the scattering of X-rays and X-rays by light elements. Phys. Rev. 21 (1923), 207 and 483.
11. Compton, A. H. and Allison, S. K.: X-Rays in Theory and Experiment. Second Edition, Ninth printing, New York 1949.
12. Debye, P.: Zerstreuung von Röntgenstrahlen und Quantentheorie. Physik. Ztschr. 24 (1923), 161.
13. Eve, A. S.: Primary and Secondary Gamma Rays. Phil. Mag. 18 (1909), 275.
14. Glocker, R.: Ueber die Streuung der Röntgenstrahlen. Fortschr. Röntgenstr. 25 (1917), 470.
15. Glocker, R.: Ueber die Berechnung der sekundären Röntgenstrahlung einer Platte. Physik. Ztschr. 19 (1918), 249.
16. Grossmann, G.: Ueber Sekundärstrahlen und Sekundärstrahlentherapie. Fortschr. Röntgenstr. 22 (1914—15), 427.
17. Grossmann, G.: Ueber die Sekundärstrahlen als Gefahrquellen. Fortschr. Röntgenstr. 23 (1915—16), 182.
18. Hacket, F. E.: The Secondary Radiation Excited by X-Rays. Roy. Soc. Dublin 9 (1905—09), 201.
19. Hine, G. J.: Secondary Electron Emission and Effective Atomic Numbers. Nucleonics 10 (1952), 9.
20. James, R. W. and Brindley, G. W.: Some Numerical Calculations of Atomic Scattering Factors. Phil. Mag. 12 (1931), 81.
21. Johansson, S. G.: The Use of Scintillation Counters in the Measurement of the Energy of X-Rays and Low Energy Gamma-Rays. Arkiv för fysik 3 (1952), 533.
22. Keane, B. E. and Spiegler, G.: Stray Radiation from Diagnostic X-Ray Beams. Brit. J. Radiol. 24 (1951), 198.
23. Klein, O. and Nishina, Y.: Ueber die Streuung von Strahlung durch freie Elektronen nach der neuen relativistischen Quantendynamik von Dirac. Ztschr. f. Physik 52 (1929), 853.
24. Klövekorn, G. H. and Gaertner, O.: Die Erythemdosis in R-Einheiten für Kupfereigenstrahlung. Strahlentherapie 24 (1926), 365.
25. Kovarik, A. F.: On Emergent β-Rays from Materials of Different Atomic Weight and Different Thickness Produced by γ-Rays. Phys. Rev. 18 (1921), 154.

26. KRAMERS, H. A.: On the Theory of X-Ray Absorption and of the Continuous X-Ray Spectrum. Phil. Mag. 46 (1923), 836.
27. KÜSTNER, HANS.: Die Streustrahlung bei der diagnostischen und therapeutischen Anwendung der Röntgenstrahlen. Die Naturwissenschaften 11 (1923), 97.
28. LORENTZON, L.: Secondary Roentgen Radiation from Wax, Al, Fe and Pb at Tube Voltages between 40 and 170 kV. Acta radiol. 41 (1953), 201.
29. POURIO, M.: Selectivity of secondary radiations. Brit. J. Radiol. 31 (1926), 502.
30. PUPIN, M. I.: Röntgen Rays and Scattered Röntgen Rays. Science 3 (1896), 538.
31. QUIMBY, EDITH H.: A Method for the Study of Scattered and Secondary Radiation in X-Ray and Radium Laboratories. Radiology 7 (1926), 211.
32. QUIMBY, E. H., LUCAS, C. DE F. and MAC COMB, W. S.: A study of back-scatter for several qualities of roentgen rays. Radiology 23 (1934), 743.
33. QUIMBY, E. H., MARINELLI, L. D., and BLADY, J. V.: Secondary Filters in Radium Therapy. Am. J. Roentgenol. 41 (1939), 804.
34. RAJEWSKY, B.: Compton-Effekt bei tiefen-therapeutischen Bestrahlungsbedingungen. Fortschr. Röntgenstr. 35 (1926), 262.
35. REES, W. J. and CLARK, L. H.: On the quality and significance of the scattered radiation produced in water subjected to beams of X-rays and gamma-rays. Brit. J. Radiol. 5 (1932), 432.
36. ROGERS, T. H.: Production of Monochromatic X-Radiation for Microradiography by Excitation of Fluorescence Characteristic Radiation. J. Appl. Physics 23 (1952), 881.
37. RÖNTGEN, W. C.: Ueber eine neue Art von Strahlen. Ann. d. Physik 64 (1898), 1.
38. SCHARDT, A. W. and BERNSTEIN, W.: Resolution of the Scintillation Spectrometer. Rev. of Sci. Instr. 22 (1951), 1020.
39. SCHENK, HANS.: Die Analyse der Sekundärstrahlung von Al, Ni, Ag und Au auf der Ein- und Austrittseite der Röntgenstrahlen. Ann. d. Physik 17 (1933), 146.
40. SIEVERT, R. M.: Secondary Rays in Radium Therapeutics. Acta radiol. 2 (1923), 268.
41. THOMSON, J. J.: Conduction of Electricity through Gases.
42. THORAEUS, R.: Tin-filters in Roentgen Therapy. Acta radiol. 15 (1934), 225.
43. VETTE, E.: Die Sekundärstrahlung fester Elemente in Abhängigkeit vom Material des Strahlers und der Härte der erregenden Röntgenstrahlen. Ann. d. Physik V5 (1930), 929.
44. WALLER, I. and HARTREE, D. R.: On the Intensity of the Total Scattering of X-Rays. Proc. Roy. Soc. 74 (19), 119.
45. WALSTAM, RUNE: Dose Measurements on Secondary Roentgen Radiation. Acta radiol. 41 (1953), 348.
46. WENTZEL, G.: Zu Theorie des Comptoneffekts. Ztschr. f. Physik 43 (1927), 779.
47. VICTOREEN, J. A.: Roentgen Rays: Measurement of Quality. Medical Physics (Ed.: Glasser) II, Chicago 1950.
48. WILSEY, R. B.: The Intensity of Scattered X-Rays in Radiography. Am. J. Roentgenol. 8 (1921), 328.
49. WILSEY, R. B.: The Effects of Scattered X-Rays in Radiography. Am. J. Roentgenol. 8 (1921), 589.
50. WILSON, C. W.: The Dependence of the Secondary Electronic Emission Produced by Gamma Radiation Upon the Direction of the Radiation. Proc. Phys. Soc. 53 (1941), 613.
51. ÅSTRÖM, B.: To be published in Arkiv för fysik.

SERVICE DE RADIOLOGIE (PROF. C WANGERMEZ) DE L'HÔPITAL DU TONDU ET DE LA CHAIRE DE PHYSIQUE MÉDICALE (PROF. C. PIFFAULT), DE LA FACULTÉ DE MÉDECINE DE BORDEAUX, FRANCE

LA MÉTHODE TOMOGRAPHIQUE DANS LA MESURE DU VOLUME D'UN VISCÈRE PLEIN. APPLICATION AU CŒUR

par

Joseph Duhamel, Pierre-Louis Martin, Michel Guillon et *Jean Broussin*

I. Introduction

Il est relativement facile, par les procédés radiographiques de déterminer les dimensions d'un viscère plein visible spontanément ou à l'aide de contrastes artificiels. La difficulté est beaucoup plus grande lorsqu'il s'agit d'évaluer son volume et l'on a dressé des tables permettant de l'obtenir quand on connait les dimensions de l'organe.

On peut faire à ces tables deux séries d'objections:

1°) Leur précision est, la plupart du temps, médiocre.

2°) Elles sont établies à l'aide de mesures faites sur le cadavre fixé ou non, et où se sont déjà manifestées des altérations cadavériques ou des modifications de tonus extrêmement importantes. On connait les progrès que l'examen radiologique a fait faire à l'anatomie morphologique ou topographique sur le vivant: il suffit de comparer aux ouvrages actuels les traités d'anatomie vieux de vingt ans à peine, au chapitre traitant de l'estomac, pour en être persuadé.

3°) Elles ne tiennent pas compte des fines modifications localisées que l'on rencontre en pathologie.

Il est donc évident que s'il existe une méthode permettant de mesurer, sur le vivant, le volume d'un organe, méthode utilisable tous les jours, au prix d'une application technique facile, renouvelable en série au cours de l'évolution d'une maladie quelles que soient les modifications de forme subies par l'organe, son champ d'application peut être extrêmement étendu.

Un viscère sur le vivant est inaccessible aux méthodes usuelles de mesure (par déplacement d'eau par exemple): la tomographie qui nous fournit des coupes sériées d'un organe, peut, en principe, permettre de calculer son volume. Nous étudierons donc succes-

Soumis à la Rédaction le 27 Avril 1953.

sivement les modes de reconstitution d'un volume à partir d'une série de tomogrammes, puis, les conditions géométriques que doit satisfaire le tomographe pour nous permettre d'obtenir des éléments utilisables.

Nous utiliserons les documents que l'un de nous a publiés dans sa thèse (8), au sujet du cœur. On peut en effet considérer le cœur, sur le vivant où ses cavités sont pleines de sang, comme un organe plein. La méthode proposée nous fournit en somme le volume global égal à la somme du volume du muscle cardiaque et de celui des cavités.

LINDEMAN (10), a publié une méthode tomographique, utilisant la technique des tomographies simultanées de M. DE ABREU, pour étudier, sur l'animal les cavités cardiaques au cours de l'angiocardiographie; on pourrait ainsi dissocier ce qui appartient au muscle de ce qui appartient aux cavités. Il s'agit, pour l'instant d'une vue toute théorique.

Avant de songer à d'aussi lointaines extensions, nous pouvons nous attaquer, plus commodément, à d'autres volumes, tels que la rate ou le rein, par les techniques de contraste gazeux (SANSONE, MACARINI et OLIVA).

II. Reconstitution d'un volume

Lorsqu'on désire calculer, géométriquement, le volume d'un objet, connaissant sa forme, on opère de la façon suivante:

On adopte un plan de référence Φ et on cherche la relation qui unit la surface S (x) d'une section de l'objet par un plan P parallèle à Φ, à la distance x qui sépare les deux plans (diagramme 1).

L'objet dont on désire connaître le volume est compris entre deux plans A et B, situés aux distances a et b du plan de référence. On sait que le volume cherché, V, est fourni par la formule.

$$V = \int_a^b S(x)\, dx$$

qui exprime simplement que le volume est égal à la somme des volumes d'une infinité de tranches successives, de surface S(x), séparées par une distance infiniment petite dx.

En pratique, on se contente de mesurer la surface de sections échelonnées et séparées par une distance m finie et mesurable, choisie de telle sorte que l'erreur ainsi commise soit minimum.

Le seul procédé permettant, sur le vivant, d'obtenir des coupes d'un organe est la méthode tomographique. Ce sont les servitudes de cette technique qui nous limitent dans le choix de la distance m séparant deux coupes successives.

On ne peut pas en effet les faire trop rapprochées pour deux raisons:

1) La tomographie est un examen coûteux en patience pour le sujet, en temps, et, naturellement, en films. Il n'est pas question de faire une infinité de coupes.

2) Des coupes très rapprochées ne fournissent qu'une illusoire précision

a) parce qu'il est difficile d'admettre que d'une coupe à une autre, le patient, qui respire entre la prise des clichés, revient en position à la fraction de millimètre près, et, qu'entre le début et la fin de l'examen, par variation de tonus musculaire, il n'a pas bougé de quelques millimètres.

b) on peut, d'autre part, définir pour tout tomographe une épaisseur de coupe: obtenir des tomogrammes situés dans la même couche de coupe est sans signification géométrique. Au contraire pourvu que la surface de l'objet ne soit pas trop tourmentée on pourra adopter pour m une valeur très supérieure à cette épaisseur.

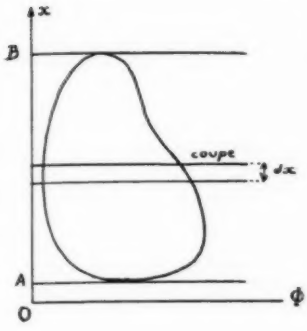

Diagramme 1. Le plan du film est désigné par Φ.

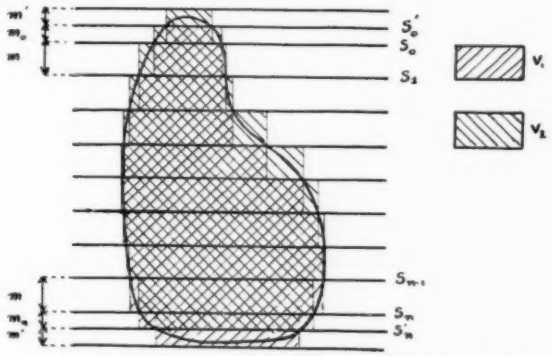

Diagramme 2. Mesure d'un volume à l'aide de coupes séparées par une distance finie m.

Nous pouvons ainsi prévoir qu'il vaudra mieux utiliser un tomographe fournissant des coupes assez fines, c'est à dire avec un angle de coupe grand. L'inconvénient de ces appareils est la grande difficulté de repérage et de centrage sur lesquelles deux d'entre nous ont encore insisté récemment (5 et 7).

La solution du problème est facilitée par le fait que les viscères qui se prêtent à l'étude (cœur, rein, rate), possèdent, sinon des formes géométriques simples, du moins des courbures très régulières, sans discontinuités brutales, et permettent d'adopter, pour la valeur de la distance séparant les coupes, une valeur assez grande, ce qui diminue le nombre de clichés nécessaires.

Nous avons choisi comme valeur de m: 1 cm. Cette distance, très suffisante, comme nous l'a montré l'expérience, a l'avantage de simplifier les calculs numériques et de correspondre aux graduations des tomographes usuels.

Technique. On prend une série de tomogrammes de l'objet, tomogrammes séparés par la distance m choisie, nous appellerons S_0, S_1 ..... S_n les surfaces de ces coupes dans l'ordre descendant.

Il faut tenir compte du fait que les limites supérieure et inférieure de l'objet sont en général assez mal connues «a priori», et, par une série de tâtonnements, on obtient une coupe S'_0 située à une distance m_0, au dessus de S_0, ($m_0 < m$), qui rencontre encore l'objet, tandis qu'une coupe située à la distance m', au dessus de S'_0, ($m'_0 < m$), ne le rencontre plus. C'est cette distance m' qui mesure l'erreur sur la limite supérieure de l'objet.

On opère de la même façon pour la limite inférieure: il existe une coupe S'_n située à la distance m_n au dessous de S_n qui rencontre encore l'objet tandis qu'une coupe située à la distance m' au dessous de S'_n ne le rencontre plus.

Les tâtonnements nécessaires pour obtenir S'_0 et S'_n sont raccourcis par la pratique; d'ailleurs il ne s'agit que de termes correstifs, et comme, de plus, les valeurs de S'_0 et S'_n sont faibles, une grande précision n'est pas indispensable.

Nous pouvons assimiler chaque tranche de section à un petit cylindre et calculer le volume V, en descendant ou en montant (diagramme 2).

Nous obtenons ainsi les deux valeurs:

en descendant: $V_1 = S'_0 m_0 + S_0 m + m\,(S_1 + S_2 + \ldots\ldots + S_{n-2} + S_{n-1}) + S_n m_n + S'_n m'$

en montant: $V_2 = S'_0 m' + S_0 m_0 + m\,(S_1 + S_2 + \ldots\ldots + S_{n-2} + S_{n-1}) + S_n m + S'_n m_n$.

Nous admettrons que le volume vrai est voisin de V_1 et de V_2, et qu'il est fourni par leur moyenne:

(I) $V \simeq {}^1/_2 S'_0 (m' + m_0) + {}^1/_2 S_0 (m + m_0) + m (S_1 + S_2 + \ldots\ldots + S_{n-2} + S_{n-1}) + {}^1/_2 S_n (m + m_n) + {}^1/_2 S' (m' + m_n)$.

Ce qui n'est qu'une généralisation de la formule obtenue en supposant égaux les intervalles séparant les coupes.

En opérant ainsi on commet une erreur assez faible, qu'on pourrait encore minimiser en adoptant pour m une valeur moindre.

Si la mesure des surfaces de section n'offre aucune difficulté par pesée ou par planimètrie, avec une bonne précision, il faut s'entourer de garanties au sujet de la signification réelle, par rapport à l'objet de la surface mesurée.

1°) Puisque l'on opère sur le vivant, l'organe tomographié peut être parasité par les ombres ou les coupes des organes voisins, et sa section, mal se dégager de leurs ombres ou de leurs sillages. Il faut donc que la section soit bien contrastée par rapport aux tissus voisins.

Dans le cas du cœur, entouré du tissu pulmonaire aérien, il n'y a pas de difficulté. Pour les autres organes il est nécessaire de s'inspirer des techniques décrites pour les contrastes gazeux et de savoir en choisir une.

2°) Une fois écartée la restriction précédente et en supposant que l'objet étudié offre un bon contraste par rapport au milieu qui l'entoure, nous devrons nous demander dans quelle mesure la surface mesurée correspond réellement à la surface de coupe. On sait, en effet, que l'image d'un volume homogène en tomographie est composée de deux parties: l'une, mal contrastée, ou plutôt à contraste variable et à contours assez mal délimités pour cette raison, est la trace, elle entoure la deuxième portion, à contours nets, qui est le «residu» ou «noyau». C'est ce résidu qui constitue ce que l'on appelle la coupe, au sens vulgaire, et c'est la surface que nous mesurons.

L'un de nous (1 et 2) a étudié géométriquement les lois de sa formation. Il a établi que ce noyau homogène était en règle générale plus grand que la coupe réelle qu'il contient, et qu'on ne peut pas discerner. En mesurant le noyau et en le considérant comme surface de coupe, on commet une erreur systématique par excès. Dans certains cas cependant le noyau est uniquement constitué par la coupe elle-même et l'erreur commise sera rigoureusement nulle. C'est dans ces cas qu'il importe de se placer pour arriver à des résultats valables. C'est ainsi que s'introduisent les conditions relatives au mouvement tomographique, dont nous avions parlé au début de ce travail.

III. Le mouvement tomographique. Image instantanée d'une sphère

Quel que soit le mode de réalisation mécanique du tomographe utilisé, on sait qu'on peut toujours, du point de vue géométrique, considérer le film Φ comme fixe, tandis que le foyer F décrit une trajectoire fictive. L'objet est animé, par rapport au film, d'un mouvement de translation, le plan de coupe est parallèle à Φ. Un point O du plan de coupe possède une image Ω fixe dans le film. La trajectoire de F et celle de O sont homothétiques par rapport à Ω, le rapport $\Omega O / \Omega F = K$ est le rapport d'homothétie.

Un volume quelconque fournit à chaque instant une ombre, qui est son image instantanée: c'est la superposition de ces images instantanées qui constitue le tomogramme définitif. Nous allons étudier en détail l'image instantanée du plus simple des solides (diagramme 3), la sphère, déjà étudiée en partie dans ce journal par de Waard (13).

Considérons une sphère Σ, de rayon R et de centre C. Le plan de coupe P la rencontre suivant un cercle g, de centre O et de rayon $\sqrt{R^2 - c^2}$, en appelant c la distance

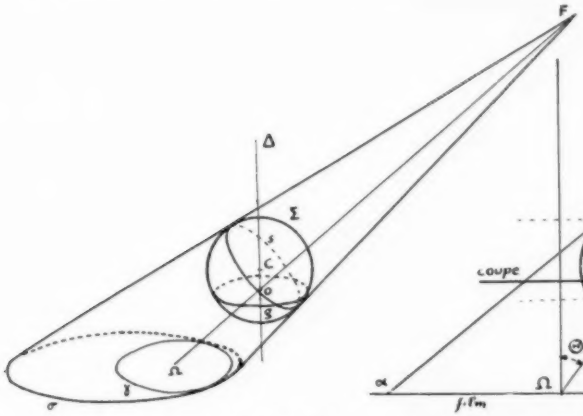

Diagramme 3. Formation de l'image instantanée d'une sphère. Le plan de coupe coupe la sphère Σ suivant un cercle g, de centre O, dont l'image est le cercle γ de centre Ω.

La sphère a pour image l'ellipse σ, trace sur le plan du film du cône de sommet F, circonscrit à Σ, suivant le cercle s.

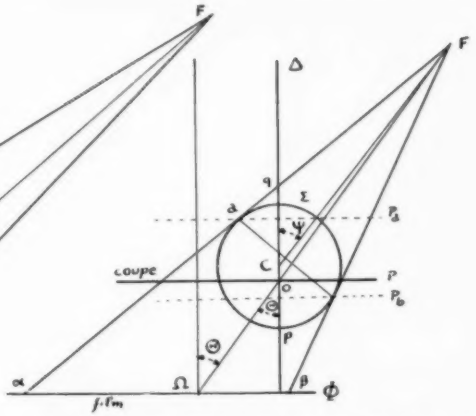

Diagramme 4. Projection de la figure précédente sur un plan perpendiculaire au film, passant par le centre C de la sphère et par le foyer F.

qui sépare le centre de la sphère, C, du plan de coupe. Par définition même du mouvement tomographique, l'image de ce cercle de coupe est un cercle γ de centre Ω et de rayon $\sqrt{R^2 - c^2}/(1 - K)$.

C'est cette surface que nous devons reconnaître et mesurer au milieu du noyau.

Le noyau est délimité par l'enveloppe des images instantanées de la sphère sur le cliché, c'est à dire par la courbe qui leur est tangente, et nous devons rechercher les conditions que doit remplir le plan de coupe pour qu'il en soit effectivement ainsi.

On peut se livrer à une étude géométrique complète du problème, nous nous bornons à en résumer les conclusions d'ailleurs évidentes sur le diagramme 3.

Puisque l'image instantanée de la sphère est la trace sur le plan Φ du film du cône tangent à la sphère et dont le sommet est le foyer F, ce sera une ellipse qui est la projection à partir de F, du cercle s.

Le diagramme 4 représente une projection sur un plan perpendiculaire au film. Le cercle s y figure par son diamètre ab, l'ellipse σ a pour grand axe $\alpha\beta$. Les droites Fa α et Fb β sont tangentes au cercle qui représente la sphère. Une droite perpendiculaire au film, Δ, et passant par C, rencontre Fa α en q et Fb β en p.

Pour que le cercle γ, image de la coupe, soit tangent à l'ellipse il faut que le plan de coupe rencontre la droite ab, c'est à dire qu'il soit situé entre les deux plans parallèles à Φ passant par a et b. Soit P_a et P_b ces deux plans.

S'il est situé au dessus du plan P_b ou au dessous du plan P_a, s'il existe un noyau, il sera plus grand que la coupe, il peut même au voisinage de p et de q exister des plans de

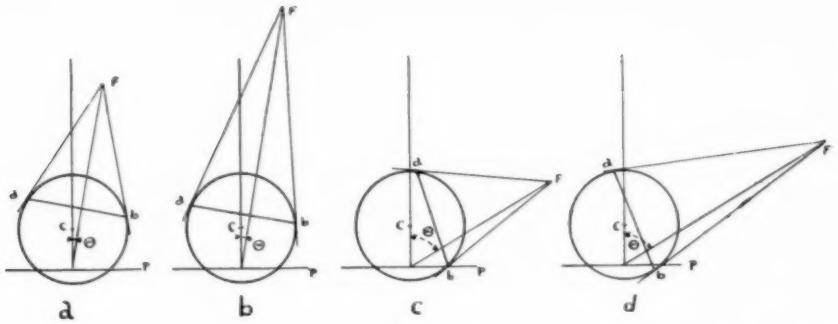

Diagramme 5. Importance de l'éloignement du foyer et de la grandeur de l'angle de coupe:

a) courte distance focale CF, petit angle de coupe, $\Theta = 10°$: résultats désastreux, le plan de coupe P peut varier énormément sans rencontrer le cercle s (symbolisé par son diamètre ab); la plupart des coupes seront affectées d'un important noyau et on aura une erreur par excès importante.

b) distance focale presque double, petit angle de coupe, $\Theta = 10°$; les résultats sont à peine améliorés.

c) Courte distance focale, grand angle de coupe, $\Theta = 60°$; grande amélioration. Les coupes affectées d'un noyau gênant sont infiniment moins nombreuses.

d) grande distance focale, grand angle de coupe, $\Theta = 60°$; l'amélioration s'est poursuivie et ce n'est que dans un tout petit domaine qu'on aura une erreur par excès sur la surface de la coupe.

coupe qui fournissent un noyau alors qu'il n'existe pas réellement de coupe. En somme s'il existe une erreur elle sera par excès.

Cette étude abrégée nous permet de formuler les conclusions suivantes:

1°) Pour que le résidu, ou noyau, se confonde exactement avec la coupe il importe que durant toute la durée du mouvement tomographique le plan de coupe rencontre le cercle s. Or ce cercle est variable pendant le mouvement et nous devons choisir un tomographe dont le mouvement soit, au mieux, compatible avec cette condition.

2°) En vertu de la remarque précédente, il faut qu'au cours du déplacement stratigraphique, la corde ab soit la plus longue possible, c'est à dire, presque égale à un diamètre. Il faut que la longueur CF soit grande devant le rayon R de la sphère. En d'autres termes on doit opérer dans les conditions de la téléradiographie.

Il en est ainsi dans les tomographes usuels, R est de l'ordre de 10 cm et CF de l'ordre du mètre, c'est à dire dix fois plus grand, ce qui suffit largement.

3°) Il faut de plus que la corde reste quasi perpendiculaire, au cours du mouvement, au plan de coupe P. Si elle l'était rigoureusement (cas irréalisable en pratique), et si elle était un diamètre, tous les plans de coupe rencontreraient *ab*, et on n'aurait jamais à redouter d'erreur par excès.

Il faut, par conséquent que l'angle Ψ soit voisin de 90°: l'angle de coupe Θ, c'est à dire l'angle de $\triangle$ et de oF, qui en diffère peu à cause de la petitesse du rapport R/CF doit donc être lui aussi voisin de 90°. Par la même occasion les points p et q se rapprochent

de la surface de la sphère ce qui diminue le risque de pseudo-coupes ne correspondant à rien.

En d'autres termes, il faut choisir un tomographe travaillant avec le plus grand angle de coupe possible.

IV. Étude des divers mouvements tomographiques

A. La stratigraphie axiale transversale (tomographie horizontale) (classe A_2)

Dans sa réalisation par VALLEBONA (diagramme 6) le film, horizontal, tourne autour d'un axe vertical ∠, tandis que le sujet tourne d'un mouvement synchrone autour de l'axe parallèle D; le foyer F est fixe. Dans la première réalisation de FRAIN et LACROIX, le patient est fixe, le foyer et le film tournent: la géométrie des deux appareils est strictement identique.

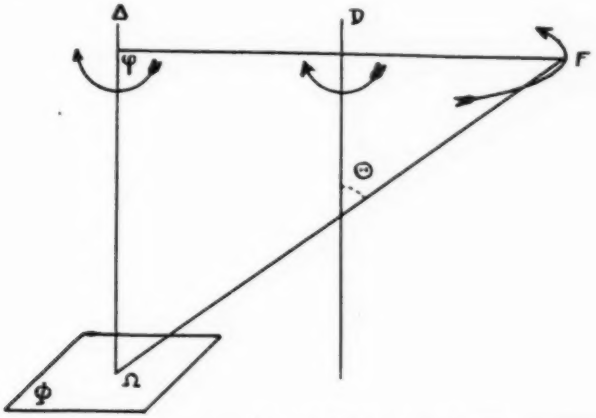

Diagramme 6. La tomographie axiale transversale (VALLEBONA). Le film tourne autour de ∠. Le sujet tourne d'un mouvement synchrone autour de D. Tout se passe comme si le film restait fixe et si le foyer décrivait une trajectoire parallèle au film, dans le sens indiqué par la flèche, de centre φ et de rayon φ F.

On démontre: que le plan de coupe est horizontal;

que par rapport au film, le foyer décrit un cercle de rayon Fφ, tandis que l'objet décrit une trajectoire homothétique;

que l'angle de coupe Θ reste constant au cours du mouvement.

L'image définitive, lue sur le tomogramme, est engendrée par la rotation de l'ellipse σ autour de Ω. Le noyau est un cercle de centre Ω (diagramme 7).

On peut distinguer trois cas

a) le plan de coupe est entre P_a et P_b. Le noyau est constitué par le cercle, image de la coupe. L'erreur commise en assimilant la surface du noyau à celle de la coupe est donc rigoureusement nulle.

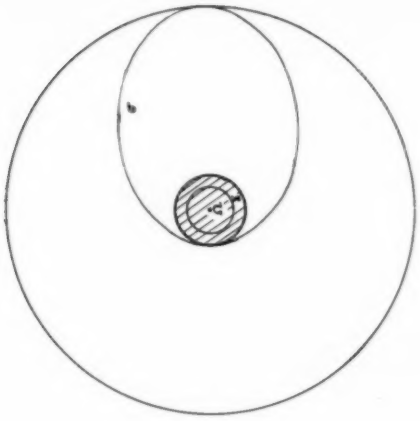

Diagramme 7. L'image lue sur le tomogramme, dans le cas où le noyau est plus grand que la coupe. La surface de la coupe réelle est le cercle γ de centre Ω.

b) le plan de coupe est entre P_a et q, ou entre P_b et p: Il existe un noyau de centre Ω. S'il existe une coupe, elle lui est concentrique et intérieure. En assimilant la surface du noyau à celle de la coupe on commet une erreur, par excès, d'autant plus grande que le plan de coupe est plus éloigné de P_a ou de P_b. En particulier, au voisinage de p et de q, il existe un noyau alors qu'il n'y a plus de coupe.

Heureusement, comme il est évident sur le diagramme, les images parasites n'ont qu'une très petite surface, lorsqu'on a soin de travailler

à grande distance
à grand angle de coupe.

(On trouve parfois, dans la littérature une confusion regrettable entre deux idées très différentes: téléradiographie, c'est à dire, radiographie à grande distance, et radiographie à faible agrandissement et à détails fouillés. S'il est vrai que la téléradiographie entraîne un faible agrandissement, lorsque le rayon central du faisceau de rayons Roentgen est perpendiculaire au film (téléradiographie pulmonaire), celà n'est plus vrai lorsque le rayon central est peu incliné sur le film, on a, comme nous le verrons un agrandissement important tout en travaillant, du point de vue métrique et énergétique dans les conditions de la radiographie à grande distance.)

c) la coupe est au dessus de q ou au dessous de p: l'image sur le tomogramme est une image annulaire, à centre non impressionné. Nous prenons ici contact avec le très important problème de l'effacement qui nous entraînerait hors de notre propos.

Ainsi en utilisant pour nos mesures la stratigraphie axiale transversale, nous commettons une erreur systématique par excès, erreur qui sera d'autant plus faible que la distance foyer—objet sera plus grande et l'angle de coupe voisin de 90°.

Ce sont justement les conditions réalisées dans tous les appareils de ce type. Elle le sont d'ailleurs pour des motifs étrangers à notre but, dont l'exposé nous écarterait de notre sujet.

Nous nous sommes servis d'un appareil pour lequel la distance CF est de 1.10 m et Θ vaut 68°.

On pourrait se servir d'un appareil à foyer et à film mobiles, décrivant des trajectoires circulaires (Bocage), géométriquement équivalent (1 et 2). Mécaniquement, pour ne pas

accroître l'encombrement, on les réalise avec des angles de coupe de l'ordre de 10°, au plus, ce qui est manifestement insuffisant: l'expérience journalière montre en effet qu'il y a loin de la pureté des images obtenues en tomographie horizontale aux images fournies par ces appareils, toujours entachées d'un noyau.

Avantages et inconvénients

Les avantages sont donc évidents. Ils découlent de notre précédente étude. Les inconvénients sont: mouvement du malade, assez désagréable à la longue, impraticable sur malade fatigué, difficulté du centrage précis (5 et 7). En revanche il est facile au moyen d'un volant divisé de faire varier la coupe par millimètre ou fraction de millimètre.

B. *Tomographie à balayage rectiligne (classe A_1)*

L'un de nous (1 et 2), a étudié en détail l'image des sphères. Il est nécessaire d'avoir un appareil à très grand angle de coupe (70° à 80°), ce qui suffit à condamner la réalisation d'une expérimentation, à cause de l'encombrement de l'appareil et de la longueur du temps de pose: il ne faut pas oublier que pour ces grands balayages on doit utiliser un tomographe rigoureux et non un appareil à oscillation. Cela est dommage, car ces appareils travaillant sur malade fixe, et, parfois, couché, permettent l'étude d'un sujet fatigué ou très déficient.

C. *Les appareils de classe B_2*

Leur type est l'appareil à coupes verticales de Vallebona-Bozzetti, qui diffère du stratigraphe horizontal, par le fait que le film est vertical, ce qui entraîne l'existence d'un plan de coupe également vertical.

Ce système possède l'avantage de fournir des angles de coupe très grands (supérieurs à 90°) et possède les avantages signalés par Duhamel (1) et Duhamel et Martin (6) pour les montages où la trajectoire fictive du foyer traverse le plan de coupe.

Nous n'avons pas pu l'essayer expérimentalement.

V. Conclusion de l'examen des techniques. Les volumes réels

Cette conclusion ressort, on ne peut plus nettement, des considérations qui précèdent. La tomographie horizontale, caractérisée par la permanence de son grand angle de coupe et par la grande distance foyer—objet est la méthode de choix pour remplir notre but.

Il faut remarquer que, dans la pratique, nous n'avons pas affaire à des volumes sphériques, mais à des volumes quelconques.

Il est, bien entendu, impossible de faire pour chacun une théorie aussi détaillée que dans le cas des sphères, mais les conclusions subsistent: le noyau est constitué par l'image de la coupe seule lorsque le plan de coupe rencontre la courbe de contact du cône circonscrit à l'objet et de l'objet. Cette courbe n'est plus nécessairement plane, mais elle aura une direction générale (pour les volumes de forme simple) quasi verticale si l'angle de coupe est grand et le foyer éloigné de l'objet.

C'est aux extrémités supérieure et inférieure de l'objet qu'on commettra des erreurs par excès en assimilant le noyau à la coupe (noyau supérieur à la coupe, ou pseudo-coupe). C'est pour cette raison même que la formule

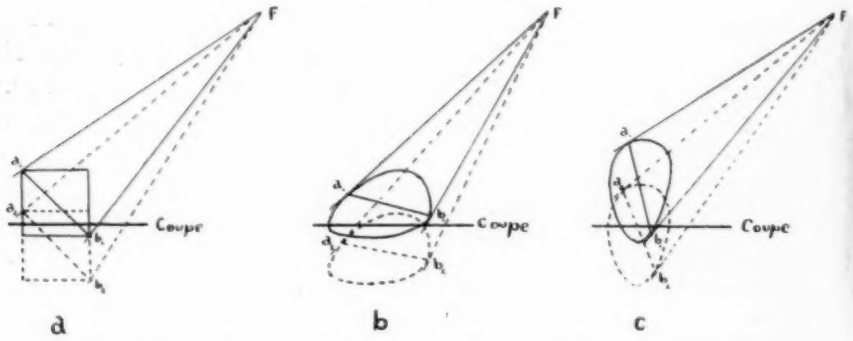

Diagramme 8. Influence de la forme de l'objet sur l'erreur de mesure.

a) objet parallélépipédique: il n'y a aucun risque d'obtenir sur le tomogramme, une image qui soit plus grande que la coupe car, à chaque coupe, le plan de section rencontre le plan ab qui définit le contour apparent.

b) et c) le même objet oblong dans deux positions différentes

en b) position défavorable, il est difficile que le plan de coupe rencontre le plan ab, lorsqu'on fait varier, comme c'est la règle, le plan de coupe en modifiant la hauteur de l'objet.

en c) position favorable, le plan de coupe rencontre toujours ab quelle que soit la hauteur de l'objet.

(1) qui attribue un poids moins élevé aux coupes de l'extrémité est intéressante.

D'ailleurs il existera des types de volumes plus favorables que la sphère (diagramme 8 a), caractérisés par des surfaces limites quasiplanes, et des volumes moins favorables (diagramme 8 b).

Le cœur, pyramide arrondie, reposant sur une de ses faces qui est horizontale, est favorable dans le bas, moins favorable dans le haut, caractérisé par une courbure plus grande.

Le tomogramme obtenu sur le film n'est pas l'image d'une coupe idéalement mince: c'est l'image d'une tranche d'épaisseur ϵ, par conséquent si nous effectuions nos coupes successives à la distance $m = e$ nous serions sûrs d'utiliser pleinement les performances de l'appareil.

L'épaisseur de coupe est fournie par la formule:

$$e \text{ (en millimètres)} = \frac{I - K}{\operatorname{tg} \Theta}.$$

Ce qui conduit à lui attribuer, en tomographie horizontale, une valeur de l'ordre de deux ou trois dixièmes de millimètre. La certitude espérée nous conduirait à une débauche de films, avec d'ailleurs une précision illusoire, car ainsi que nous l'avons montré le repérage précis du plan de

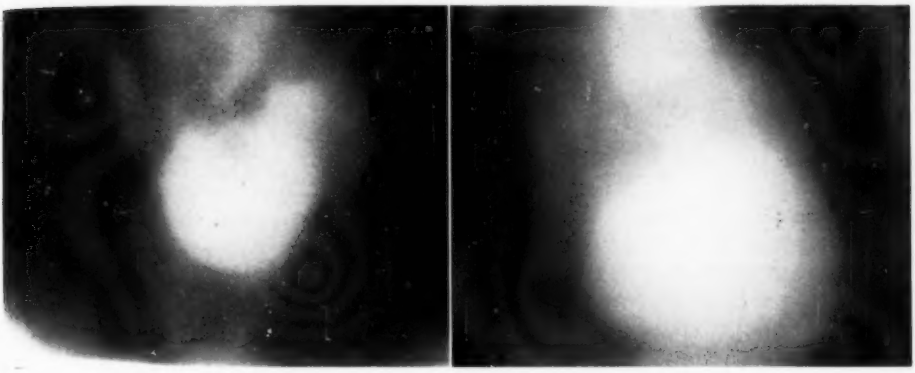

a. b.

c.

Figure 1. a) Coupe supérieure passant par la bifurcation trachéale.
b) Coupe moyenne,
c) Coupe inférieure.

coupe sur le malade, en stratigraphie horizontale, est impossible expérimentalement (difficultés de la recherche des corps étrangers).

Nous avons adopté pour *m* la valeur 1 cm qui restreint les films utiles à une douzaine. Seule l'expérience peut nous dire si cette valeur fournit une bonne appréciation.

Il ne faut pas oublier non plus qu'un temps primordial de la technique est la mesure, aussi précise qu'il est possible, de la hauteur du volume étudié.

En tomographie horizontale la distance de l'objet au foyer est assez grande, mais on ne travaille pas dans les conditions de téléradiographie, au sens où on l'entend en général. En effet, le rapport d'agrandissement

linéaire de l'image par rapport à l'objet (section du volume par le plan de coupe) est:

$$A = \frac{\Omega F}{OF} = \frac{1}{I - K} = \frac{\varphi F}{\triangle D}$$

Il est toujours très nettement supérieur à l'unité: quand on dit que la stratigraphie axiale est une téléradiographie, l'affirmation est exacte puisque ΩF est grand, mais il s'introduit dans la plupart des esprits une confusion avec la «téléradiographie pulmonaire» où ΩF est grand aussi, mais où A est voisin de un, ce qui implique que l'objet est au contact du film. Il y a là un chevauchement de termes, générateur d'obscurités dans les discussions, comme nous avons pu nous en rendre compte par nous-mêmes. Nous tenions à le signaler.

Si on appelle S la surface de la coupe mesurée sur le tomogramme, la surface réelle de la coupe sera:

$$\frac{S}{A^2}$$

Pour accélérer les calculs il suffira de calculer la formule (1) avec les valeurs des surfaces mesurées sur le film et de diviser le résultat obtenu par A^2.

L'appareil que nous avons utilisé était caractérisé par les valeurs suivantes:

$$\Theta = 68°, \quad A = 1.4, \quad A^2 = 1.96$$

VI. L'expérimentation sur volume inerte

Elle nous fournira l'erreur commise sur un volume mesurable directement.

Elle se proposera deux buts:

Vérification sur un volume bien défini des lois de la tomographie, c'est-à-dire, par exemple, puisqu'on peut calculer A à partir des dimensions du tomographe, nous pourrons mesurer le rapport de la section réelle à son image tomographique. La différence entre la valeur de ce rapport et A^2 permettra de chiffrer les erreurs dues au flou tomographique d'un volume complexe.

1°) La première série d'expériences a consisté à étudier et à pratiquer des sections tomographiques d'un prisme de base carrée, de côté 3 cm et de hauteur 2 cm.

Nous avons pu vérifier que l'image tomographique était bien un carré dont le côté avait pour longueur 4.2 cm ce qui entraîne un rapport d'agrandissement expérimental rigoureusement égal à 1.4. La surface de cette image est 17.64 cm^2 c'est-à-dire dans le rapport 1.96 à la coupe réelle. Ainsi les flous tomographiques sont sans grande importance. L'un de nous (1 et 3) avait déjà insisté sur les bons résultats métriques fournis par la

méthode tomographique, à angle de coupe faible (10°): l'expérience montre qu'il en est de même pour des angles de coupe sept fois plus grands.

La question des pseudo-coupes ne se pose pas ici, dans la recherche expérimentale de la hauteur du volume. En effet, le solide est de la forme «favorable», et une pseudo-coupe se trahirait par sa forme et ses dimensions. Nous n'en avons pas trouvé expérimentalement.

Au contraire nous avons pu trouver qu'une coupe était entièrement blanche, tandis que la coupe suivante située 0.1 cm plus bas était positive: on a donc déterminé S'_o qui vaut 17.64 cm² et m' qui vaut 0.1 cm. La coupe suivante située à 1 cm au dessous de S'_o nous fournit la même image, c'est S_o; une autre coupe, 1 cm plus bas, ne nous fournit rien tandis qu'une coupe située à 0.075 cm au dessus nous donne un résultat positif; c'est cette dernière image qui est ici S'_n, tandis que S_n est confondu avec S_o.

Nos résultats se résument ainsi:

$S'_o = S_o = S_n = S'_n = 17.64$ cm²

$m' = 0.1$ cm en haut et 0.075 en bas. La formule (1) nous donne

$$V \simeq \frac{17.64}{2} [(0.1 + 1) + (1 + 0.925) + (0.075 + 0.925)] \frac{1}{1.96}$$

$$V \simeq \frac{17.64}{2} \cdot 4.025 \cdot \frac{1}{1.96} = 18.11 \text{ cm}^3$$

Le volume mesuré est de 18.11 cm³. Le volume réel est de 18 cm³ ce qui entraine une erreur par excès de 0.6 %.

La méthode est donc remarquablement correcte, et nous pouvons caresser l'espoir d'obtenir une bonne précision en l'appliquant à des solides quelconques.

2°) Dans un premier groupe d'expériences, nous avons étudié des solides opaques de forme quelconque. En voici un qui possédait une forme vaguement cardiaque.

Sa hauteur directe était de 5.8 cm. Les résultats trouvés furent les suivants:

$m' = 0.25$ cm, $m = m_o = 1$ cm, $m_1 = 0.5$ cm
$S'_o = 41.1$ cm², $S_o = 131.4$ cm², $S_1 = 160.7$ cm²,
$S_2 = 195$ cm², $S_3 = 173.1$ cm², $S_4 = 209$ cm², $S'_4 = 209$ cm²

Nous remarquerons ici que la hauteur de l'objet, mesurée tomographiquement, est comprise entre 5.5 cm et 6 cm (erreur $\pm$ 3.4 %).

$$V \simeq \frac{1}{1.96} \left[\frac{41.1}{2} 1.25 + \frac{131.4}{2} 2 + 160.7 + 195 + 173.1 + \frac{209}{2} 1.5 + \frac{209}{2} 0.75 \right]$$

$$\simeq \frac{946.7}{1.96} = 483 \text{ cm}^3.$$

Le volume réel mesure 501 cm³: l'erreur est, par défaut, de 3.5 %.

3°) En prenant comme objet un cœur de veau, nous avons pu nous livrer aux expériences résumées dans le tableau suivant.

La colonne I correspond au cœur frais, la colonne II au cœur injecté de baryte et devenu plus globuleux. Nous ne donnons pas la numérotation des coupes en S'_o, S_o, etc.

Le cœur était pointe en bas pour assurer une meilleure contention. On utilisait un repère en film de plomb pour délimiter la base de l'aorte, c'est-à-dire la fin du cœur, et on a mesuré le volume du cœur par immersion jusqu'au repère; dans nos coupes nous nous sommes arrangés pour que la première contienne le repère et par conséquent nous pouvons affirmer que:

$m' = o$ pour la base du cœur, et que $m' = 0.5$ cm pour la pointe

$$m = m_o = m_n - 1 \text{ cm}.$$

Experience	I		II	
Surfaces mesurées sur le film....	87	cm²	56	cm²
» » » » »	113.75	»	85	»
» » » » »	156.7	»	114.2	»
» » » » »	133	»	170	»
» » » » »	118	»	163	»
» » » » »	108	»	141	»
» » » » »	94	»	126	»
» » » » »	77.2	»	89	»
» » » » »	61	»	75	»
» » » » »	44	»	35	»
» » » » »	25	»	14.4	»
» » » » »	6	»	9.3	»
» » » » »	2.3	»	4	»
Volume calculé	496	cm³	537	cm³
Volume réel	468	cm³	486	cm³
Erreur	+ 6	%	+ 10	%

L'erreur maximum est de 10 %. Encore faut-il remarquer que le cœur étant placé la pointe en bas (diagramme 8 c), on se trouvait dans des conditions assurément défavorables: en effet les dernières coupes sont entachées de l'erreur par excès due au noyau et à la pseudo-coupe. En position normale il constitue un volume beaucoup plus favorable.

C'est ainsi que sur le cadavre, fixé au formol, avec base du cœur repérée, l'un de nous a pu dresser le tableau suivant:

Cadavre I: volume réel 815 cm³; volume calculé 790 cm³, erreur — 3 %.
Cadavre II: volume réel 1,215 cm³; volume calculé 1,240 cm³, erreur + 2 %.

D'ailleurs une fois le cœur plein de liquide lourd, il se déforme et lorsqu'on mesure son volume par immersion aqueuse, pointe en bas pour que le repère de la base affleure la surface de l'eau, la pointe se déforme par poussée d'Archimède. Aussi considérons nous le chiffre de 10 % comme un maximum jamais atteint, et nous admettrons comme erreur moyenne, l'erreur maximum rencontrée: 6 % dans nos expérimentations.

Volume du cœur chez les vivants

D'ailleurs sur le vivant on se heurte à d'autres causes d'erreur:

1°) le volume du cœur est variable: il existe plusieurs volumes correspondant aux diverses diastoles et systoles. Les auteurs sont muets au sujet des ordres de grandeur de ces volumes. Le temps de pose utilisé est de 3.8 s, soit de quatre révolutions cardiaques. La méthode nous fournira donc un volume moyen. Nous avons systématiquement effectué nos mesures en inspiration forcée: nous aurons donc un volume inspiratoire moyen, compris entre la systole et la diastole globale. Peut-être plus près de cette dernière, car les bords des images sont nets et non bougés:

l'image doit donc être celle d'un extrêmum qui ne peut être que diastolique.

2°) Sur le vivant le cœur est mal délimité: on n'a pas la ressource de marquer la base du pédicule vasculaire au fil de plomb, et la base du cœur est indiscernable des vaisseaux. Contraint de prendre des repères anatomiques, on a le droit d'hésiter. Le plus fidèle, le plus proche du cœur est la bifurcation de la bronche souche gauche, pour la partie supérieure. Il est malheureusement parfois peu visible et nous avons préféré la bifurcation trachéale, commettant ainsi une erreur, par excès de 10 cm³ environ, soit de 1.6 % au plus.

Dans la portion diaphragmatique le problème est analogue, mais on dispose des coupoles diaphragmatiques toujours visibles. D'ailleurs on peut se servir du repère trachéal pour mesurer en radioscopie la hauteur cardiaque et, ainsi déterminer m_n avec précision. D'après les anatomistes consultés l'erreur doit être de l'ordre de 10 cm³, soit aussi 1.6 %.

En ajoutant l'erreur géométrique de 6 %, à ces erreurs d'ordre anatomique on arrive à une erreur totale de 10 %: c'est ce chiffre que nous retiendrons pour le cœur.

Il n'entre pas dans notre propos, qui ne veut être que technique, de faire une étude anatomo-chimique des résultats trouvés.

Nous nous bornerons à signaler que, dans un lot de malades cardiaques ou non, examinés soit dans le Service de Radiologie du Professeur C. WANGERMEZ, soit dans celui de Cardiologie du Professeur BROUSTET, nous avons trouvé les nombres suivants: 700 cm³, 1,080 cm³, 880 cm³, 570 cm³, 680 cm³ qui fournissent l'ordre de grandeur du volume du cœur chez le sujet normal.

Autres volumes

Les circonstances nous ont amenés surtout à étudier le volume cardiaque: d'autres viscères pourraient utilement faire l'objet d'une étude précise, par exemple les petites rates chez les leucémiques, ou le rein.

Dans chaque cas il sera nécessaire de déterminer auparavant, sur un volume de forme analogue, l'erreur géométrique commise.

Addendum

Depuis la rédaction de ce travail, FUCHS et BAYER, ont publié au mois de juin 1953, une technique de mesure du volume cardiaque très voisine de la nôtre. (Eine neue Methode zur Bestimmung des Herzvolumens. Fortschr. Röntgenstr. 78 (1953), 709.)

Elle conjugue l'utilisation de coupes tomographiques en petit nombre (trois ou quatre), avec des mesures de diamètres, comme les méthodes classiques et une formule mathématique qui se ramène d'ailleurs à la formule (I), à condition d'assimiler le volume du cœur à une forme géométrique simple. A ce titre, donc, elle ne s'applique qu'à des cœurs quasi normaux, et est à priori moins souple, moins générale et moins précise que

la nôtre; pour les cœurs qui ne sont pas trop déformés par un processus pathologique elle est plus expéditive et moins coûteuse.

Comme sa nature mathématique profonde est la même on peut la considérer comme une variante abrégée, et les résultats expérimentaux de FUCHS et BAYER et les nôtres se prêtent un mutuel appui.

RÉSUMÉ

Les auteurs font l'exposé critique d'une méthode tomographique capable de fournir la mesure du volume moyen du cœur sur le vivant. Cette méthode est susceptible de donner, dans les cas les plus défavorables, une précision supérieure à 10 %.

SUMMARY

The authors describe in detail a tomographie method of measuring the average volume of the heart in human subjects. The method, even in the most unfavourable cases, has an accuracy better than 10 %.

ZUSAMMENFASSUNG

Eine tomographische Methode, die es ermöglicht, den durchschnittlichen Umfang des Herzens am Lebenden zu messen, wird kritisch dargestellt. Diese Methode ist in der Lage, in den ungünstigsten Fällen eine Genauigkeit von mindestens 10 % zu geben.

BIBLIOGRAPHIE

1. DUHAMEL, J.: La tomographie. Etude théorique et physique. Thèse de Médecine. Bordeaux 1950.
2. — Les procédés géométriques en radiologie. La tomographie. Scienc. et Industr. Photogr. 21 (1950), 170.
3. — Vérifications expérimentales des théories tomographiques. Scienc. et Industr. Photogr. 21 (1950), 401.
4. — L'épaisseur de la couche de coupe en tomographie. J. de radiol. et d'électrol. 32 (1951), 758.
5. — Sur la mise en évidence et la mesure de l'excentrement des tubes en stratigraphie axiale transversale (tomographie horizontale). Scienc. et Industr. Photogr. 24 (1953), 98.
6. DUHAMEL, J. et MARTIN, P. L.: Essais de tomographie horizontale avec un tomographe à coupes verticales. J. de radiol. et d'électrol. 32 (1951), 113.
7. — Riflessioni sulla determinazione esatta della posizione del piano dei punti fissi in stratigrafia assiale trasversa. Radiol. med. 39 (1953), 1.
8. GUILLON, M.: Etude radiologique du cœur et des gros vaisseaux par la tomographie axiale transversale. Thèse de Médecine. Bordeaux 1952.
9. LACROIX, F.: Procédé rapide de repérage du niveau du plan de coupe en tomographie horizontale. J. de radiol. et d'électrol. 34 (1953), 180.
10. LINDEMAN, B.: Simultane Angiocardio-tomographie. Fortschr. Röntgenstr. 73 (1950), 261.
11. VALLEBONA, A.: Nuovi orizzonti della stratigrafia nei vari campi della medicina. Istit. Radiol. Università di Genova 1948.
12. — Trattato di stratigrafia. F. Vallardi, Milano 1951.
13. DE WAARD, R. H.: On a fundamental property of planigraphic image formation. Acta radiol. 19 (1938), 465.